1987

Coherent electronic energy transfer and nonlinear polariton effects in anthracene-doped naphthalene crystals

Maureen Anne Connolly
Iowa State University

INFORMATION TO USERS

While the most advanced technology has been used to photograph and reproduce this manuscript, the quality of the reproduction is heavily dependent upon the quality of the material submitted. For example:

- Manuscript pages may have indistinct print. In such cases, the best available copy has been filmed.
- Manuscripts may not always be complete. In such cases, a note will indicate that it is not possible to obtain missing pages.
- Copyrighted material may have been removed from the manuscript. In such cases, a note will indicate the deletion.

Oversize materials (e.g., maps, drawings, and charts) are photographed by sectioning the original, beginning at the upper left-hand corner and continuing from left to right in equal sections with small overlaps. Each oversize page is also filmed as one exposure and is available, for an additional charge, as a standard 35mm slide or as a 17"x 23" black and white photographic print.

Most photographs reproduce acceptably on positive microfilm or microfiche but lack the clarity on xerographic copies made from the microfilm. For an additional charge, 35mm slides of 6"x 9" black and white photographic prints are available for any photographs or illustrations that cannot be reproduced satisfactorily by xerography.

Connolly, Maureen Anne

COHERENT ELECTRONIC ENERGY TRANSFER AND NONLINEAR POLARITON EFFECTS IN ANTHRACENE-DOPED NAPHTHALENE CRYSTALS

Iowa State University PH.D. 1987

PLEASE NOTE:

In all cases this material has been filmed in the best possible way from the available copy. Problems encountered with this document have been identified here with a check mark __✓__.

1. Glossy photographs or pages _____
2. Colored illustrations, paper or print _____
3. Photographs with dark background _____
4. Illustrations are poor copy _____
5. Pages with black marks, not original copy _____
6. Print shows through as there is text on both sides of page _____
7. Indistinct, broken or small print on several pages ✓
8. Print exceeds margin requirements _____
9. Tightly bound copy with print lost in spine _____
10. Computer printout pages with indistinct print _____
11. Page(s) _____ lacking when material received, and not available from school or author.
12. Page(s) _____ seem to be missing in numbering only as text follows.
13. Two pages numbered _____. Text follows.
14. Curling and wrinkled pages _____
15. Dissertation contains pages with print at a slant, filmed as received _____
16. Other _____

_____

_____

Coherent electronic energy transfer and nonlinear polariton effects in anthracene-doped naphthalene crystals

by

Maureen Anne Connolly

A Dissertation Submitted to the
Graduate Faculty in Partial Fulfillment of the
Requirements for the Degree of
DOCTOR OF PHILOSOPHY

Department: Chemistry
Major: Physical Chemistry

Approved:

Signature was redacted for privacy.

In Charge of Major Work

Signature was redacted for privacy.

For the Major Department

Signature was redacted for privacy.

For the Graduate College

Iowa State University
Ames, Iowa

1987

TABLE OF CONTENTS

CHAPTER I. INTRODUCTION

The subject of energy transfer, and in particular energy transfer involving excitons, has been actively pursued for several decades and a plethora of experimental and theoretical results exists. Nevertheless, a detailed understanding of the mechanisms involved in the transfer of energy by excitons has not been attained yet.

Central to the issue of energy transfer are questions involving coherence: do excitons transfer energy in a coherent, wavelike manner, or instead, in an incoherent, random, hopping, or diffusive manner? Although some studies have indicated coherent motion plays a role in energy transfer, other studies have shown evidence of incoherent behavior. In fact, exciton motion in real molecular crystals can exhibit both coherent and incoherent limits as well as behavior intermediate between the two (1).

The problem of finding a truly satisfying solution to exciton energy transfer can be thought of as a two-fold one: 1. development of a theoretical approach which mimics exciton motion in both coherent and incoherent limits as well as all intermediate behavior for large ranges of temperature, defect concentration, and other physical conditions applied to the molecular crystal; 2. design of experiments which can generate data of sufficient quality to be used in the theory or in comparison to predictions brought forth by the theory.

This dissertation is a study of electronic energy transfer at frequencies near the lowest-lying naphthalene exciton resonance in anthracene-doped

naphthalene crystals, using the nonlinear spectroscopic techniques of two-photon fluorescence excitation and second harmonic generation as probes. This chapter presents an overview of some of the more important contributions which have led to the present theoretical and experimental understanding of electronic energy transfer by excitons. Because this dissertation is a study of exciton-polariton behavior, a brief historical overview of progress in the understanding of polariton behavior in molecular crystals is also presented. Later chapters discuss the theoretical approaches more fully, describe the experimental procedures employed in this investigation, and present the results obtained.

Electronic Energy Transfer

Numerous theories and experimental results of studies of exciton motion and energy transfer have appeared in the literature. Although it is not conceivable to cite each and every theoretical and experimental effort, this section endeavors to present a wide sampling of the experimental techniques employed in the study of energy transfer and of the theories developed to explain the experimental results.

A recent introductory review of energy transfer mechanisms, including discussions of resonant and nonresonant energy transfer, electronic charge transport and energy transfer, exciton energy transfer, Auger processes, and inelastic collisional energy transfer, is presented by Bernard et al. (1) and is a good starting point for anyone interested in learning about any of the above mentioned energy transfer mechanisms.

Silbey (2) presented a review of the theoretical developments in the field of electronic energy transfer and exciton transport in molecular crystals. Theoretical and related experimental treatments of coherent energy transfer in solids, with special attention paid to lineshape analysis, have been reviewed by Harris and Zwemer (3). A brief overview of some basic experimental techniques employed in studies of excited state interaction and energy transfer is given by Wolf (4). Kopelman (5) reviewed energy transport, theory and experiments, in mixed molecular crystals. Kenkre (6) recently presented a review of mathematical methods used in the description of energy transfer; this review presents several different theories within the framework of the generalized master equation (GME) approach (vide infra). Theory and experiments involving excitons and polarons in charge transfer crystals are discussed in a review by Haarer and Philpott (7).

Sensitized luminescence techniques have been used extensively in the study of energy transfer. Generally, in this technique the molecular crystal of interest, referred to as the host, is doped with an impurity molecule, called the guest, which serves as a trap for the excitation. Excitation of the crystal, using a frequency range suitable for exciting either the host or the guest, is followed by monitoring of the luminescence intensity of the host and/or guest. It should be pointed out, however, that defects in the molecular crystal lattice can also act as traps for the excitation and can produce sensitized luminescence. The most common observation of such defects comes in the form of X-trap emission. X-trap emission is often used in conjunction with impurity sensitized luminescence to study the effects of

energy transfer in system with shallow (X-traps) and deep (impurity) traps, with the latter often referred to as supertraps. Sensitized luminescence has been utilized in studies of energy transfer involving singlet excitons (fluorescence) and triplet excitons (delayed fluorescence or phosphorescence).

A fine discussion of energy trapping processes in aromatic crystals, with special attention paid to X-trap and impurity sensitized fluorescence, is presented by Wolf and Benz (8). Discussions of electron spin resonance (ESR) data, temperature dependence of observed delayed fluorescence spectra, and kinetics schemes for sensitized prompt fluorescence and sensitized delayed fluorescence are included.

Recently Peter, Ries, and Bässler (9) have examined singlet exciton motion in an organic glass doped, by vapor deposition, with phenanthrene, anthracene, and tetracene. The results are discussed in terms of random walks involving anthracene dimers and tetracene, and Förster transfer involving anthracene excimers and tetracene.

A study of the effect of crystal imperfections on the phosphorescence of triplet excitons in 1,4-dibromonaphthalene single crystals was performed by Vankan and Veeman (10). Their results indicate the need for imperfections, which provide traps, for the observation of the exciton emission. Fluorescence spectra of annealed and deformed anthracene crystals were obtained by Williams et al. (11) in a study of singlet exciton traps. Traps were observed at $\approx$300 cm^{-1} and 1500 cm^{-1} below the S_1 level and were attributed to displaced molecules of anthracene in the area of dislocations.

Studies of detrapping of the lowest triplet state of naphthalene X-traps created by doping naphthalene crystals with β-halonaphthalenes ($\approx 10^{-3}$ mole/mole) were made by Weinzierl and Friedrich (12). The pre-exponential detrapping rate was observed to increase with the halogen mass; this is attributed to an increase in electron-phonon coupling brought about by a heavy-atom-induced enhancement of the charge-transfer character in the lowest triplet trap state. Other investigators who have utilized the external heavy-atom effect in studies of the lowest excited triplet states of naphthalene X-traps include Giachiano and Kearns (13) and Yamauchi and coworkers (14).

Powell and Soos (15) extended the usefulness of sensitized luminescence as a probe of energy transfer by first introducing the use of time-resolved spectroscopic techniques to the field. This technique became even more powerful with the introduction of picosecond lasers. Time evolution of anthracene and tetracene fluorescence in tetracene-doped anthracene crystals was examined by Powell and Kepler (16); their results indicate energy transfer via a long-range resonant interaction in contrast to the usual interpretation of singlet exciton diffusion, in which the transfer is considered to be a short-range process occurring between the excited host molecule and a nearest neighbor impurity. A theory combining both diffusion and long-range interactions best fit their data. Powell (17a,b) subsequently extended these investigations to anthracene crystals of various tetracene concentration, anthracene-doped naphthalene crystals and tetracene-doped naphthalene crystals. Again the combined theory of exciton diffusion and long-range interaction provide a good fit to the

experimental results, however, phenomenalogical fitting parameters (for example, the critical energy transfer distance and the diffusion constant) and values predicted by theory or measured using other techniques were seen to differ by as much as two orders of magnitudel Rosenstock (18) compares data from (16a) to calculations of time-dependent luminescence based on a random walk model for exciton motion; he found good agreement with experiment and made a controversial statement that the long-range energy transfer assumption considered by Powell and Kepler (16) and Powell (19) was not required. Singlet exciton migration and energy transfer in pyrene-doped naphthalene crystals were investigated by Powell (17c) using time resolved fluorescence measurements. In this study, Powell considers a generalized random walk formulation for the migration of singlet excitons, and extracts a value of $\approx 1.5 \times 10^{-10}$ sec for the exciton hopping time at room temperature. The results are shown to be consistent with thermal defect scattering and trapping.

Kinetic models for host to trap exciton energy transfer in doped organic crystals are discussed by Powell and Soos (20). One model based on a modulated random walk with a finite range for the trapping interaction appears to be consistent with time-resolved host-sensitized energy transfer in doped organic crystals. Extensions of this random walk model are discussed in Soos and Powell (21).

Random walk formalisms for the description of energy transfer also have been investigated extensively by Blumen and coworkers (22,23). Random walks with nearest neighbor stepping and long-range stepping on three-dimensional and two-dimensional lattices are studied by Blumen and

Zumofen (22a) and Zumofen and Blumen (22b), respectively. These results are extended to the continuous time domain in reference (22c). Nearest neighbor random walks assuming the excitation to be quenched at first encounter with a trap is investigated by Zumofen and Blumen (23a). Decay functions are calculated for various trap concentrations. Similar studies are described in reference (23b). Additional results of random walk studies assuming long-rang stepping motion are presented in references (23c,d).

First passage continuous time random walk (CTRW) and master equation formalisms are compared and treated within a unifying framework by Klafter and Silbey (24) to study trapping rates and incoherent migration in one-dimensional crystals. Comparison to experimental results (25) is included. A discussion of direct and indirect energy transfer in the framework of CTRW is presented by Klafter and Blumen (26).

More recently, Chow and Powell (27) have developed two approaches to energy transfer dynamics. One method is suited to cases in which weak direct sensitizer-activator interaction acts as a small perturbation on the transfer by diffusion among sensitizers. The other method is a Monte Carlo technique which simulates energy migration on a random distribution of sensitizers. Comparisons of these results with those of other theories and experimental data are given.

A kinetic model with exciton and trap decay rates, the trapping rate, and the detrapping rate used as parameters was proposed by Shelby, Zewail, and Harris (28). This model fit the data from the time evolution of exciton and trap phosphorescence resulting from the laser excitation of the

triplet band states of 1,2,4,5-tetrachlorobenzene (TCB) and 1,4-dibromonaphthalene (DBN); however, the experiment was deemed ambiguous. Guttler, Von Schutz, and Wolf (29) indicate that the trapping rate may be limited by the final trapping step and not by the migration to the trap region.

Pure and anthracene-doped phenanthrene single crystals were excited by short light pulses in a study performed by Heidersdorf (30). The fluorescence spectra and fluorescence decay time of emission bands were obtained in the temperature range of 4 to 300 K; emission was observed for phenanthrene 0-0 band, phenanthrene X-traps, and (for the case of the doped crystals) anthracene. The temperature dependence shows a lack of direct exciton energy transfer to anthracene at temperatures below 50 K, although the anthracene fluorescence is sensitized at these temperatures by indirect energy transfer. A transition scheme is presented.

Photon-echo decay measurements of the lowest singlet exciton state of naphthalene were studied by Aartsma and Wiersma (31) for single crystals of naphthalene-doped durene (deep trap) and naphthalene in perdeutero-naphthalene (shallow trap). They observed different relaxation behavior for the shallow and the deep traps. The photon echo relaxation in the shallow trap case, i.e., the isotopically mixed crystal, is characterized as owing to scattering of the guest excited state into the host singlet exciton band; relaxation in the deep trap crystal is interpreted in terms of a resonant phonon scattering process in the ground and excited states. The photon-echo decay times for both crystal systems were shorter than expected based on fluorescence decay values, and this discrepancy is

attributed to energy transfer.

Skinner et al. (32) discuss the theory of photon echoes based on four level system composed of a pair of coupled two level systems. Results are discussed with regard to experiments performed. Further discussions of picosecond photon echo experiments are included in Fayer (33).

An investigation of the build-up and decay of delayed fluorescence and phosphorescence in chrysene-doped naphthalene crystals, containing both a physical defect and additional impurity associated with the dopant, was undertaken by Talapatra and Misra (34). Their results provide information regarding the heterofusion processes of triplet excitons in the system.

Temperature dependence and impurity concentration effects also have been studied widely. Exciton diffusion in very thin ($\leq 5\ \mu$) anthracene-doped naphthalene crystals was examined as a function of temperature and impurity concentration by Kazzaz and Zahlan (35). Additionally, they looked at the effects of annealing and excitation wavelength. Their results are discussed in terms of surface, incoherent and coherent free excitons. These data were reanalyzed by Agranovich and Konobeev (36a) using a diffusion approximation; their analysis shows agreement with the assumption that "free" excitons are responsible for the energy transfer from host to guest. Further revision of their diffusion theory is presented in Agranovich and Konobeev (36b).

The dependence of singlet exciton energy transfer rate on the anthracene concentration in single crystals of anthracene-doped naphthalene was investigated by Auweter et al. (37) using two-photon

picosecond excitation. At high concentrations of anthracene (anthracene concentration per unit volume, $N_A > 5 \times 10^{16}\ cm^{-3}$), the rate was found to be independent of time. However, at medium concentrations ($6 \times 10^{15}\ cm^{-3} < N_A < 5 \times 10^{16}\ cm^{-3}$) and at low concentrations ($N_A < 6 \times 10^{15}\ cm^{-3}$), the rates were determined to depend upon time as $t^{-1/2}$. The exciton motion is characterized as an incoherent, hopping process at high concentration, diffusive at medium concentrations, and coherent, or wavelike, at low concentrations. In their treatment the capture radius is considered to be a property of the energy transfer mechanism rather than of the dopant molecule.

Shatz and Halpern (38) study theoretically the dependence of exciton trapping on impurity concentration. They calculate the mean probability for exciton capture by an impurity using a diffusion equation which can account for exciton-impurity interactions. The probability is determined to be proportional to the concentration only if the impurities act as absorbing spheres of finite radius.

Triplet exciton absorption lineshapes of DBN were examined in the temperature range ≈2-40 K by Burland et al. (39). They attribute dephasing below 10 K to the scattering of excitons off impurities or lattice defects and above 10 K to scattering by optical phonons.

The temperature dependence of the intensity of the intrinsic TCB X-trap has been examined by Fayer and Harris (40). Their results were fit to Boltzmann statistics giving a trap concentration of one part in 90,000. The interpretation is based on a model dependent upon coherent migration at low temperatures. Dlott, Fayer, and Wieting (25) also have performed

similar experiments on TCB. The phosphorescence build-up rate in the TCB X-trap observed was smaller than the prediction of the coherent model, and much larger than the prediction for the completely incoherent exciton. No unequivocal statement can be made about coherence from these studies.

Picosecond coherent antistokes Raman spectroscopy (CARS) experiments have been performed by Dlott et al. (41) to study the temperature-dependence of vibrational excitons and dephasing in naphthalene crystals. They have observed evidence consistent with a phonon-promoted energy transfer process. Another study of vibrational dephasing in naphthalene crystals was performed by Hess and Prasad (42), who looked at the thermal broadening of the 390 cm^{-1} Raman active vibration in neat and isotopically doped naphthalene single crystals. A discussion of resonance energy transfer and motional narrowing are included. Picosecond delayed CARS experiments were performed on naphthalene crystals at 1.5 K by Hesp and Wiersma (43); their Raman lineshape analysis indicates motional narrowing at low temperatures, and exciton trapping was observed at higher temperatures.

Magnetic resonance experiments of various types have been performed by many groups; the major observable in these experiments is the lineshape. Francis and Harris (44a, b) first showed the existence of coherence in triplet excitons in TCB using optically detected ESR to monitor the band-to-band transition in the lowest triplet state at 3.3K. Comparison of experiment and theory (44c) established that the exciton bandwidth, the minimum coherence time, and the density of states function in the band is obtainable from zero field optically detected magnetic resonance at liquid

helium temperatures. Using the same optically detected electron spin resonance (OD-ESR) technique, Zewail and Harris (45) established the coherent nature of dimer transfer in the lowest triplet state of TCB. The dimers, the translationally equivalent pair along the a-axis embedded in a deuterated solid, has coherent states which are the symmetric and antisymmetric linear combination of the individual molecule excited states and are split by 2β, where β is the exchange integral. In optical absorption only one dimer state has oscillation strength to the ground state; spin-orbit coupling between observed triplet sublevels and higher singlet states allows for the dimer splitting to be observed in ESR. A minimum coherence lifetime of 5×10^{-7} sec was determined; this lifetime is approximately 4 orders of magnitude greater than the intermolecular transfer time (10^{-11} sec), which indicates that the excitation oscillates coherently many times between the dimer molecules before scattering to the other dimer state.

Botter, Dicker, and Schmidt (46a) used two- and three-pulse spin echo to study the ESR linewidth of TCB at temperatures of 15 K and below. Below 1.6 K a constant memory dephasing time is observed and ascribed to impurity and trap scattering; above 2.2 K no spin echoes appear. These studies also show the transition from a double maximum band-to-band transition at 4.2 K to a symmetric Lorentzian at the center of the band at 8 K; this observation is in agreement with predictions made by Harris and Fayer (47). The coherence time of translationally inequivalent naphthalene dimers in perdeuteronaphthalene was measured by Botter et al. (46b) employing both zero-field ESR and electron spin echo techniques. Recently, Schmidt (48) has discussed electron spin echo results for TCB.

ESR and OD-ESR lineshape studies of DBN were performed by Schmidberger and Wolf (49). At low temperatures, the lineshape was found to be constant, indicating coherence by the Haken and Strobl (50) definition. The lineshape was observed to increase proportional to T^3 up to a maximum value at 16 K. Since the population density of acoustic phonons in a Debye solid goes as T^3, the interpretation of lineshape behavior in this temperature region involves dephasing by scattering with acoustic phonons. Above 16 K, the lineshape decreases asymptotically to a constant value at room temperature. The motion here is characterized as incoherent and motionally narrowed. Additionaliy, at low temperatures exciton transfer between magnetically inequivalent chains limits coherence. An upper limit on the coherence time, 10^{-8} sec, was determined from measurements of this cross-chain hopping rate.

EPR was used to probe triplet exciton transport between differently oriented sites in crystals of anthracene-doped tetracyanobenzene (TCNB) at temperatures below 30 K by Park and Reddoch (51). Their observation that the transfer rate increases as temperature decreases is attributed to the onset of coherent transfer as phonon interactions decrease.

Schmid and Reineker (52) calculated the temperature dependence of ESR lineshapes of triplet excitons in molecular pairs starting from a microscopic model with spin, electronic, and vibrational degrees of freedom included in the Hamiltonian. The Nakajima-Zwanzig projection formalism is used to eliminate the phonon bath from the density operator equation of motion.

Optical experiments and optically detected electron spin coherence

experiments were used by Lewellyn et al. (53) to study direct and indirect energy transfer in isotopically mixed crystals of TCB at low temperature. Transfer was found to be highly sensitive to trap concentration. Predominantly indirect transfer was observed at low trap concentrations; as trap concentration increases the transfer is observed to become direct.

Other experiments have been performed in which the detector molecule or trap is layered on the surface of the crystal. Singlet excitons in crystalline tetracene were studied by Vaubel and Bässler (54). Tetracene crystals were coated with either capriblue or tetraquinone which acted as sinks for the excitons; and fluorescence measurements were made in the temperature range 160 K to 293 K. They found the diffusion length to increase exponentially with decreasing temperature until reaching a constant value below 190 K. Their results are explained in terms of singlet exciton fission. The photosensitized emission from the dye Rhodamine B on the crystal surface in a microfluorimetry experiment designed to study the effect of surface irregularities on the singlet exciton diffusion lengths in anthracene crystals was examined by Cohen et al. (55).

Studies of exciton energy transfer across the molecular crystal-metal interface have also been performed. Studies of energy transfer across crystalline anthracene-metal surfaces have been performed in the Bässler group (56). In a study using gold layer on the crystal surface, it was observed that the quenching rate constant of singlet excitons decreases with increasing distance between the gold and crystal surfaces. Other studies on this topic have been undertaken by Glushko (57) who used a microscopic model to calculate thermal broadening behavior of exciton

luminescence in molecular crystals in contact with a metal. An investigation of the diffusion coefficient and diffusion length of singlet excitons in the c' direction in naphthalene crystals was undertaken by Heisel et al. (58). Their experiment involved a temporal analysis of the singlet exciton annihilation at an aluminum-naphthalene interface.

Time-of-flight methods have been employed by several investigators in the study of exciton-polaritons and energy transfer. Yuan and Rabinovich (59) used a time-of-flight extension of the variable encounter method (VEM) to study vibrational energy transfer at the cyclobutene-silica interface at high temperatures.

Exciton-exciton annihilation rates have been examined (58) in investigations of energy transfer. A time-dependent singlet exciton annihilation rate was observed in polycrystalline thin films of β-hydrogen phthalocyanine (H_2Pc) by Greene and Millard (60) using subpicosecond time-resolved absorption spectroscopy.

Brown et al. (61a) discuss experimental results on the fusion (annihilation) of triplet excitons in isotopically mixed naphthalene crystals. Transfer of energy from trap to supertrap (β-methylnaphthalene, referred to hereafter as βMN) was investigated. They concluded that the results were sensitive to the source of excitation, namely the selective or nonselective excitation of trap; clustering of traps contributes to poor transfer efficiency at medium concentration levels; and temperature independent phosphorescence and delayed fluorescence is observed below 4 K, but above 4 K the temperature dependence is attributed to phonon activation. A later study (61b) employing the master equation for triplet

exciton energy transfer at low temperatures in isotopically doped naphthalene offered arguments favoring Anderson transitions between localized and extended states. Scattering was found to be dominated by optical two-phonon processes.

Studies of energy transfer using percolation and random walk formalisms have been performed extensively by Kopelman and coworkers. Argyrakis and Kopelman (62) and Monberg and Kopelman (63) have considered exciton percolation in isotopic mixed crystals as a means of determining the coherence length. The naphthalene first singlet exciton system was modeled with a nearest neighbor interaction and square lattice topology. The number of sites visited was found as a function of the exciton mean free path (62b,c). Supertraps are utilized as sensors in their time-resolved luminescence experiments. Triplet exciton tunnelling is investigated in reference (63a). Investigations have been extended to discussions of fractal behavior (64). Additional discussions of fractal-like kinetic schemes and related experiments can be found in Kopelman (65) and Kopelman and coworkers (66).

Exciton energy funnels and triplet exciton transport in βMN-doped isotopically mixed crystals of naphthalene are studied by Gentry and Kopelman (67) using time-resolved spectroscopy. A kinetic analysis of trapping and annihilation (67b) and analysis based on the master equation (67c) are presented. Percolation and diffusion are discussed with regard to singlet exciton energy transfer in this same system in reference (68).

βMN-doped isotopically mixed crystals of naphthalene are studied also by Parson and Kopelman (69) using time-resolved spectroscopy. Results

are discussed in terms of percolation and homogeneous energy transport (69a), two-particle CTRW, trapping, and exciton annihilation (69b), two-particle coherent approximation (69c), and a self-consistent diagrammatic approximation (69d,e).

Calculations of ideal percolation thresholds for singlet and triplet excitons have been performed by Colson et al. (70) and have been compared to fluorescence and phosphorescence data obtained for isotopically mixed crystals of benzene in which pyrazine was used as a supertrap. Differences observed between theory and experiment are discussed in terms of the Anderson localization model (71).

Rips and Jortner (72) consider coherence effects in electronic energy transport between randomly distributed donors. Memory effects are explored by working within the framework of the generalized master equation (GME) approach (73). The GME approach is used by Kenkre (74) to study exciton transport in the strong intersite coupling regime; the analysis produces long-range energy transfer rates. Discussions of both the GME approach and the stochastic Liouville equation (SLE) approach, and applications to experimental results are included.

Wong and Kenkre (75a) present sensitized luminescence calculations for various trapping models based on a theoretical formalism for exciton transport based on a Boltzmann-like equation in momentum-space (75b). One surprising result of these calculations is the absence of a $t^{-1/2}$ time-dependence in the energy transfer rate.

Quantum yields were calculated for excitons in molecular crystals by Kenkre and Wong (76) within the framework of the GME approach and

using two different trapping models: the sink model and the substitutional trap model. They found that the exciton diffusion constant could be underestimated if coherence was not taken into account in analyzing quantum yield data. A theoretical approach to exciton trapping valid for arbitrary trap concentrations then was developed by Kenkre (77) using the sink trapping model. Extension of the theory to cover long-range capture processes is presented in Parris and Kenkre (78).

Kenkre and Schmid (79) look at the annihilation constant and energy transfer rate in naphthalene and anthracene crystals. They find lower bounds for the motion rates and diffusion constants, but show that in certain temperature ranges the experimental observables provide little information regarding the motion of excitons. Further discussions of the unsuitability of some experiments to provide useful information about the motion of excitons are provided in Kenkre, Parris and Schmid (80).

Interesting studies of the diffusion coefficient of excitons have been performed using Ronchi rulings or transient grating techniques. Kenkre and Schmid (81) present results of transient grating experiments performed on pure anthracene crystals. Coherence times and mean free paths are calculated for singlet excitons at 1.8 K, 10 K, and 20 K; the mean free path was determined to be $\approx$100 intersite distances at 20 K and $>$1500 intersite distances at 1.8 K, with the latter indicating coherence at low temperatures. Ronchi ruling experiments were used to determine diffusion constants for triplet excitons; these results indicate a loss of coherence within distances of the order of a lattice constant in the temperature range studied ($T>100$ K).

Energy transfer problems also have been studied in systems other than molecular crystals. Semiconductor systems which have been studied extensively and the methods of investigation include: CdS crystals using low temperature spectral- and/or time-resolved luminescence (82,83); CdSe utilizing picosecond energy- and time- resolved luminescence (84); and CuCl using picosecond transient grating techniques (85a) and picosecond induced absorption (85b) at low temperatures. A recent review of some energy transfer processes in semiconductors is given by Klingshirn (86).

Other systems which have been studied include ion impurity sytems such as transition metal and rare earth metal compounds (87,88,89), solid rare gases (90), and charge transfer complexes (91).

Nonlinear Spectroscopy in the Study of Exciton-Polaritons

Nonlinear optics and spectroscopy

The spectroscopy of molecular crystals has been actively pursued for many years. Linear spectroscopic techniques have been reviewed extensively by McClure (92), Wolf (93), and Hochstrasser (94) and will not be discussed in this thesis.

The field of nonlinear spectroscopy has grown rapidly since the introduction of lasers in the early 1960s. Nonlinear behavior was described by Armstrong and coworkers (95) using a semiclassical approach. Since that time, the field has developed tremendously and many review articles have been published on the subject of nonlinear optics and

spectroscopy (96-98). Excellent books which have appeared on the subject include those by Butcher (99) and Bloembergen (100).

The development of lasers, and in particular of tunable dye lasers, has had a tremendous impact on the field of nonlinear spectroscopy because of the generally small cross sections for optical nonlinear processes; lasers provided the necessary high power densities which allowed for the observation of the weak nonlinear effects. In 1961, Franken et al. (101) published results of the first such observation, namely, the observation of second harmonic generation of light from a ruby laser by quartz. Shortly after Kaiser and Garrett (102) first observed two-photon absorption for Eu^{2+} ions in CaF_2. Since then nonlinear optical experiments have been performed by many groups. Because this thesis employs both two-photon fluorescence excitation (TPE) and second harmonic generation (SHG) spectroscopic techniques, special attention is paid to these two areas of nonlinear optics and to the related area of two-photon absorption (TPA).

Two-photon absorption, first predicted by Göppert-Mayer (103) as early as 1931, occurs when two photons are absorbed simultaneously and an excited state is created. Theoretical treatments of this phenomenon can be found in references (104-109), and early experiments on organic crystals were performed by Hopfield and Worlock (110) and Peticolas and Rieckhoff (111).

After tunable dye lasers became available, many experimental groups began to collect two-photon absorption and excitation spectra of various organic molecular compounds, for example, benzene (112,113), naphthalene (113-117), biphenyl (114a), anthracene (118,119),

phenanthrene (120), fluorene (121), diphenylbutadiene (115), and acenaphthene (116).

Second harmonic generation (SHG), the phenomenon whereby a single photon of wavelength λ is transformed into two photons each with wavelength $\lambda/2$, has also been widely investigated. Treatments of some of the theoretical aspects of SHG have been given by Giordmaine (122), Ovander and Petrenko (123), Meredith (124), Bloembergen (125) and others (126-129). SHG spectra have been obtained for naphthalene (117,130,131), anthracene (130), and phenanthrene (120,132). Additional SHG studies include references (133-139), and other types of nonlinear effects which have been investigated theoretically and/or experimentally include three-photon absorption (140), third harmonic generation (141), TPE with application to photochemical (142) and nonphotochemical hole burning (143), four-wave mixing (144-149), surface enchanced nonlinear effects (150-153), and nonlinear effects with optical waveguides (154-156).

Excitons and polaritons

In 1931, Frenkel (157) proposed a theory which described elementary collective electronic excitations in weakly bound molecular solids in terms of the molecular exciton. Davydov (158,159) further developed the theory to apply to organic aromatic crystals. Several monographs and review articles (160-164) have been published on exciton theory and processes and the interested reader is referred to these for details.

Crystal spectra of organic molecular crystal were obtained by many

groups, and special attention was paid to observations of Davydov splitting which was predicted to occur in crystals with more than one molecule per unit cell. Theoretical calculations of the Davydov splitting were done for benzene by Craig and Walmsley (165a) and for benzene and naphthalene by Greer and coworkers (166a). The crystal spectra of naphthalene (165-168), anthracene (169-173), and phenanthrene (174) have all been studied extensively.

Effects of exciton-phonon interactions on the spectra of molecular crystals also has been a widely investigated field. Agranovich and Konobeev (175) applied the Green function method to the problem. Cho and Toyozawa (176) studied the exciton-phonon system in terms of a model consisting of Frenkel excitons and Einstein oscillators. Colson et al. (177) considered exciton-phonon coupling in benzene crystals using the localized exciton sideband method (178). Other studies include those involving exciton-lattice interactions (179), second-order coupling terms (180), structural disorder (181), and Frenkel and Wannier limits (182).

The concept of polaritons was first developed in the 1950s for coupling between the phonon and photon field. Initially, Huang (183) used classical equations of motion to describe phonons in a crystal. These equations of motion then were subjected to Maxwell's equations and phonon-polariton curves were obtained. Later that decade Fano (184) obtained the same results using a quantum mechanical treatment for the phonons. It was Hopfield (185), though, who applied Fano's approach to couple excitons with the quantized radiation field and applied the approach to the problem of exciton absorption. Further contributions to the theory

of exciton-polaritons were made by Pekar (162) and Agranovich (163a,186), Benson and Mills (187), Lang (188), Sumi (189), and Philpott (190). Reviews on the theory of polaritons have been presented by Hopfield (191) and more recently by Johnson and Small (192).

The theory of two-photon absorption by polaritons is discussed by Boggett and Loudon (193). Experimental evidence of polaritons has been obtained by several groups using both linear (194-199) and nonlinear (117,120,131,132,200) techniques. Polariton dispersion curves have been measured by many groups (131c,199,201-205). Detailed discussions of the spectroscopy of excitons can be found in Broude, Rashba, and Sheka (206). Reviews of nonlinear spectroscopy of polaritons (207) and surface polaritons (208) also should be consulted.

As a final note, it should be mentioned that the application of nonlinear optics to the study of the (0,0) a-exciton of pure strain-free naphthalene crystals and the development of polariton fusion theory are detailed in reference (131c).

CHAPTER II. THEORY

A detailed theoretical understanding of the nature of energy transfer processes in crystals, amorphous solids, solutions, and biological systems has been sought for many decades by scientific groups throughout the world. Many methods of energy transfer are known to exist, for example, resonant energy transfer, nonresonant energy transfer, exciton energy transfer, electronic charge transport and energy transfer, and collisional energy transfer (1). However, these processes are not necessarily mutually exclusive.

Electronic energy transfer by exciton-polaritons is the subject of this thesis, and this chapter provides basic details of some of the more prominent theoretical treatments of exciton energy transfer currently being applied to the problem. Also included in this chapter is a brief discussion of polariton fusion theory.

Electronic Energy Transfer

The process of energy transfer in crystals generally is considered to be due to the motion of the exciton. Two classes of excitons can be considered: 1. Frenkel (tight binding) excitons, and 2. Wannier (effective mass) excitons (1). It is the former which is most important in discussions of energy transfer in molecular crystals. The Frenkel exciton can be thought of as a quasiparticle which can occupy a delocalized Bloch state, a localized Wannier state, or any other allowable state (6).

Before presenting descriptions of specific energy transfer theories, a brief discussion of exciton transport limiting behavior must be given. Coherent transport and incoherent transport, band transport and hopping transport are all keywords in energy transfer related literature (2b,5,209) and their meanings are discussed below.

The band model is a description applied to delocalized or extended exciton states (5); in the limit of band transport, the exciton states are characterized by a wavevector $\underline{k}$, and transport between different $\underline{k}$ states occurs via scattering events, such as phonon or defect/impurity scattering (2b,209). In the opposite limit is hopping transport; in this case the exciton states are identified by a site index n, and the phonons or defects scatter these nearly localized states (2b,209).

Diffussive behavior is most commonly described by the quantity called the exciton diffusion coefficient D, which is a description of the rate of relaxation of a nonequilibrium distribution of excitons towards the uniform distribution found at infinite time (2b,209). One definition of the diffusion coefficient is given by (2b,209):

$$D = \frac{1}{2d} \lim_{t\to\infty} \left\{ \frac{\langle R^2(t) \rangle}{t} \right\} = \frac{1}{2d} \lim_{t\to\infty} \left\{ \frac{d\langle R^2(t) \rangle}{dt} \right\} \qquad [1]$$

where d refers to the dimensionality of the system, and $\langle R^2(t) \rangle$ is the mean square displacement of an exciton at time t from its t=0 position. The

mean square displacement can be written as (209):

$$\langle R^2(t) \rangle = \sum_n R_n^2 P_n(t) \qquad [2]$$

where R_n is the distance between site n and the origin, and $P_n(t)$ is the probability that an exciton will be found at site n at time t.

The concept of the diffusion coefficient is important in the discussion of the nature of exciton transport. If the exciton propagates through the crystal in a wavelike manner without scattering by phonons or crystal imperfections, the exciton can be associated with a wavevector $\underline{k}_0$ and the motion is well described by the Schrödinger equation for the system; exciton motion in this limit is termed coherent (1,2b). In this limit, because scattering does not occur, $\langle R^2(t) \rangle$ is not proportional to time and the diffusion coefficient can not be defined (2b,209). Alternatively, if scattering events do occur, the exciton motion becomes incoherent, that is, the exciton distribution loses momory of its initial state and equilibrium is attained in a diffusive manner (2b,209). For this case $\langle R^2(t) \rangle$ is nonzero and the diffusion equation is valid.

Classically, various theoretical treatments have been valid only in one or the other limit, but exciton motion in real crystals generally falls intermediate between these limits, or may display behavior corresponding to the limits of coherent or incoherent motion only under extreme physical conditions, such as very low or very high temperature. Treatments generally used in discussions of incoherent motion include the master equation approach (6), cluster models (5), random and correlated walks (5), and percolation (5). Several of these approaches are discussed briefly in

this chapter.

Several theories have appeared during the past twenty years which allow consideration of both coherent and incoherent behavior of exciton motion. Three such unified theoretical treatments have been chosen for brief discussion in this chapter: 1. the stochastic Liouville equation approach (210,211); 2. the Grover-Silbey polaron-like approach (2,209,212); and 3. the generalized master equation approach (6,213). The first two treatments are discussed together because the resulting equations are quite similar; the latter is discussed separately.

Percolation, random walks, and clusters

Kopelman and coworkers (5,62,63,67) have studied percolation, cluster formation and random walks extensively; many of their results have been applied to the exciton systems of neat and doped naphthalene crystals. Kopelman (5) has reviewed energy transport in mixed crystals and much of the discussion which follows is based on that review and on references therein.

Four types of percolation can be described: classical, lattice, static and dynamic (63a). The following discussion concerns itself with the latter two. Briefly, static percolation as applied to excitons deals with the transition from localized to extended (delocalized) exciton states as concentration of a binary mixed crystal is increased (63a). In this interpretation only nearest neighbor interactions are considered and the excitation lifetime is assumed to be relatively long (63a). In dynamic percolation a cut-off in the interaction time, and therefore, a cut-off in the interaction space, is applied

(5,63a).

In order to explain percolation, and its application to hopping mechanisms, consider a random binary crystal with guest sites labeled A; clusters of guest sites are assumed to exist. In the case for static percolation only nearest neighbor interactions are considered to be directly connected; sites in the cluster also can be connected indirectly through a chain of directly connected sites (5). If the lattice is infinite, there exists a critical concentration C_{cr} such that for a concentration of guest sites $C_A > C_{cr}$ there is one and only one infinite cluster and for $C_A < C_{cr}$ there is no infinite cluster (5). In calculations, the infinite lattice is not strictly feasible and must be approximated by very large finite lattices ($\approx 10^9$ sites (214)). In the limit of the finite lattice and infinite cluster can not exist, but a maxicluster can be defined as one which extends from one edge of the lattice to any other edge (5). Finite clusters which do not meet the above definition of a maxicluster are termed miniclusters. For the large finite lattice, the critical concentration is defined as the concentration above which one maxicluster exists, and below which no maxicluster exists (5). It is important to realize that the finite miniclusters can exist above and below the critical concentration (5). It is clear then that above C_{cr} both extended (delocalized) and localized states can exist, but that below C_{cr} only localized states are found. The percolation transition refers to the transition from localized (hopping) exciton transport to delocalized (bandlike) exciton transport which occurs when the C_{cr} threshold is crossed from below (5).

The assumption of a cut-off in the pair-wise interaction parameter at

some relative coordinate induces a cut-off both in the hopping rate and in the hopping distance. For a given cut-off, only pairs of sites with distances smaller than the cut-off are considered to be directly connected. This is the case for extension to dynamic percolation (5,63). It should be emphasized that hopping can occur on both miniclusters and maxiclusters, but that the exciton created on the maxicluster is free to hop over large distances during its lifetime whereas the exciton located on a minicluster well may be confined to hopping only within its own minicluster cage during its lifetime (5). In light of the above comments, exciton transport would be expected to be more significant above C_{cr}.

Argyrakis and Kopelman (5,62) have performed extensive studies of random walk properties on random binary lattices using Monte Carlo simulations. Behavior is expected to be very different above and below the critical percolation concentration, and Kopelman (5) points out some problems involved in solving random walks for binary random lattices; solutions for concentrations above C_{cr} are emphasized. Kopelman (5) also discusses correlated walks on random lattices; correlated walks allow for directional memory to be retained over a specified number of steps. The number of steps is termed the correlation or coherence parameter (5). Results and discussions are presented in papers by Kopelman (5) and Argyrakis and Kopelman (62) and will not be discussed here.

Stochastic Liouville equation and Grover-Silbey approaches

The first unified treatment of coherent and incoherent exciton motion was given by the stochastic Liouville equation (SLE) approach which was

originated by Haken and Strobl (210a) and which has undergone further development by Haken and Reineker (210b) and Haken and Strobl (50). An extensive review of the SLE formalism by Reineker (211) is replete with references and is recommended to the interested reader. The discussion which follows is based in large part on that review.

Briefly, the SLE approach, as initiated by Haken and Strobl (210a), was based on semistochastic considerations; exciton motion was treated differently for coherent and incoherent limits. The coherent motion was treated by a Hamiltonian and the incoherent motion was treated as a random process. This was developed such that the Hamiltonian contains the excitation energy of the molecules at lattice sites and the transfer matrix elements between them (viz., Coulomb and exchange interaction integrals); this coherent, wavelike motion has an associated phase which decays owing to interactions with intra- and intermolecular vibrations. Fluctuations of the excitation energies and of the transfer matrix elements arising from these vibrations are accounted for in the Hamiltonian by an additional stochastic contribution which is time-dependent. The equation of motion of the exciton density operator is averaged over the fluctuations to yield the SLE. The form of the SLE (1,211,213) is given by:

$$\frac{d\rho_{mn}(t)}{dt} = -i\,[H_0\,,\,\rho]_{mn} - 2\delta_{mn}\sum_k \gamma_{|m-n|}\,(\rho_{mm} - \rho_m) - 2(1-\delta_{mn})\,\Gamma\,\rho_{mn} + 2(1-\delta_{mn})\,\bar{\gamma}_{|m-n|}\,\rho_{mn} \qquad [3]$$

where the ρ's are the density matrix elements, H_0 is the Hamiltonian, the

γ's are transition rates, and Γ is defined by:

$$\Gamma = \sum_{n} \gamma_{|m-n|} \qquad [4]$$

Coherent motion is accounted for in the first term on the right hand side (RHS), that is, by the Hamiltonian. Incoherent motion appears through the second term on the RHS where the transition rate is given by $2\gamma_{|m-n|}$ for sites a distance |m-n| apart. Phonon bath interactions, specifically the destruction of off-diagonal density elements at rates 2Γ and $2\gamma_{|m-n|}$, are taken into account through the last two terms.

The treatment of exciton motion offered by Grover and Silbey (GS) (212) has been reviewed by Silbey (2). Although this approach has a launching point quite different from that of the SLE treatment of Haken, Reineker, and Strobl (50,210), the equation describing the transport is formally the same as that developed by the latter (6). In the GS approach, a canonical transformation of the Hamiltonian is performed to eliminate the linear part of the exciton-phonon coupling and residual terms are treated perturbatively (2,209,212). The microscopic equations of motion for the exciton density are derived and solved. Further extensions and applications of this theory can be found in (209,215,216,217).

Generalized master equation

Energy transfer in real crystal systems generally falls between the limits of coherent and incoherent behavior (1). The importance of formulating a theory of energy transfer which encompasses both coherent and incoherent motion is then readily apparent. The generalized master

equation (GME) approach was developed by Kenkre and Knox (73) in order to unify the treatment of coherent and incoherent exciton motion in a general manner. Sufficient detailed reviews of the GME approach have appeared in the literature (6,213) so that only the basic approach and equations will be presented here.

The starting point of the GME approach (213) is the Von Neumann equation for the density matrix ρ of the exciton and interacting bath (the bath may include phonons, lattice imperfections, etc.):

$$i \frac{d\rho}{dt} = [H,\rho] = L\rho \qquad [5]$$

where L is the Liouville operator and H is the Hamiltonian. The application of the projection operator and its complement to equation [5] yields an equation which differs from the GME by one term, which, for crystals, vanishes for the initial occupation of a delocalized state. The GME then is the probability equation given by:

$$\frac{dP_m(t)}{dt} = \int_0^t dt' \sum_n [\, W_{mn}(t-t')\, P_n(t') - W_{nm}(t-t')\, P_m(t') \,] \qquad [6]$$

where the W(t)'s are the memory functions which inject non-Markoffian (not totally chaotic) nature into the GME. The functional forms of these memory functions depend upon factors such as the interactions in the Hamiltonian and the extent of crossgraining (i.e., the elimination of the bath coordinates). Detailed discussions of the procedure used to determine the

functional forms of the memory function is given in (213) and references therein. The proper choice of $W(t)$ leads to recovery of the solution either for precisely coherent motion (the limit of constant memory: $W(t)=2V^2/\hbar^2$, where V is the exciton energy matrix element), or for completely incoherent motion (the limit of infinitely rapidly decaying memory: $W(t)=F\delta(t)$, where F is the transition or hopping rate, and is proportional to V^2). It is clear then that the GME does present a unified treatment of the problem of energy transfer via coherent and incoherent motion.

It has been pointed out by Kenkre (6,213) that the SLE approach can be interpreted within the framework of the GME approach by the proper choice of the memory function and the neglect of phonon bath interaction term (the term was not neglected in a similar treatment by Reineker and Kühne (218), but novel physical behavior owing to this term has not been observed (213)).

Polariton Fusion Theory

The theoretical development of the polariton model and nonlinear polariton behavior has been presented in detail by Stevenson (131c), and has been reviewed by Johnson and Small (192); therefore only a brief discussion is included in this thesis.

The polariton model was necessitated by the inability of the classical exciton model to address the problem of light absorption in crystals in which the electromagnetic field is strongly coupled to the absorbing medium (185). Classically, Beer's law has been used to describe light

absorption in terms of an exponential decrease of the incoming light beam intensity as it passes through the absorbing medium. The derivation of this law is based on perturbation theory and is valid for media which interact only weakly with the radiation field and for sufficiently weak light intensities. However, crystals are a dense media and the interactions with the field are not sufficiently weak; thus, perturbation theory breaks down.

In 1958, Hopfield (185) pointed out that the semiclassical theory of radiation, which generally had been used successfully for calculating the dielectric constant in frequency regions of no absorption, does not satisfactorily explain optical absorption by excitons. According to the semiclassical approach to absorption, in the absence of scattering processes, within the crystal the energy from the radiation field would simply oscillate between the photon and exciton states, and would eventually exit the crystal as a photon (with its wavevector $\underline{k}$ preserved) without the occurance of absorption. Hopfield (185) goes on to describe the coupling of the exciton and photon states to create mixed exciton-photon states, which he termed polaritons. The one-photon absorption process was described as a two-step process involving the coupling of the photon and exciton to create the polariton, followed by the scattering of the polariton.

The procedure used by Hopfield (185), and later by Agranovich (186), to couple the photons and excitons was the second quantization approach in which the exciton and photon fields are modeled as quantum mechanical harmonic oscillators and Bose creation and annihilation operators are utilized in the Hamiltonian. Derivation is provided in detail in reference (131c,192) and will not be given here; the Hamiltonian for the complete

system is given by:

$$H = H_{ex} + H_{ph} + H_{int} \qquad [7]$$

where H_{ex}, H_{ph}, and H_{int} are the Hamiltonians for the exciton, the photon, and the exciton-photon interaction, respectively. The Hamiltonian for the system of interacting excitons and photons in the second quantization form is:

$$\begin{aligned} H = & \sum_{k\mu} E_{k\mu} B^{+}_{k\mu} B_{k\mu} + \sum_{q,j} \frac{\hbar q c}{n} a^{+}_{q,j} a_{q,j} \\ & + \sum_{q,j,\mu} \{ I(j,-q,\mu)\, a_{q,j} B_{-q\mu} + I(j,q,\mu)\; a^{+}_{q,j} B_{q\mu} \\ & \qquad + I^{*}(j,q,\mu)\, a_{q,j} B^{+}_{q\mu} + I^{*}(j,-q,\mu)\; a^{+}_{q,j} B^{+}_{-q\mu} \} \\ & + \sum_{j} \frac{\hbar \omega_p^2}{4qcn} (a_{q,j} a_{-q,j} + a_{q,j} a^{+}_{q,j} + a^{+}_{q,j} a_{q,j} + a^{+}_{q,j} a^{+}_{-q,j}) \end{aligned} \qquad [8]$$

where the following definitions apply:

$$\omega_p^2 = \frac{4\pi N e^2}{m} \qquad [9]$$

ω_p^2 is the square of the plasma frequency,

N is the number of electrons per unit cell;

B^{+}, B are the Bose delocalized exciton creation and annihilation operators,

a^+, a are the Bose photon creation and annihilation operators,

k, q are the exciton and photon wavevectors,

qj refers to a photon of polarization j transverse to q,

μ refers to the exciton branch, and

$$I(j,q,\mu) = ie\left[\frac{2\pi}{qVcn\hbar}\right]^{1/2} \sum_{\alpha} D_{\alpha j}^{f0} \left[U_{\alpha\mu}(q) + V_{\alpha\mu}(q)\right] E_{q\mu} \qquad [10]$$

$D_{\alpha j}^{f0}$ is the transition dipole between states $|0\rangle$ and $\langle f|$
at polarization j and site α,

U,V are Tyablikov coefficients, and

V is the unit cell volume.

The polariton creation and annihilation operators, $\xi_\rho^+(k)$ and $\xi_\rho(k)$, for polaritons with wavevector k and on branch ρ are used in the transformation of the Hamiltonian in equation [8] to one of the form:

$$H = \sum_{\rho k} E_\rho(k)\, \xi_\rho^+(k)\, \xi_\rho(k) \qquad [11]$$

via the Tyablikov diagonalization method (192).

The polariton energies can be obtained then, and for the simple case where only one exciton level is important, the energies are given by:

$$E_{\rho jk}^2 = \frac{\hbar^2 k^2 c^2}{n^2} + (2-j)\frac{\omega_\rho^2}{n^2}\left[\frac{E_{\rho jk}^2}{E_{\rho jk}^2 - E_{\mu k}^2}\right] F_\mu \sin^2\phi \qquad [12]$$

where ϕ is the angle between the transition dipole and the wavevector $\underline{k}$. Polarization j-2 represents the case for photons not coupled with the exciton. The solutions to equation [12] are identical to solutions using the semiclassical approach:

$$\omega^4 - \omega^2\left[\frac{c^2k^2}{\epsilon_0} + \omega_0^2 + \frac{\omega_p^2 F}{\epsilon_0}\right] + \frac{\omega_0^2 c^2 k^2}{\epsilon_0} = 0 \qquad [13]$$

where ω_0 is the transverse exciton frequency and ϵ_0 is the dielectric constant. However, a distinction between the second quantization (polariton) approach and the semiclassical approach is seen with the introduction of damping, which occurs in the polariton model through a complex dielectric constant:

$$\epsilon_0 = \frac{c^2k^2}{\omega^2} \qquad [14]$$

When $\underline{k}$ is complex and ω is real, the result is spatial damping; when $\underline{k}$ is real and ω is complex, temporal damping occurs. The damping affects the dispersion of the polariton. It should be noted that damping occurs in the semiclassical model also, but it occurs as temporal damping of the uncoupled exciton, whereas in the polariton model the excitonic character of the polariton is responsible for the damping but it is the polariton state which is damped (131c). Discussion of the calculation of the temporally damped polariton dispersion curves for the 31475 cm^{-1} $\underline{a}$-exciton of

naphthalene is presented in detail by Stevenson (131c).

Nonlinear optical effects can be obtained in the framework of the polariton model by expanding the exciton and interaction Hamiltonians to higher orders than expressed in equation [8]. For details on the procedure the reader is referred to references (131c,192,219).

The importance of this expansion is related to the terms of the third order Hamiltonian which describe the annihilation of two polaritons and the creation of a third; this process is known as "polariton fusion" (201b) and is related to second harmonic generation (SHG). Additionally, the two-photon absorption (TPA) or two-photon fluorescence excitation (TPE) can be thought of as being due to scattering of fused polaritons. The two processes then compete with each other for signal intensity as the scatterers, eg. phonons or crystal imperfections, is increased. The relationship between the SHG and TPE signal intensities has been worked out in detail by Stevenson (131c) and only the resulting equations for the intensities are given here:

$$I_{SHG} = \frac{v_g}{\gamma L}\left[1 - \exp\left(\frac{\gamma L}{v_g}\right)\right] \qquad [15a]$$

$$I_{TPE} = 1 - \frac{v_g}{\gamma L}\left[1 - \exp\left(\frac{\gamma L}{v_g}\right)\right] = 1 - I_{SHG} \qquad [15b]$$

where v_g is the polariton group velocity, L is the crystal thickness, and γ is the damping frequency.

The purpose of this thesis is to demonstrate experimentally the existence of coherent electronic energy transfer in doped strain-free mounted (DSF) single crystals of naphthalene at liquid helium temperatures via well-defined directional polaritons in the region of the lowest frequency zero-phonon singlet exciton. The energy transfer was probed using the techniques of two-photon fluorescence excitation and second harmonic generation. The temperature behavior and dispersion of the TPE and SHG signals were also studied and compared to results obtained by Stevenson (131), and will be discussed in detail in Chapter IV.

CHAPTER III. EXPERIMENTAL

Sample Preparation and Analysis

Aldrich Chemical naphthalene (98% purity) was further purified by sodium fusion reaction for several hours at 110°C under a nitrogen atmosphere of ≈50 mm Hg to remove β-methylnaphthalene. The reacted material subsequently was zone-refined a minimum of 110 passes. The anthracene was used as received from Aldrich Chemical.

All crystals were grown by sublimation; the apparatus, depicted in Figure 1, was a modified sublimator equipped with an inverted copper collection bell and has been described in detail elsewhere (131c). A mixture of 1-2 x 10^{-5} mole anthracene to mole naphthalene was ground thoroughly and was placed in the bottom of the sublimator, which then was flushed repeatedly with dry nitrogen before closing off the apparatus under ≈600 mm Hg of nitrogen. The sublimator was wrapped with a short length of heating tape and was placed in an oil bath kept at ≈75°C for several hours. The sublimation flakes generally were shaped like a slightly elongated diamond and exhibited a sharp twinning line which ran from the vertex attached to the sublimation bell to the opposite vertex. These crystals were examined coniscopically, using a Leitz Ortholux-Pol polarizing microscope, and were judged to be ab-face crystals.

The crystals were aligned in a strain-free sample holder, shown in Figure 2 (the design of which is discussed fully in reference (131c)), such that the b-axis was parallel to the sample rod and was the axis of rotation

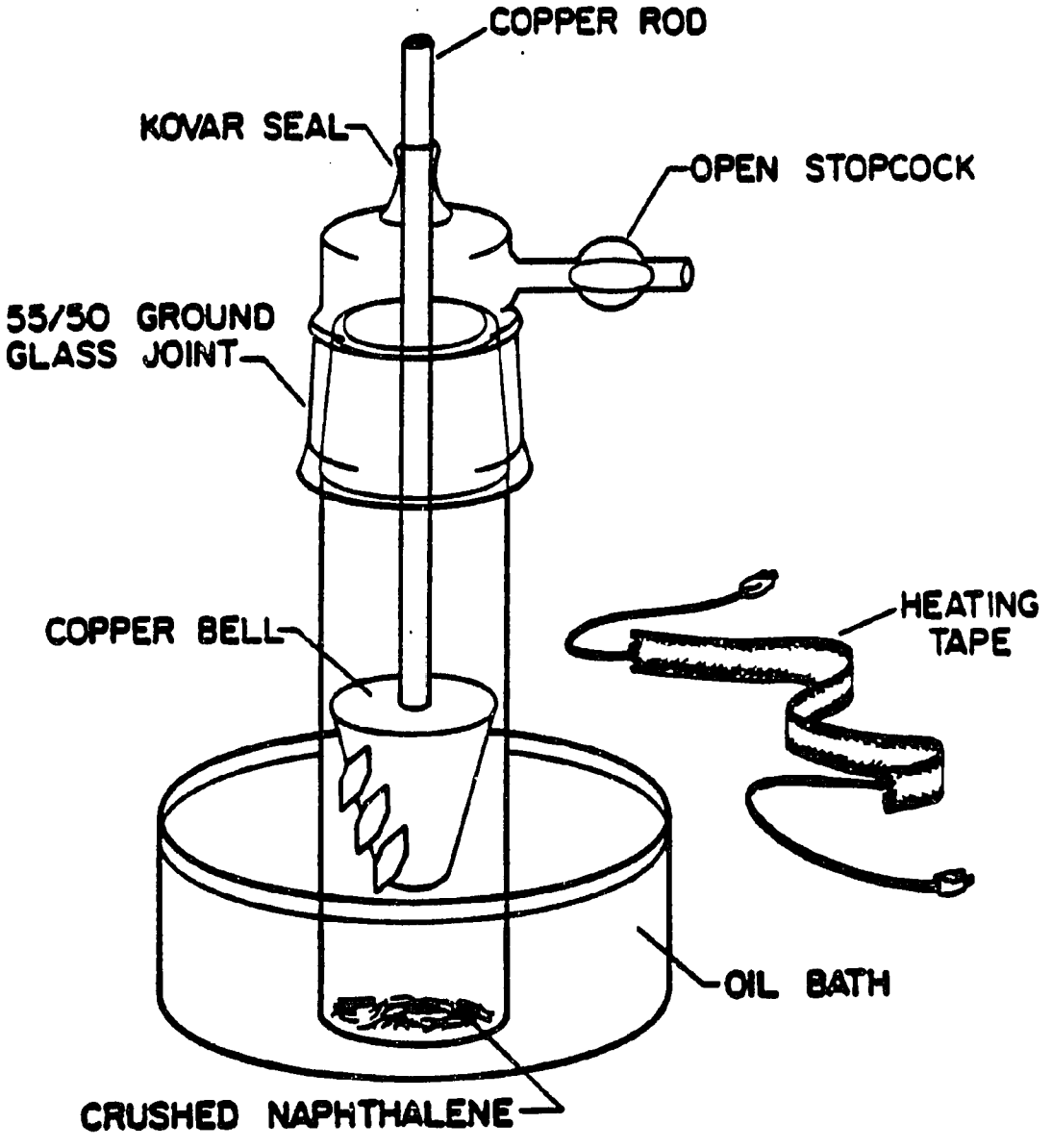

Figure 1. Modified sublimator for growing single crystals

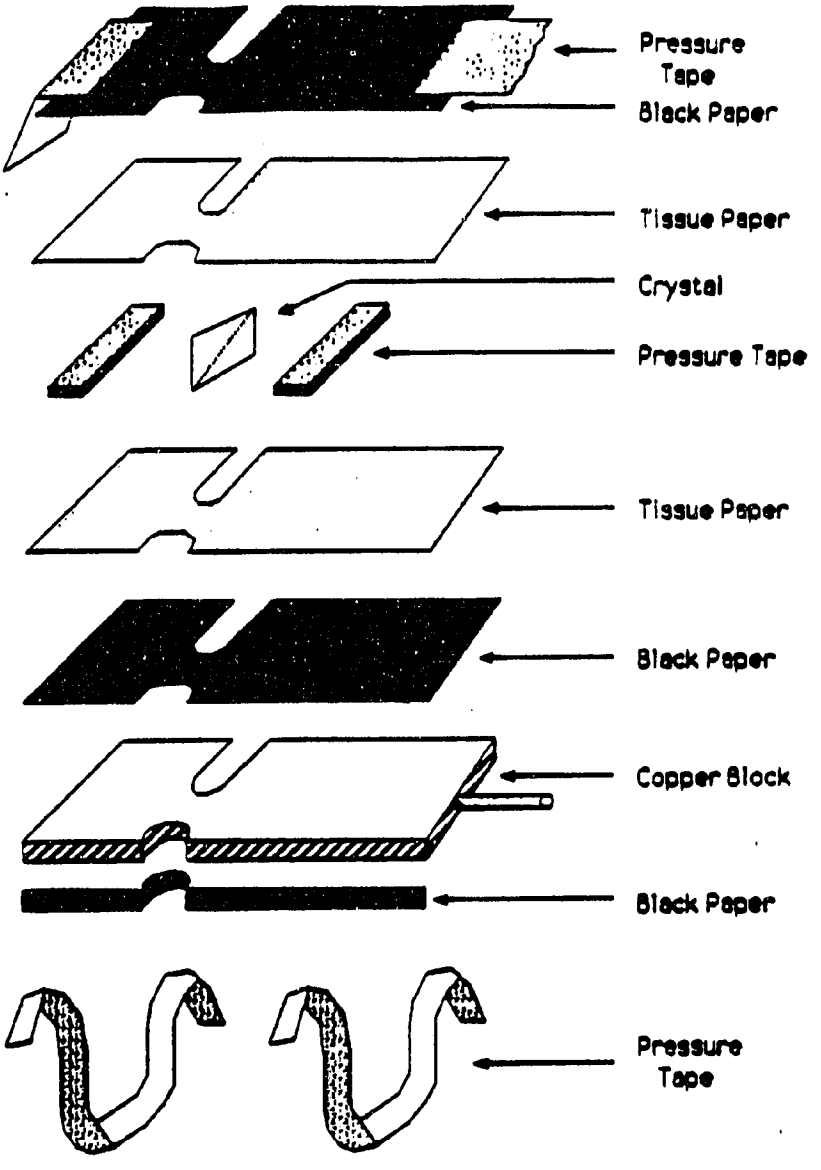

Figure 2. Strain-free sample holder

for experiments. Crystals were mounted such that the twinning line was positioned away from the slot through which the laser beam passed; the twinning line was essentially parallel to the a-axis brush and the sample holder slot. Crystals which under coniscopic examination exhibited surface striations or any other obvious surface flaws were rejected for use in these experiments. All coniscopic examinations and alignment and mounting procedures were performed with equipment and crystals placed inside an upright freezer with modified door, T ≈ 5°C.

Cryoscopic temperatures were attained using a Janis 8DT "Supervaritemp" stainless steel optical dewar. Temperatures of ≈4.2 K and above were obtained by controlling the flow of liquid helium or cold helium gas between a reservoir and sample chamber. Lower temperatures (≈1.6 K to 5 K) were reached by using a large capacity vacuum pump to pump on liquid helium in the sample chamber while varying the helium flow rate and pumping rate. The temperature was measured with a Lakeshore Cryotronics DT-500K silicon diode calibrated for use between 1.4 K and 100 K. The diode was held in intimate contact with the sample holder at the same level as the crystal. The temperature was monitored using either a Lakeshore Cryotronics DTC-500 Cryogenic Temperature Controller or a homemade constant current box (220) in conjunction with a voltmeter with digital readout.

Crystal thickness was measured with micrometers. Ten to twenty measurements were made of the thickness of two glass microscope slides held together and then the crystal was placed between the slides and the

measurements repeated. The measurements were good to within ±3 μ.

The concentration of each crystal was determined by scraping the residual crystals from the crystal collection bell, dissolving these in benzene, and running the uv-visible absorption spectra of the sample solutions and standard solutions.

Laser System and Optics

The configuration of the laser system and optics used in these experiments is shown schematically in Figure 3. The frequency doubled output (532 nm) of an actively Q-switched Nd:YAG laser (Quantel YAG 480) was used to pump a tunable dye laser (Quantel TDL-III). The average power at 532 nm was ≈800-850 mW with a pulse width of 8 ns; the output of the dye laser typically was attenuated to give an average power of ≈1 mW. The linewidth of the dye laser was ≈0.14 cm^{-1}, measured using a 30 GHz spectrum analyzer (221). The laser dye system was Exciton DCM dye dissolved in methanol to give optimum lasing in the wavelength region of interest (≈6350Å - 6355Å).

The configuration of optics is similar to that described elsewhere (131c). Briefly, the polarized dye laser output was rotated to vertical polarization by means of two beam steering prisms, was then passed through a NRC variable beam attenuator or through neutral density filters to attain the desired power, measured with a Laser Precision energy meter (model Rj7100). The attenuated beam was then split using a glass wedge beam splitter. One of the beams then was focused loosely onto the sample

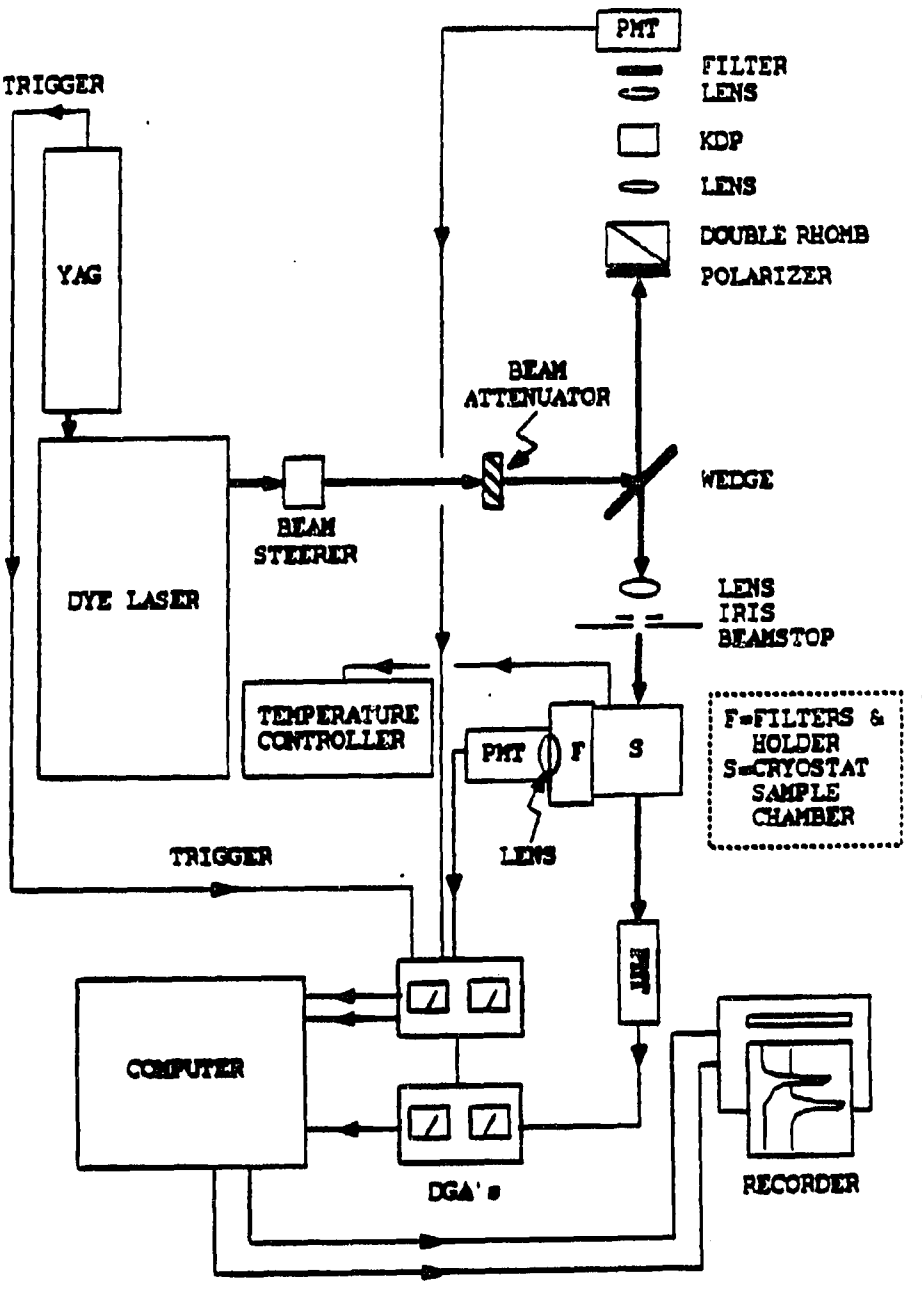

Figure 3. Schematic of experimental apparatus

with a 50 cm lens. An iris diaphragm generally was placed between the lens and sample to eliminate any stray reflections.

Second harmonic generation (SHG) was detected collinearly with an Amperex 56DVP photomultiplier tube in a Products For Research type "B" fast response base, filtered by a Schott UG-11 filter and a Corion 3200Å interference filter to remove fundamental excitation. SHG was detected ≈0.4 m from the sample to reduce the probability of detection of the incoherent two-photon emission signal. The two-photon fluorescence excitation (TPE) signal was detected 90° to the incident beam with an Amperex XP2232B photomultiplier tube in a Products For Research type "B" base. A filter holder was attached to the PMT housing and placed as close as possible to the sample. A Schott UG-11 filter was used to filter out the anthracene emission while passing the naphthalene signal. A combination of three filters, Hoya B-390, Corning C5-5-56, and 3-757 (source unknown), were used to filter the naphthalene emission while passing the anthracene signal.

A beamstop placed between the sample and lens was marked to show retroreflected laser beam spots between ≈-10° and +10°. These spots enabled reproducible angle-tuning of the crystal and helped to establish the proper positioning of the angle tuning rod for normal incidence.

The laser beam split off by the glass wedge was used as the normalizing reference beam. The beam was passed through a double Fresnel rhomb to rotate polarization and then was focussed onto a Lasermetrics KDP frequency-doubling crystal by a 10 cm focal length lens. The frequency-doubled beam was focused onto a RCA 1P28

photomultiplier tube filtered by a Schott UG-11 filter and a Molectron TF interference filter.

Data Acquisition and Control

Two Quanta-Ray Dual Gated Amplifiers (DGAs) were used to collect the two-photon fluorescence excitation, second harmonic generation, and reference signals. Gates of ≈50 μs were triggered by a pulse from the Nd:YAG laser.

Control and monitoring of the experiments and data acquisition and storage was accomplished by the program QLSCAN (222) run on a Digital Equipment Corporation LSI-11/03 computer. All information was saved on 8" floppy disks for later processing and analysis. The analog output was sent to a dual-pen stripchart recorder (either a Heathkit model SR206 or Houston Instruments model 4523).

Two methods were used to measure integrated peak intensities. The first of these was the cut and weigh method described in detail in reference (131c).

The second method used a computer graphics program GPLOT (222) to plot and integrate each signal profile. Using this program, each peak profile was plotted, with optional smoothing and two points selected by the program operator determined the baseline for each scan. The peak profile, then, was integrated using a simple Simpson's approximation method.

CHAPTER IV. RESULTS AND DISCUSSION

Electronic Energy Transfer

This section presents new and significant results and discussion of electronic energy transfer (EET) data obtained for anthracene doped, strain-free mounted (DSF) naphthalene single crystals in the concentration range of 4×10^{-6} to 7×10^{-6} mole/mole. Two-photon fluorescence excitation (TPE) and second harmonic generation (SHG) were used as the probe techniques under the following sets of conditions:

1. temperatures T≈1.6 K and T≈20-25 K;
2. excitation of the ac-polarized zero-phonon naphthalene exciton at ≈31475 cm^{-1} and excitation of the associated ≈131 cm^{-1} vibronic band;
3. angles of orientation with respect to the c'-axis which correspond to mapping onto the lower branch of the polariton dispersion curve: Θ_{ext} = +10°, +15°, +20°, +25°, +30°.

Additionally, full temperature studies (≈1.6 K to 25 K) were performed at set angles of orientation, and full dispersion studies (Θ_{ext} ≈ -40° to +40°) were performed at set temperatures. Power dependence studies were done to eliminate concern regarding possible power broadening of the signals. Results of these investigations will be discussed in turn in the following subsections.

Coherent and incoherent transfer

If coherent EET is to occur in the system of interest (i.e., anthracene-doped naphthalene crystals), it is likely to occur at low temperatures (T≈0 K) where competition from polariton-phonon scattering is at a minimum. In this case, any fluorescence due to anthracene would be a direct result of coherent EET. At higher temperatures where polariton-phonon scattering becomes increasingly important, thermalized excitons are produced, thereby lessening the opportunity for direct trapping of the polariton (see Figure 4). This effect, thus, would be manifested as an increase in the naphthalene-to- anthracene fluorescence ratio with increasing temperature.

Table I presents the results of studies performed on a 30 μ DSF naphthalene crystal at the lower limit temperature, T≈1.6 K, and at the upper limit temperature, T≈25 K, for several different polariton velocities, and for excitation into the zero-phonon band and the 311 cm^{-1} vibronic band. The important observations to be discussed in turn are:

1. coherent excitation (zero-phonon band)-high temperature (≈20-25 K) naphthalene-to-anthracene TPE intensity ratios (labeled $(I_N/I_A)_{CH}$) are the same as the incoherent excitation (vibronic band)-high temperature ratios (labeled $(I_N/I_A)_{IH}$);
2. incoherent excitation-low temperature (1.6 K) (labeled $(I_N/I_A)_{IL}$) and incoherent excitation-high temperature intensity ratios are equivalent;
3. coherent excitation-low temperature intensity ratios (labeled $(I_N/I_A)_{CL}$) are less than the coherent excitation-high temperature

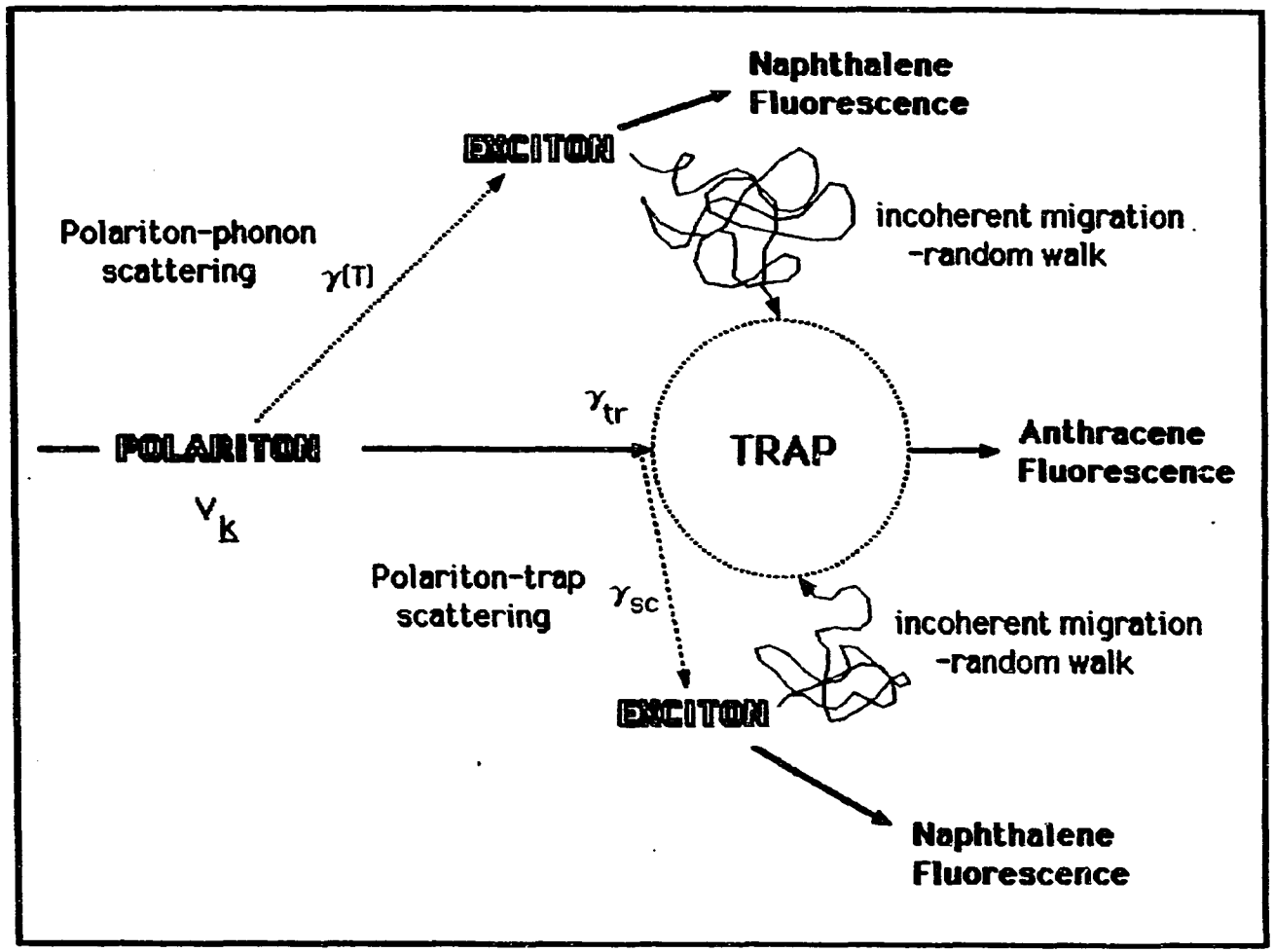

Figure 4. Model for polariton scattering processes

Table I. Naphthalene-to-anthracene TPE intensity ratios for a 30 μ DSF crystal[a]

θ_{ext}	Polariton velocity ($cm\text{-}sec^{-1}$)	$(I_N/I_A)_{CL}$[b]	$(I_N/I_A)_{CH}$[c]	$(I_N/I_A)_{IL}$[d]	$(I_N/I_A)_{IH}$[e]
+10°	2.6×10^7	1.3	1.5	1.5	1.5
+15°	1.4×10^7	1.2	1.6	1.4	1.5
+20°	9.2×10^6	1.2	1.6	1.6	1.5
+25°	7.1×10^6	1.2	1.6	1.5	1.6
+30°	6.0×10^6	1.2	1.7	1.5	1.7

[a] Concentration $\approx 7 \times 10^{-6}$ mole/mole anthracene/naphthalene.

[b] Naphthalene-to-anthracene TPE intensity ratio, coherent (zero-phonon band) excitation, T = 1.6 K.

[c] Naphthalene-to-anthracene TPE intensity ratio, coherent (zero-phonon band) excitation, T = 20 K.

[d] Naphthalene-to-anthracene TPE intensity ratio, incoherent (311 cm^{-1} vibronic band) excitation, T = 1.6 K.

[e] Naphthalene-to-anthracene TPE intensity ratio, coherent (311 cm^{-1} vibronic band) excitation, T = 20 K.

intensity ratios;

4. the intensity ratios are consistent for all values of Θ_{ext} within each category of excitation type and temperature.

These points will be discussed in terms of the model shown schematically in Figure 4, in which $\gamma(T)$ is the temperature dependent polariton-phonon scattering frequency, γ_{so} is the polariton-trap scattering frequency, and γ_{tr} is the polariton trapping frequency. In this model, anthracene exhibits fluorescence only if trapping occurs; naphthalene fluorescence can occur following the formation of a thermalized exciton via polariton-phonon scattering or following the formation of an exciton (or a slower, different $\underline{k}$-sense polariton) via polariton-trap scattering. A polariton can be trapped directly, that is coherently, or the exciton can be trapped subsequent to a random walk, or some other incoherent type of migration.

Consider point 1 above. Values for $\gamma(T)$ have been calculated previously (223) for naphthalene, and from these calculations it has been determined that $\gamma(20\ K) \approx 10^{14}\ sec^{-1}$. The trapping frequency, γ_{tr}, can be taken to be approximately equal to γ_0 (the temperature independent contribution to the damping constant due to the presence of the anthracene impurity), and in this investigation γ_0 has been determined to be $\approx 3 \times 10^{10}\ sec^{-1}$ from TPE and SHG temperature studies (vide infra) of the anthracene-doped naphthalene system. In the above case, with $\gamma(T) \gg \gamma_{tr}$, polariton-phonon scattering is more probable than direct trapping of the coherent polariton. The coherence lengths (vide infra), l_{coh}, at 20 K are expected to be ≈6-26 Å for the angles $\Theta_{ext} = +30°$ to $+10°$, respectively. The average

host-trap separation (vide infra), $\langle R \rangle$, for the concentrations studied is $\approx 2 \times 10^4$ Å. Therefore, the coherence length at 20 K is much smaller than the average separation ($l_{coh}(20\ K) \ll \langle R \rangle$), and it is expected that at 20 K the energy transfer will be incoherent even for excitation of the zero-phonon band. This behavior indeed is observed, since the ratio $(I_N / I_A)_{CH} = (I_N / I_A)_{IH}$ as seen in Table I. The fact that these values agree in the high temperature regime provides a rigorous check on the experimental procedure used in this investigation.

The second observation, i.e., that the incoherent excitation yields equivalent intensity ratios for both the high and the low temperature regimes, is not a surprising one. Experiments performed by Schmid (224) show that, for incoherent exciton migration in naphthalene, the energy transfer is capture-limited; that is, the actual capture or trapping event occurs on a timescale which is long compared to the timescale of the migration of the exciton to the trap site. Therefore, for this situation the trapping event is the rate determining step, and information regarding the motion of the exciton within the host crystal is lost. Since the trapping event should be temperature independent, the results from incoherent excitation should be temperature independent, as indeed is observed.

The situation changes significantly for the case of coherent excitation at low temperature. If coherent EET actually occurs at low temperature, then the ratio of naphthalene to anthracene fluorescence should differ from the ratio obtained for coherent excitation at high temperature. Recall that at high temperature ($\approx$20 K), $l_{coh} \ll \langle R \rangle$ (vide supra); however, at low temperature ($\approx$1.6 K), the coherence length, l_{coh}, is $\approx 2 \times 10^4$ Å to 9×10^4 Å

for the external angles, Θ_{ext} = +30° to +10° (vide infra), so the coherence length at 1.6 K is greater than or equal to the average host-trap separation (l_{coh}(1.6 K) ≥ ⟨R⟩), and thus coherent transfer is expected to occur. Also, from reference (223), γ(2 K) is found to be ≈ 1.26 sec^{-1}, and, therefore, $\gamma(2\ K) \ll \gamma_0$, so that polariton-phonon scattering will not be a major concern at low temperatures. For the case when $\gamma(2\ K) \ll \gamma_0$, then, one expects a decrease in the naphthalene to anthracene fluorescence ratio from that in the high temperature regime, and, as shown in Table I, it is observed that $(I_N/I_A)_{CL}$ is definitely less than $(I_N/I_A)_{CH}$.

Coherence length

For the pure crystal and donor exciton migration, an exciton may move with a well-defined group velocity, v_k, over some distance before losing memory of its velocity. The distance traveled is referred to as the coherence length (33). The memory of the velocity can be lost due to scattering events with phonons or lattice imperfections which occur at a rate γ. The coherence length l_{coh} can be given then by:

$$l_{coh} = \frac{v_k}{\gamma} \qquad [16]$$

Coherent migration generally is considered to occur for the case for which the coherence length, l_{coh}, is greater than the lattice spacing, a. (33). Therefore, the magnitude of l_{coh} gives a measure of the extent of coherent migration of the polariton in the crystal.

In previous studies (131) of pure strain-free (PSF) naphthalene

crystals, the low temperature value for polariton damping was determined to be dominated by the temperature independent (i.e., residual) value of $\gamma_0 = 3\text{-}4 \times 10^9$ sec^{-1}. If this value of γ_0 ($\approx\gamma$(T=0 K)) is taken to be the lowest possible value for damping in the naphthalene 31475 cm^{-1} a-exciton system, then the coherence length for an exciton at absolute zero, l_{coh} (exc, 0 K), is ≈ 250-300 Å, assuming a typical value for the naked exciton (that is, one with little or no photon character) group velocity, $v_{ex} \sim 10^4$ cm-sec^{-1}. This velocity corresponds to a coherence length (vide infra) on the order of 30 unit cell lengths, so clearly this is within the realm of coherent migration. Consider next a so-called "dressed" polariton (i.e., one with a good amount of photon character) with a typical group velocity, $v_{pol} \sim 10^7$ cm-sec^{-1}; the coherence length becomes l_{coh}(pol, 0 K) $\approx 2.5\text{-}3.0 \times 10^5$ Å, or 25-30 μ, a value which is equivalent to the crystal thickness typically used in these experiments. It is clear, therefore, that the addition of photon-like character to an otherwise "sluggish" exciton greatly enhances the exciton migration coherence length.

In the previous section, it was pointed out that at high temperatures, for example, T= 20 K, the temperature dependent polariton-phonon scattering frequency, γ(T), becomes much larger than the temperature independent contribution to the scattering frequency, γ_0. This, of course, significantly affects the coherence length, l_{coh}. The coherence lengths are expected to be approximately 6 Å and 26 Å at a temperature T = 20 K, for $\Theta_{ext} = +30°$($v_{pol} = 6.0 \times 10^6$ cm-sec^{-1}) and +10° ($v_{pol} = 2.6 \times 10^7$ cm-sec^{-1}), respectively. Such short coherence lengths indicate, as mentioned above, that the energy is expected to be incoherent at high temperatures.

Table II. Summary of coherence lengths calculated for several velocities and temperatures[a]

Θ_{ext}	Polariton (exciton) velocity (cm-sec^{-1})	Temperature (K)	γ (sec^{-1})[b]	l_{coh} (Å)[c]
+5°	9.0×10^7	1.6	4×10^9	2×10^6
+10°	2.6×10^7	1.6	4×10^9	7×10^5
+30°	6.0×10^6	1.6	4×10^9	2×10^5
-30°	1.2×10^6	1.6	4×10^9	3×10^4
+5°	9.0×10^7	20	1×10^{14}	90
+10°	2.6×10^7	20	1×10^{14}	26
+30°	6.0×10^6	20	1×10^{14}	6
-30°	1.2×10^6	20	1×10^{14}	1.2

[a] Calculated from equation [16].

[b] Scattering frequency.

[c] Coherence length.

Coherence lengths for several angles (i.e., velocities) and temperatures, calculated using equation [16], are tabulated in Table II.

In this study, the major concern lies with the existence of coherent donor to trap electronic energy transport (EET) in anthracene-doped strain-free mounted (DSF) crystals of naphthalene. Figure 4 provides a schematic of several possible fates of a polariton prepared in these experiments. In this investigation, what is meant by EET is that an polariton with a well defined $\underline{k}$-sense is prepared and that the phase memory of this polariton is maintained until the polariton is scattered by the trap and trapping actually occurs. There is, of course, the possibility that the polariton can be scattered by the trap but that trapping does not occur, and instead, that a thermalized exciton with no phase memory is formed. Thus, in the above scenario for trapping there are two competing processes each with their own damping frequency: 1) scattering with the trap followed by trapping, γ_{tr}; 2) scattering with the trap followed by formation of a thermalized exciton, γ_{sc}. The damping frequency associated with the trap is the sum of these two contributions:

$$\gamma\,(\text{trap}) = \gamma_{so} + \gamma_{tr} \qquad [17]$$

It is clear that coherent EET corresponds to the case where:

$$\gamma_{tr} \gg \gamma_{so} \qquad [18]$$

and it is reasonable to assert that if:

$$\gamma_{so} \gg \gamma_{tr} \qquad [19]$$

then coherent EET will not occur to any appreciable extent.

Migration time vs. trapping time

It is clear that there is a difference between the migration time and the trapping time for the polariton. First, define <R> as the average host-trap separation distance, and then ask the question "how long does it take for the polariton to travel from a host (naphthalene) molecule to a trap (anthracene) molecule?". Clearly this is given by $\langle R \rangle / v_k$; the time it takes for the polariton to become trapped is given by γ_{tr}^{-1}. Then in the case where:

$$\left[\frac{v_k}{\langle R \rangle}\right]^{-1} < \gamma_{tr}^{-1} \qquad [20]$$

the actual trapping is slow compared to the migration of the polariton from host to trap; thus, trapping is the rate determining step. The migration time given above, of course, is the coherent migration time. But it is also obvious from Figure 4 that a thermalized exciton can reach the trap via incoherent migration. This type of migration becomes very important at higher temperatures.

Capture limited regime vs. migration limited regime

The difference between migration time and trapping time was discussed briefly in the previous section. The situation given by equation [20] corresponds to a capture limited regime, i.e., the trapping (capture) is the rate determining step. The opposite situation, then, corresponds to the migration (motion) limited regime, i.e., the excitation migration occurs on a timescale, which is long compared to the trapping event, and, therefore, is the rate determining step. These two limiting regimes, and their applicability to the results of the present investigation, are discussed in this subsection.

The first approach corresponds to the migration limited regime (vide infra). Consider the expression for the number of scattering events of a polariton with traps per unit time (given by equation [17]):

$$\gamma\,(\text{trap}) \;=\; \gamma_T \;=\; \gamma_{so} \;+\; \gamma_{tr} \qquad [21]$$

where γ_{so} and γ_{tr} are as defined in an earlier section, and γ_T, the total polariton-trap damping frequency, is given by:

$$\gamma_T \;=\; R_{enc} \times P \qquad [22]$$

where R_{enc} is defined as the number of encounters of the polariton with a trap per unit time, and P is the probability of a scattering event per encounter. This probability can be thought of in terms of a probability of a scattering event per unit time, ρ, multiplied by an encounter time or

duration, τ_{enc}, so that:

$$\gamma_T = R_{enc} \times \rho \times \tau_{enc} \qquad [23]$$

The probability of a scattering or a trapping event per unit time is unity, provided that the polariton lies within the scattering or trapping cross section, σ_{sc} or σ_{tr}, respectively. So that under this restriction:

$$\gamma_T = R_{enc} \qquad [24]$$

An expression for R_{enc} can be obtained by an analogy with induced absorption rate. For the induced absorption rate, the rate of absorption, R_{abs}, is obtained from the product of the photon flux and an absorption cross section. The photon flux is given by the photon energy density times the speed of light. For the above situation, the photons are moving and the absorbers are stationary. The polariton-trap situation can be thought of in similar terms, although in this case it is somewhat easier to think in terms of a "trap flux", that is, to consider the polaritons to be stationary, and the traps to be moving at the polariton velocity. This scenario yields, for the rate of encounters:

$$\begin{aligned} R_{enc} &= \text{trap flux} \times \text{event cross section} \\ &= \phi_T \times \sigma_T \end{aligned} \qquad [25]$$

where

$$\phi_T = n_T \times v_{pol} \qquad [26]$$

and n_T is the number density of traps. Therefore,

$$R_{enc} = n_T \times v_{pol} \times \sigma_T \qquad [27]$$

Also, since $R_{enc} = \gamma_T$, one can write:

$$R_{enc} = \frac{v_{pol}}{\langle R \rangle} \qquad [28]$$

where ‹R› is the average host-trap separation. An expression for ‹R› can be obtained readily following the mathematical approach of Chandrasekhar (225) by modifying his approach to account for a cylindrical model rather than a spherical model. In this picture a polariton wavepacket will be scattered within a radius **a** of the impurity. Therefore, the polariton can be thought to sweep out a cylinder of radius **a** and length ‹R›. The probability that the impurity-impurity nearest neighbor lies between r and r+dr, where r is measured relative to an impurity placed at the origin, is given by $\omega(r)dr$ (following the terminology in reference (225)). If one thinks of the rest of the cylinder being filled with host molecules, it becomes obvious that $\omega(r)dr$ is also the probability that with a host at the origin, a nearest

neighbor impurity lies between r and r+dr. One can write, then:

$$\omega(r)\,dr = \left[1 - \int_0^r \omega(r')\,dr' \right] \times \eta_r \qquad [29]$$

where η_r is th number of impurities in the region between r and r+dr. For the cylinder model:

$$\omega(r)\,dr = \left[1 - \int_0^r \omega(r')\,dr' \right] \pi a^2 n_T \qquad [30]$$

and

$$\frac{d\omega(r)}{d(\pi a^2 n_T r)} = -n_T \pi a^2 \frac{\omega(r)}{n_T \pi a^2} \qquad [31]$$

so that

$$\omega(r) = n_T \pi a^2 \exp[-\pi a^2 n_T r] \qquad [32]$$

Using this function in equation [30] yields:

$$< R > = \int_0^\infty r\,\omega(r)\,dr = \frac{1}{\pi a^2 n_T} \qquad [33]$$

Returning to equation [28], the number of encounters of the polariton with a trap per unit time becomes:

$$R_{enc} = \frac{v_{pol}}{< R >} = v_{pol} \pi a^2 n_T = \gamma_T \qquad [34]$$

Equation [34] is recognized as being the same as equation [27] with $\sigma_T = \pi a^2$. This cross section, σ_T, and therefore, the radius, a, is a constant for a given chemical system. Consequently, one concludes that R_{enc} or γ_T must be dependent upon the polariton velocity. This looks similar to the Smoluchowski result for the energy transfer rate (see reference (78)) which is given by:

$$k = \frac{4 \pi \rho R D}{V} \qquad [35]$$

where k is the energy transfer rate, ρ is the mole-mole trap concentration, R is a capture radius, V is the unit cell volume, and D is the exciton diffusion constant. The number density of traps, n_T, in equation [34] is equivalent to ρ/V in equation [35], and the radius a in equation [34] is proportional to the radius, R, in equation [35]. The polariton velocity, v_{pol}, in equation [34] has the diffusion constant, D, as its counterpart in equation [35]. Equation [34], then, corresponds to the migration (or diffusion) limited regime.

The conclusion, then, that the scattering or trapping frequency is polariton velocity dependent, is contrary to what has been understood

previously (131). In studies of PSF naphthalene crystals (131c), the value of the scattering frequency, γ_0 (obtained experimentally by fitting TPE and SHG data) was found to be independent of the polariton velocity for crystals ≥ 27 μ (although the theoretical fits were less than satisfactory for thin crystals, eg., the 12.5 μ and 5 μ crystals, and for angles of orientation < |10°|). This lack of dependence on the polariton velocity, which was varied by approximately 3 orders of magnitude in those experiments (131c), suggests that the capture limited regime is appropriate for this type of investigation.

In the present investigation the crystals were all of very similar thickness, i.e., 30-36 μ, so that any anomalies associated with crystal thickness were not be a problem. In general, the angles chosen for study in this investigation were ≥ |10°| , so that the common problems associated with fitting the TPE and SHG data at small angles was avoided.

The above discussion suggests that the PSF naphthalene system corresponds to the capture limited regime. This also agrees with the result obtained by Schmid (224). One can argue that since the distance between scatterers is smaller, and, therefore, the migration time is shorter for DSF crystals than for PSF crystals, the capture limited regime also must be appropriate for the DSF system.

It is the capture limited result, then, which is of primary interest in this study, and, therefore, the following derivation corresponds to this regime. Consider equation [23], which can be rewritten, by substitution of

equation [28], as:

$$\gamma_T = R_{enc} \times \rho \times \tau_{enc} = \left[\frac{v_{pol}}{<R>}\right] \times \rho \times \tau_{enc} \qquad [36]$$

τ_{enc} is considered to be inversely proportional to the polariton velocity:

$$\tau_{enc} \propto \frac{1}{v_{pol}} \qquad [37]$$

and, assuming the polariton wavepacket to be narrow with respect to the average host-trap separation, <R>, and the trapping radius, R_{tr}, the encounter time for the trapping or scattering event can be expressed as:

$$\tau_{enc} = \frac{R_{tr}}{v_{pol}} \qquad [38]$$

where R_{tr} can be expressed in terms of the cylinder radius, **a**, discussed above:

$$R_{tr} = 2a \qquad [39]$$

Therefore, substitution of equations [38] and [39] into equation [36] yields the result:

$$\gamma_T = \frac{2a}{<R>} \times \rho \qquad [40]$$

Obviously, from this expression, γ_T is independent of polariton velocity, and, therefore, should be appropriate to the capture limited regime. Equation [40] can be simplified further by substituting for <R>, using equation [33]:

$$\gamma_T = 2\pi a^3 n_T \rho \qquad [41]$$

This result is similar to that reported for the capture limited regime by Parris and Kenkre (78):

$$k_s = \frac{c \rho R^3}{V} \qquad [42]$$

where k_s is the energy transfer rate, c is a capture frequency or probability, ρ is mole/mole trap concentration, R is the capture radius, and V is the unit cell volume. It should be noted, however, that n_T in equation [41] is equivalent to ρ/V in equation [42], and ρ in equation [41] can be likened to c in equation [42].

Recalling equation [21], equation [41] can be rewritten for the cases for trapping and for scattering off a trap:

$$\gamma_{tr} = 2\pi a_{tr}^3 n_T \rho_{tr} \qquad [43a]$$

$$\gamma_{sc} = 2\pi a_{sc}^3 n_T \rho_{sc} \qquad [43b]$$

It should be emphasized that the approach used by Parris and Kenkre (78) considers only capture and not the possibility of scattering off the trap without subsequent capture. The results obtained in the present investigation indicate that scattering with the trap, without subsequent capture, is indeed significant (vide infra), and must be considered in any discussion of energy transfer.

Equation [41] can be used to evaluate the trapping probability, ρ, for various values of the radius, **a**. For the DSF crystals studied, $n_T \approx 5 \times 10^{-8}$ Å^{-3}, and γ_0 ($\approx \gamma_T$) is $\approx 3 \times 10^{10}$ sec^{-1}. The polariton velocities typically studied are in the range $v_{pol} = 6.0 \times 10^6 - 2.6 \times 10^7$ cm-sec^{-1}. Therefore, for the trapping or scattering radii, **a** = 10 Å and **a** = 100 Å, ρ is $\approx 10^{14}$ sec^{-1} and is $\approx 10^{11}$ sec^{-1}, respectively. Using equation [28], the number of encounters of the polariton with a trap per unit time, i.e., R_{enc}, can be calculated. For the polariton velocity, $v_{pol} = 2.6 \times 10^7$ cm-sec^{-1}, which corresponds to the experimental external angle $\Theta_{ext} = +10°$, R_{enc} is $\approx 5 \times 10^{10}$ sec^{-1} and is $\approx 5 \times 10^{12}$ sec^{-1}, for **a** = 10 Å and **a** = 100 Å, respectively. For $v_{pol} = 6.0 \times 10^6$ cm-sec^{-1}, which corresponds to the experimental external angle $\Theta_{ext} = +30°$, R_{enc} is $\approx 1 \times 10^{10}$ sec^{-1} and is $\approx 1 \times 10^{12}$ sec^{-1}, for **a** = 10 Å and **a** = 100 Å, respectively. Comparing the values obtained for R_{enc} to those obtained for ρ, it is observed that for **a** = 10 Å, the encounter rate, R_{enc}, is much less than the trapping or trap scattering rate, ρ, so the time it takes to encounter a trap is much longer than the time it takes for the trapping event to occur; this clearly corresponds to the motion, or migration, limited regime. For a radius,

a = 100 Å, the opposite result is found, i.e., $\rho < R_{enc}$, so that the trapping event occurs on a timescale which is long compared to the time of encounter, or the motion. This corresponds to the trapping or capture limited regime. It should be pointed out, however, that there are about three orders of magnitude difference between the rates calculated using a = 10 Å, whereas, for a = 100 Å, there is approximately one order of magnitude difference. It may be that, for a clearcut case of capture limited energy transfer, a value for the trapping radius of $a > 100$ Å should be considered appropriate. The value of a = 100 Å is taken approximately to be a lower bound for the trapping or capture radius in the capture limited regime (for a radius, a = 200 Å, $\rho \approx 10^{10}$, which is two orders of magnitude less than R_{enc}). It becomes obvious that the trap scattering radius must be at least as large as the capture radius, and is likely to be larger than the capture radius. One additional point must be made; that is, that for a "sluggish" polariton, for example, $v_{pol} = 4.3 \times 10^5$ cm-sec^{-1} (corresponding to the external angle, $\Theta_{ext} = -45°$), the radius, a = 10 Å, definitely corresponds to the motion limited regime, however, a radius, a = 100 Å, results in a value for the encounter rate, R_{enc}, which is of the same order of magnitude as the trapping probability, ρ. This supports the suggestion that a lower bound for the radius, a, is 100 Å. The results of the calculations given above are summarized in Table III.

Branching ratios

Using the results from Table I, it is possible to estimate the branching ratio γ_{sc}/γ_{tr}. A discussion of the procedure for this estimate follows.

The probability for a polariton scattering of a trap is given by P_{incoh}, and the probability for a coherent polariton trapping event is given by P_{coh}. Since the probability of the two trap-related events must sum to one:

$$P_{coh} = 1 - P_{incoh} \qquad [44]$$

Therefore, the branching ratio is given by:

$$\frac{\gamma_{sc}}{\gamma_{tr}} = \frac{P_{incoh}}{1 - P_{incoh}} \qquad [45]$$

Assuming that the scattering event creates an exciton, the quantum yield for populating anthracene is defined to be Φ. The probability of detecting anthracene fluorescence is given by p^A; the probability of detecting naphthalene fluorescence is p^N. The fluorescence intensity ratio at low temperature is given then by:

$$\frac{I_A}{I_N} = \frac{P_{incoh}\,\Phi\,p^A + P_{coh}\,p^A}{P_{incoh}\,(1-\Phi)\,p^N} = \frac{1}{1.2} \qquad [46]$$

where the value 1.2 is from Table I, $(I_N / I_A)_{CL}$. It is recognized that P_{coh} can be replaced by $(1-P_{incoh})$, thus giving:

$$\frac{P_{incoh}\,\Phi\,p^A + (1 - P_{incoh})\,p^A}{P_{incoh}\,(1-\Phi)\,p^N} = \frac{1}{1.2} \qquad [47]$$

Table III. Summary of trapping event rate calculations for motion and capture limited regimes in DSF crystals

a (Å)	$\rho(sec^{-1})^a$	$\langle R \rangle$ (Å)[b]	v_{pol} (cm-sec^{-1})	R_{enc} (sec^{-1})[c]	regime
10	1×10^{14}	6×10^{4}	2.6×10^{7}	5×10^{10}	motion limited
10	1×10^{14}	6×10^{4}	6.0×10^{6}	1×10^{10}	motion limited
10	1×10^{14}	6×10^{4}	4.3×10^{5}	7×10^{8}	motion limited
100	1×10^{11}	6×10^{2}	2.6×10^{7}	5×10^{12}	capture limited
100	1×10^{11}	6×10^{2}	6.0×10^{6}	1×10^{12}	capture limited
100	1×10^{11}	6×10^{2}	4.3×10^{5}	7×10^{10}	motion or capture limited ?

[a] Calculated from equation [41] using the values $\gamma_T = 3 \times 10^{10}$ sec^{-1} and $n_T = 5 \times 10^{-8}$ Å^{-3}.

[b] Calculated from equation [33] using the value $n_T = 5 \times 10^{-8}$ Å^{-3}.

[c] Calculated from equation [28].

Restating this expression in terms of the branching ratio yields:

$$\frac{\Phi p^{A}}{(1-\Phi)p^{N}} + \frac{\gamma_{tr}}{\gamma_{so}} \frac{p^{A}}{(1-\Phi)p^{N}} = \frac{1}{1.2} \qquad [48]$$

In this last expression, the reciprocal of the ratio $\Phi p^{A}/(1-\Phi)p^{N}$ is recognized to be the "incoherent" contribution to the intensity ratio I_N/I_A, which experimentally was determined to be ≈1.6. In addition, the term $p^{A}/(1-\Phi)p^{N}$ can be approximated by unity since in these experiments the detection efficiencies for anthracene and naphthalene were essentially the same, the quantum yields for naphthalene and anthracene fluorescence are ≈0.3, and the anthracene concentration was such that the intensities measured for naphthalene and anthracene were comparable. Based on these approximations the branching ratio is estimated to be $\gamma_{so}/\gamma_{tr} \approx 5$.

The branching ratio can be used in calculating values for trap scattering frequency, γ_{so}, and the trapping frequency, γ_{tr}, from equation [21]. The total trapping frequency, γ_T, is assumed to be equivalent to the temperature independent damping frequency, γ_0, for a doped strain free (DSF) crystal (vide supra), and has been determined (vide infra) in this study to be 3×10^{10} sec^{-1} (vide supra). From equation [21], and from the branching ratio estimate that $\gamma_{so} \approx 5\ \gamma_{tr}$ (vide supra), the trapping frequency, γ_{tr}, is found to be $\approx 5 \times 10^{9}$ sec^{-1}. Using this value for the trapping frequency in equation [21], the trap scattering frequency γ_{so} is found to be 2.5×10^{10} sec^{-1}. Using the trapping or scattering radii, **a** = 10 Å and **a** = 100 Å, equations [43] can be used to calculate the trapping and

scattering probabilities, ρ_{tr} and ρ_{so}, respectively. The values obtained for the trapping probability, ρ_{tr}, are $\approx 2 \times 10^{13}$ sec^{-1} and $\approx 2 \times 10^{10}$ sec^{-1} for the trapping radii, **a** - 10 Å and **a** - 100 Å, respectively. The values obtained for the trap scattering probability, ρ_{so}, are $\approx 8 \times 10^{13}$ sec^{-1} and $\approx 8 \times 10^{10}$ sec^{-1} for the trap scattering radii, **a** - 10 Å and **a** - 100 Å, respectively. As stated in the previous section, these results correspond to the motion limited regime for **a** - 10 Å, and to the capture limited regime for **a** - 100 Å.

Temperature Behavior of TPE and SHG Signals

Temperature-dependent behavior of the TPE and SHG signals were studied for several crystals in the thickness range of 30-36 μ. Several angles of orientation were chosen to be studied in the temperature range 1.6 K to 30 K. Data of this type have been reported by Stevenson and Small (131) for the system of pure, strain-free (PSF) naphthalene single crystals. The theoretical fits discussed in this section are based on the treatment presented in reference (131c).

Thermal broadening of the nonlinear signals

For each crystal studied, temperature broadening data were collected. Several of these thermal broadening curves are presented in Figures 5-11. The theoretical curves are based on the work of Stevenson and Small (131). Assuming the linewidth Γ to broaden thermally in proportion to the thermal occupation number of a phonon of frequency Ω, the linewidth can

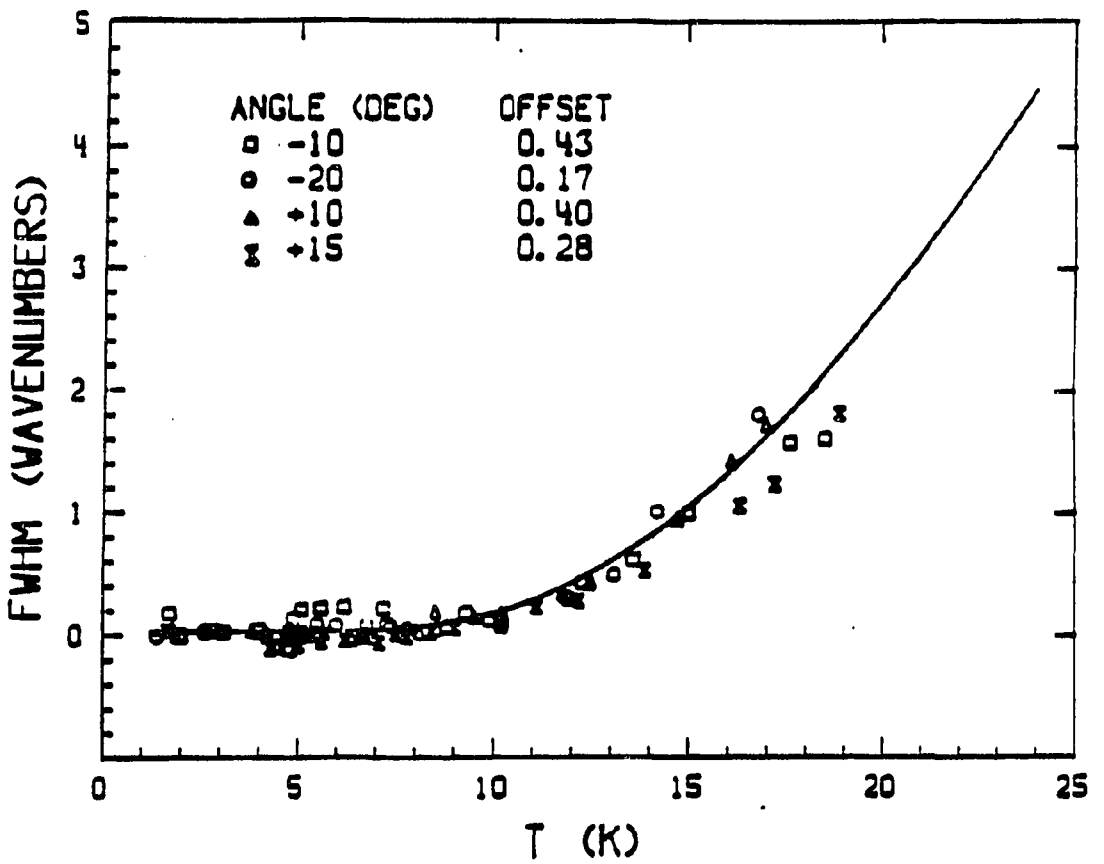

Figure 5. **Temperature broadening data for a 27 μ PSF naphthalene crystal at four angles of incidence with respect to the c' axis. Data are offset at each angle by the residual low-temperature width observed for that orientation. The solid curve is obtained from expression [40], using an effective phonon frequency of $\Omega = 39\ cm^{-1}$ and preexponential value $C = 43\ cm^{-1}$ (from reference 131c)**

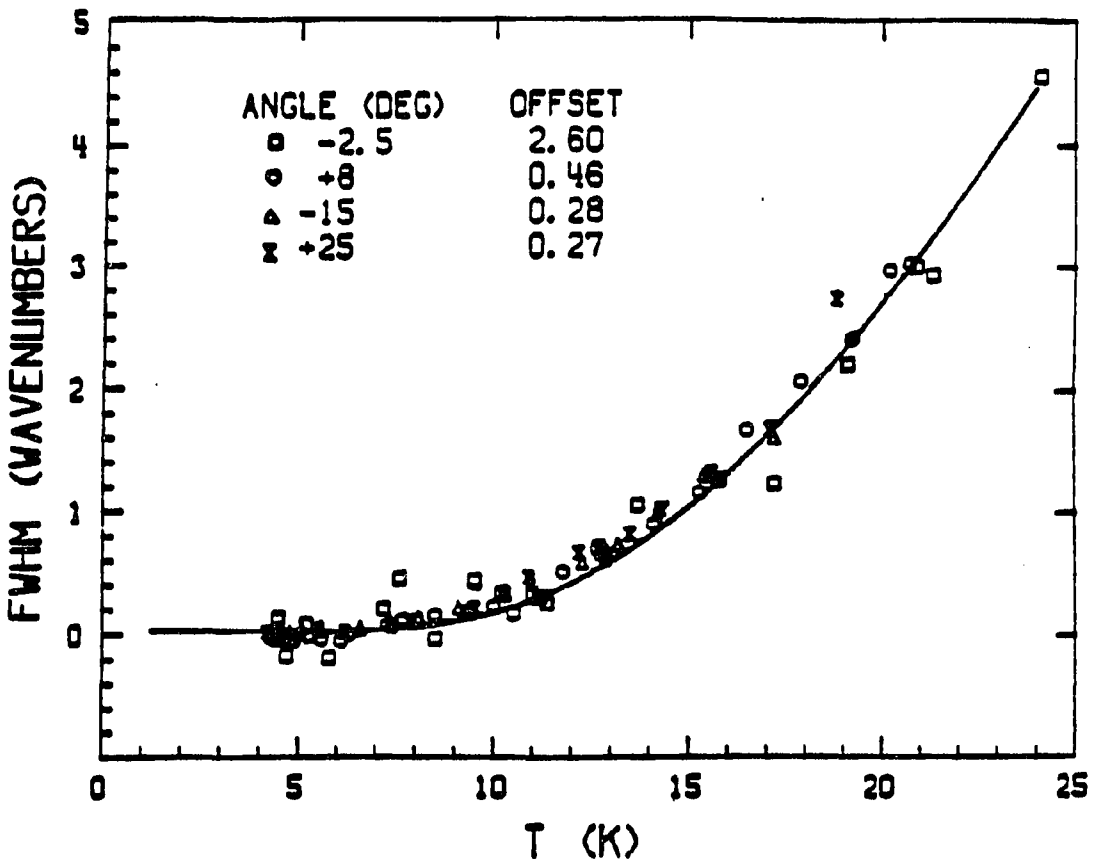

Figure 6. Temperature broadening data for a 30 μ PSF naphthalene crystal at four angles of incidence with respect to the c' axis. Data are offset at each angle by the residual low-temperature width observed for that orientation. The solid curve is obtained from expression [40], using an effective phonon frequency of $\Omega = 39\ cm^{-1}$ and preexponential value $C = 43\ cm^{-1}$ (from reference [131c])

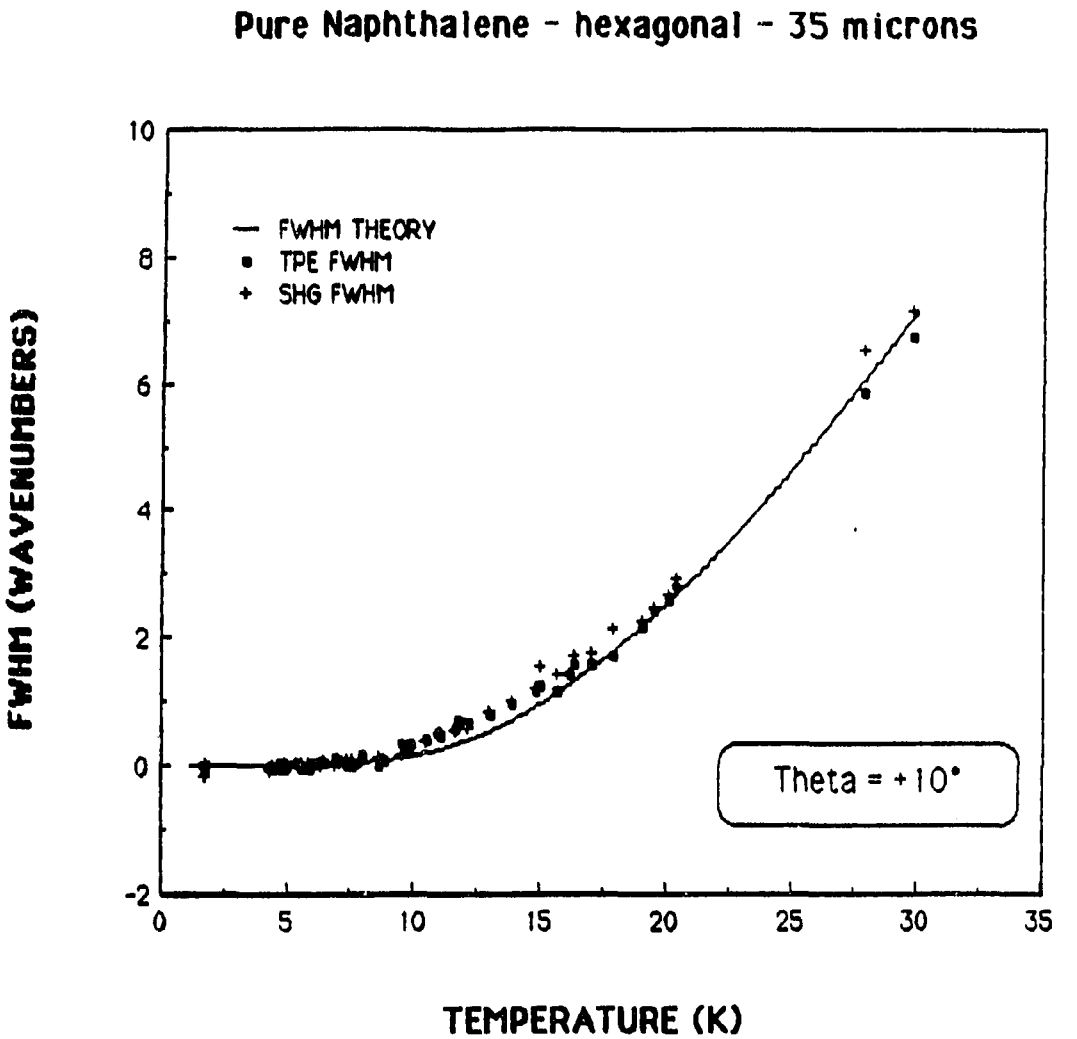

Figure 7. Temperature broadening data for a 35 μ PSF naphthalene crystal (hexagonal habit) at an angle of incidence of +10° with respect to the c' axis. Data are offset by the residual low-temperature width (0.84 cm^{-1} and 0.76 cm^{-1} for TPE and SHG, respectively) observed for this orientation. The solid curve is obtained from expression [40], using an effective phonon frequency of Ω = 39 cm^{-1} and preexponential value C = 43 cm^{-1}

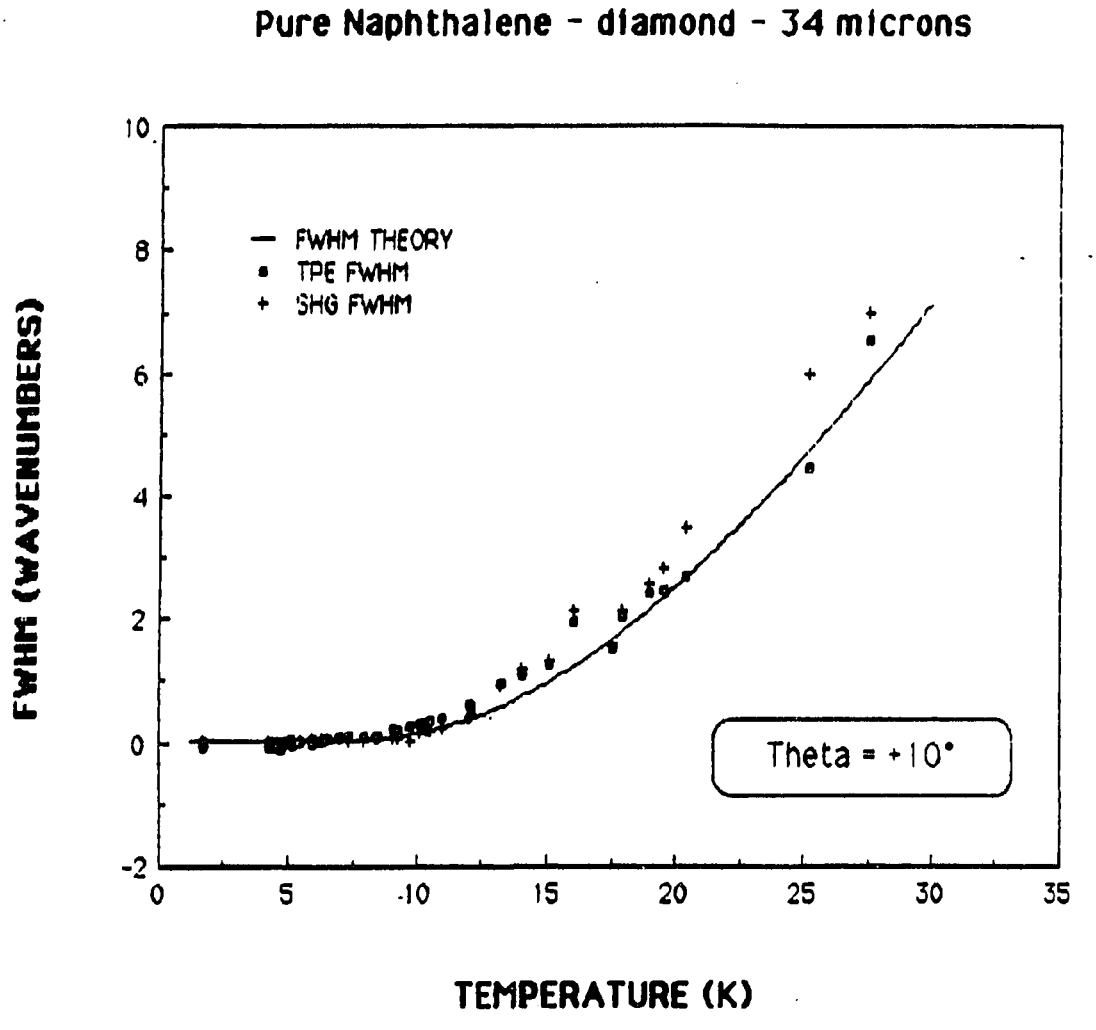

Figure 8. Temperature broadening data for a 34 μ PSF naphthalene crystal (diamond habit) at Θ_{ext} = +10° and +30° angles of incidence with respect to the c' axis. Data are offset by the residual low-temperature width observed for that orientation (0.65 cm^{-1} and 0.50 cm^{-1} for Θ_{ext} = +10° TPE and SHG; 0.51 cm^{-1} and 0.46 cm^{-1} for Θ_{ext} = +30° TPE and SHG, respectively). The solid curve is obtained from expression [40], using an effective phonon frequency of Ω = 39 cm^{-1} and preexponential value C = 43 cm^{-1}

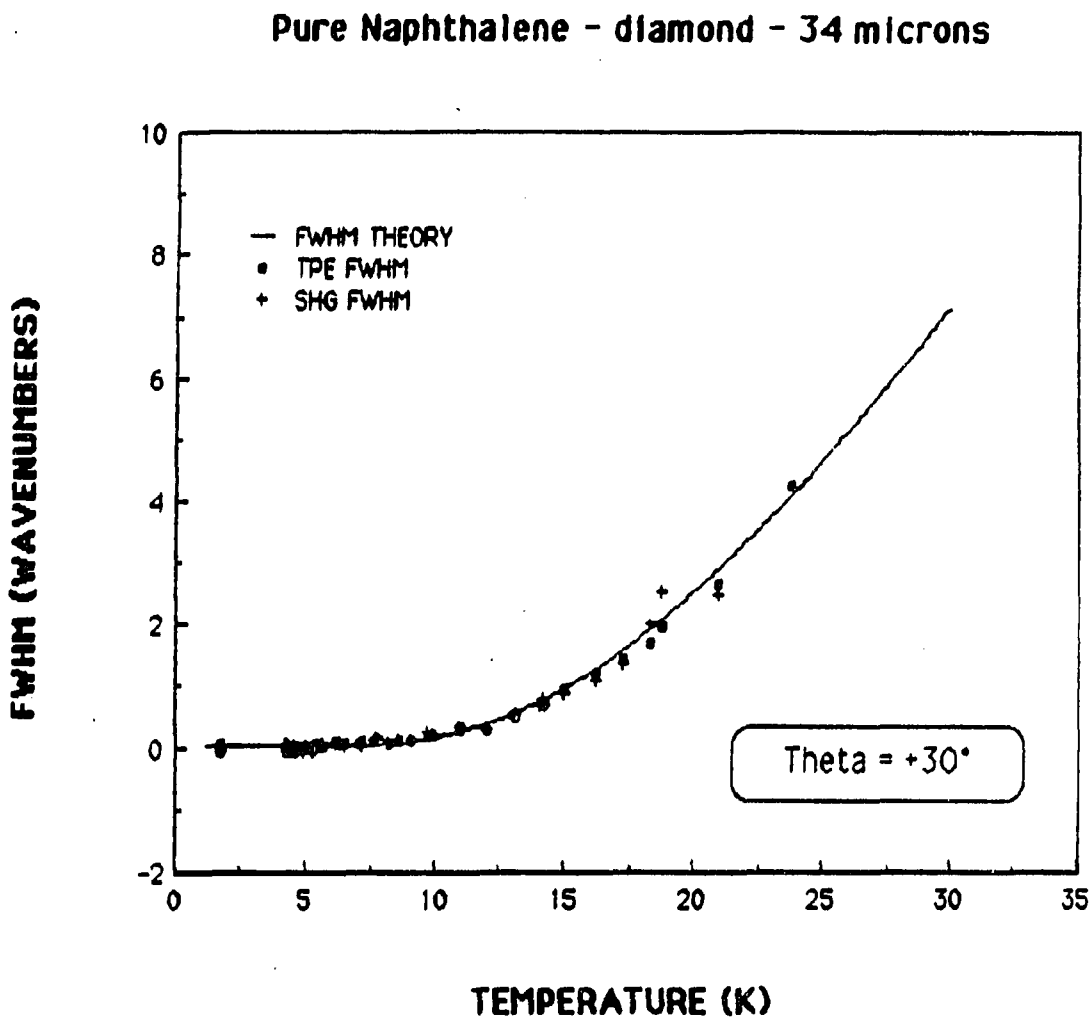

Figure 8. (continued)

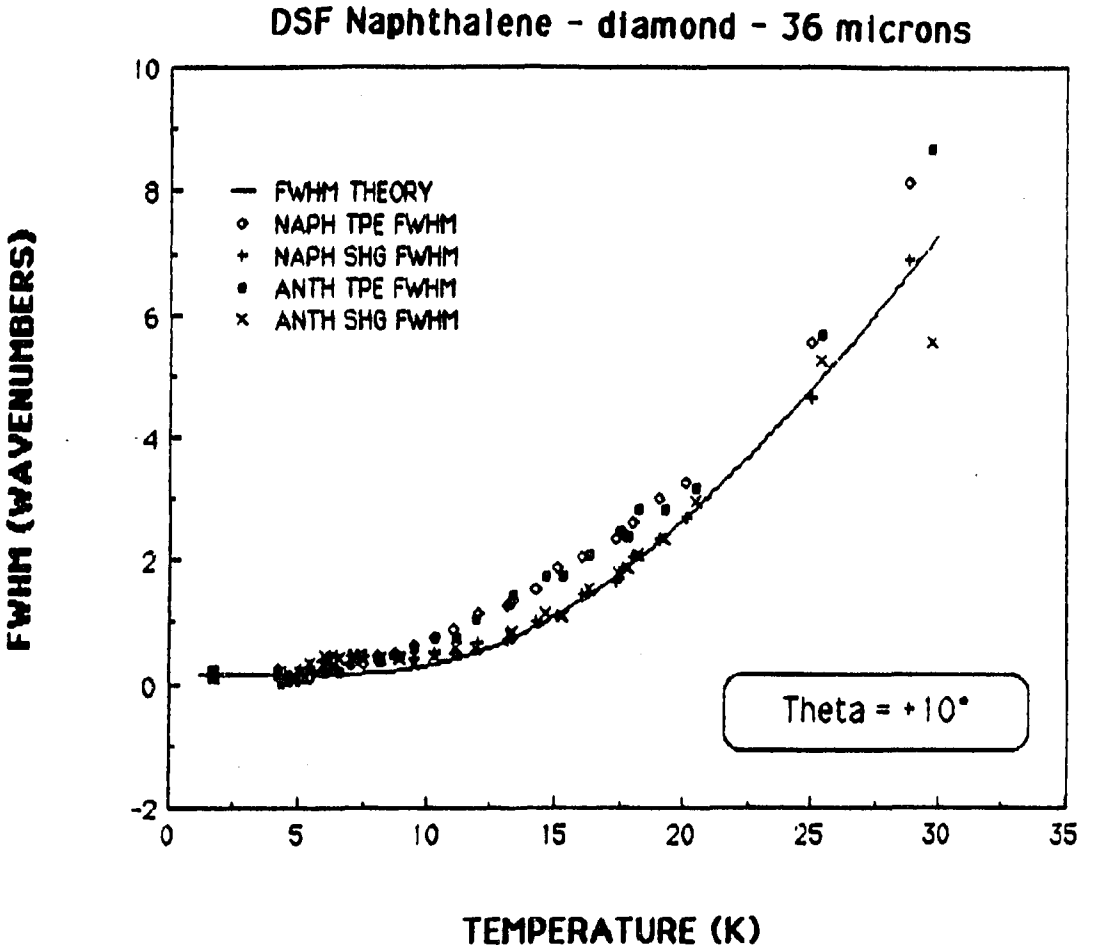

Figure 9. Temperature broadening data for the naphthalene and anthracene nonlinear signals for a 36 μ DSF naphthalene crystal (diamond shape) at Θ_{ext} = +10° and +30° angle of incidence with respect to the c' axis. Data are offset by the residual low-temperature width observed for that orientation The solid curve is obtained from expression [40], using an effective phonon frequency of Ω = 39 cm^{-1} and preexponential value C = 43 cm^{-1}. Offsets for Θ_{ext} = +10° are 0.33 cm^{-1} and 0.36 cm^{-1} for naphthalene TPE and SHG, and 0.31 cm^{-1} and 0.35 cm^{-1} for anthracene TPE and SHG

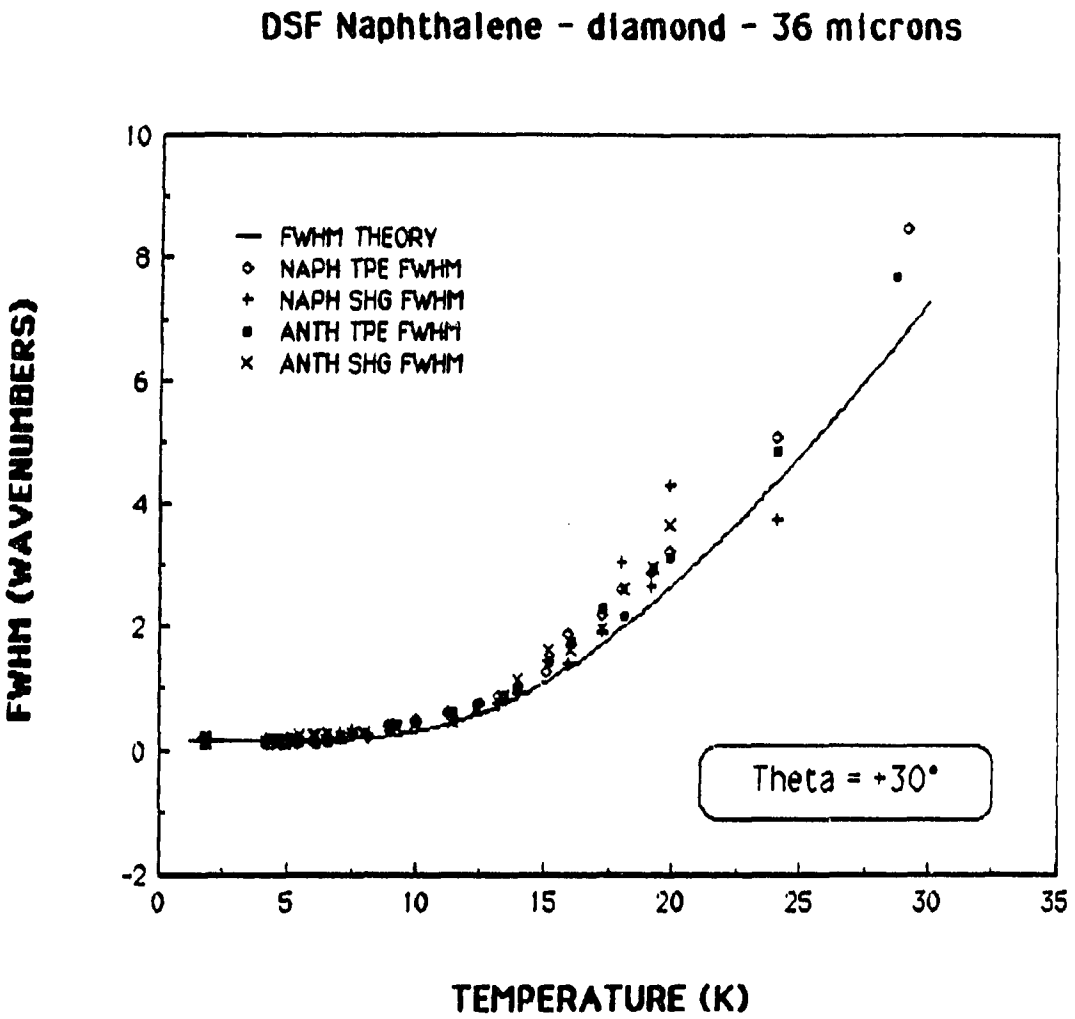

Figure 9. (continued). Offsets for Θ_{ext} = +30° are 0.20 cm^{-1} and 0.14 cm^{-1} for naphthalene TPE and SHG, and 0.20 cm^{-1} and 0.18 cm^{-1} for anthracene TPE and SHG

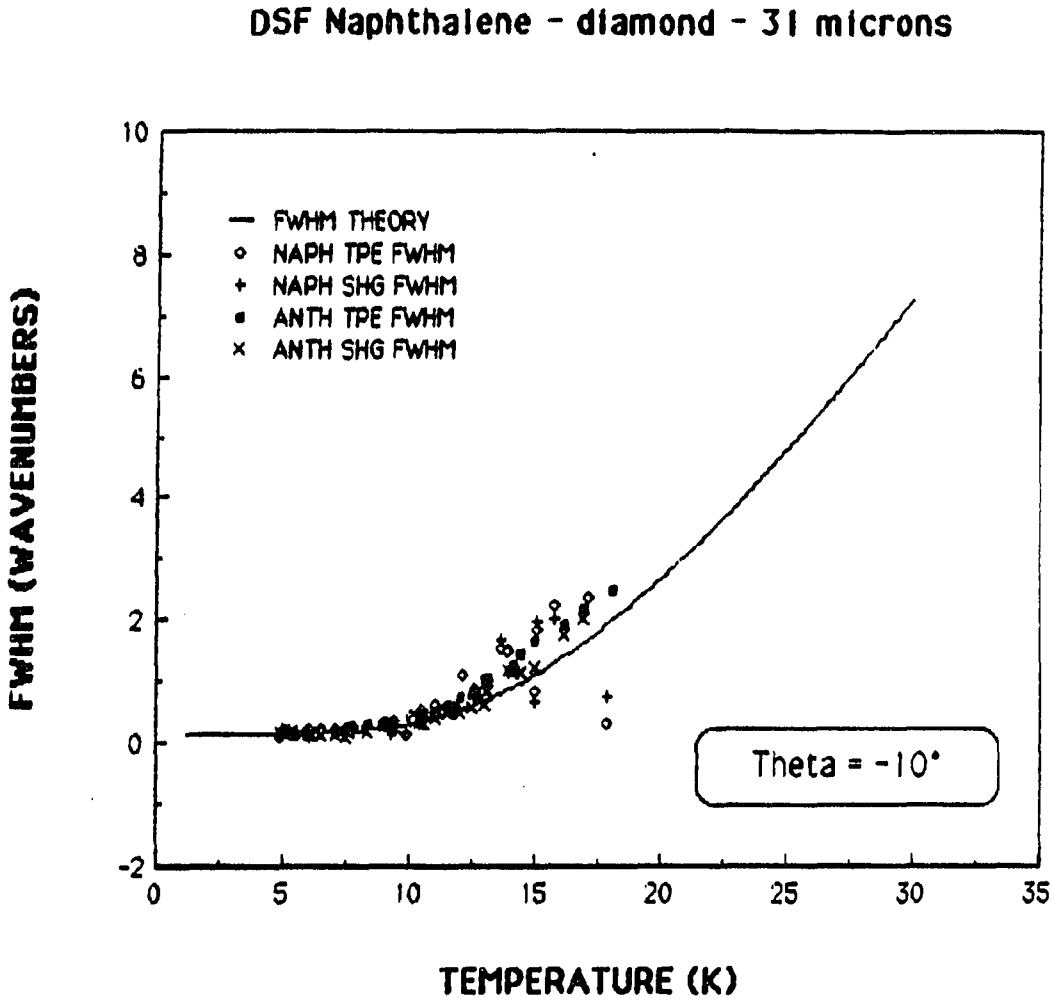

Figure 10. Temperature broadening data for the naphthalene and anthracene nonlinear signals for a 31 μ DSF naphthalene crystal (diamond habit) at Θ_{ext} = -10° and -30° angles of incidence with respect to the c' axis. Data are offset by the residual low-temperature width observed for that orientation. The solid curve is obtained from expression [40], using an effective phonon frequency of Ω = 39 cm^{-1} and preexponential value C = 43 cm^{-1}. Offsets for Θ_{ext} = -10° are 0.44 cm^{-1} and 0.39 cm^{-1} for naphthalene TPE and SHG, and 0.43 cm^{-1} and 0.40 cm^{-1} for anthracene TPE and SHG

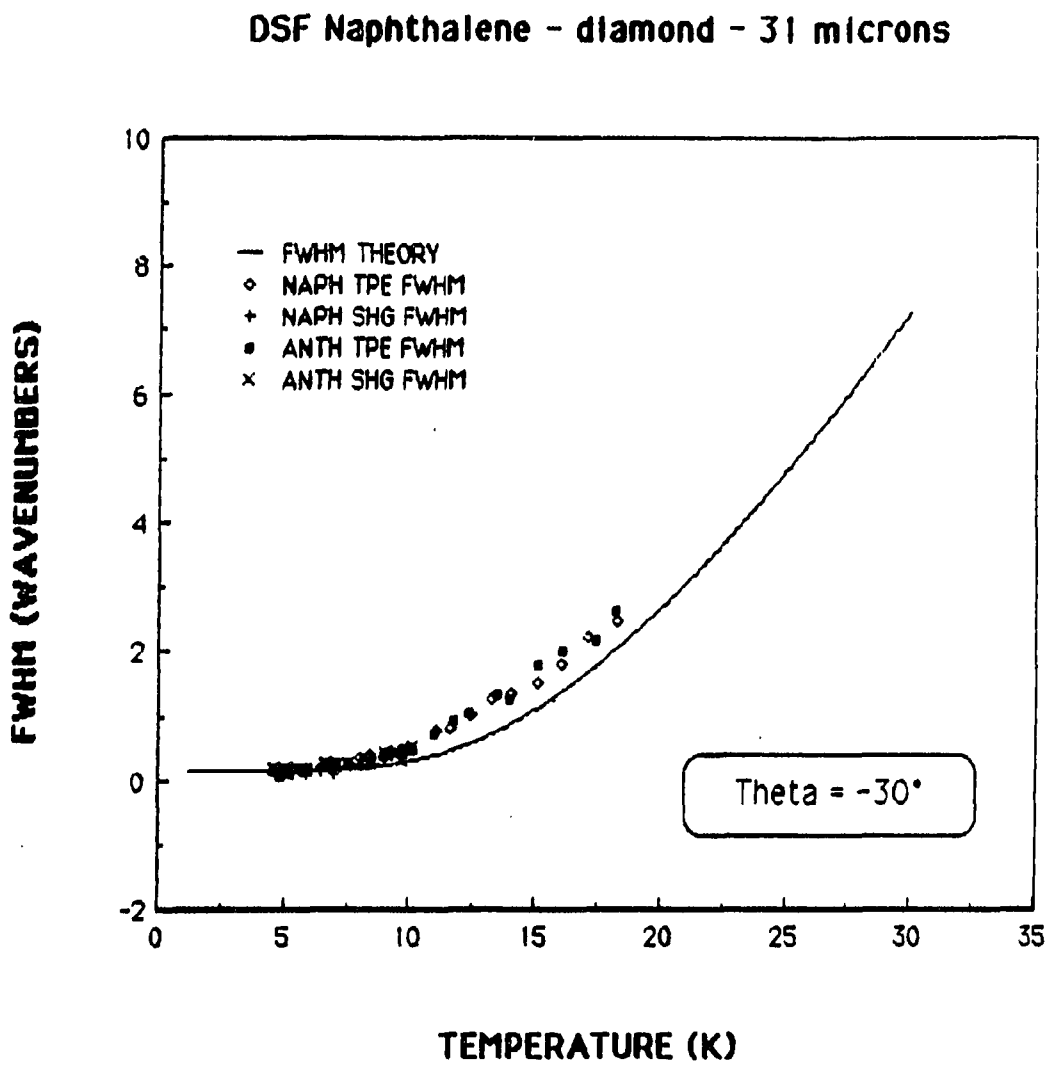

Figure 10. (continued). Offsets for Θ_{ext} = -30° are 0.31 cm^{-1} and 0.29 cm^{-1} for naphthalene TPE and SHG, and 0.30 cm^{-1} and 0.24 cm^{-1} for anthracene TPE and SHG

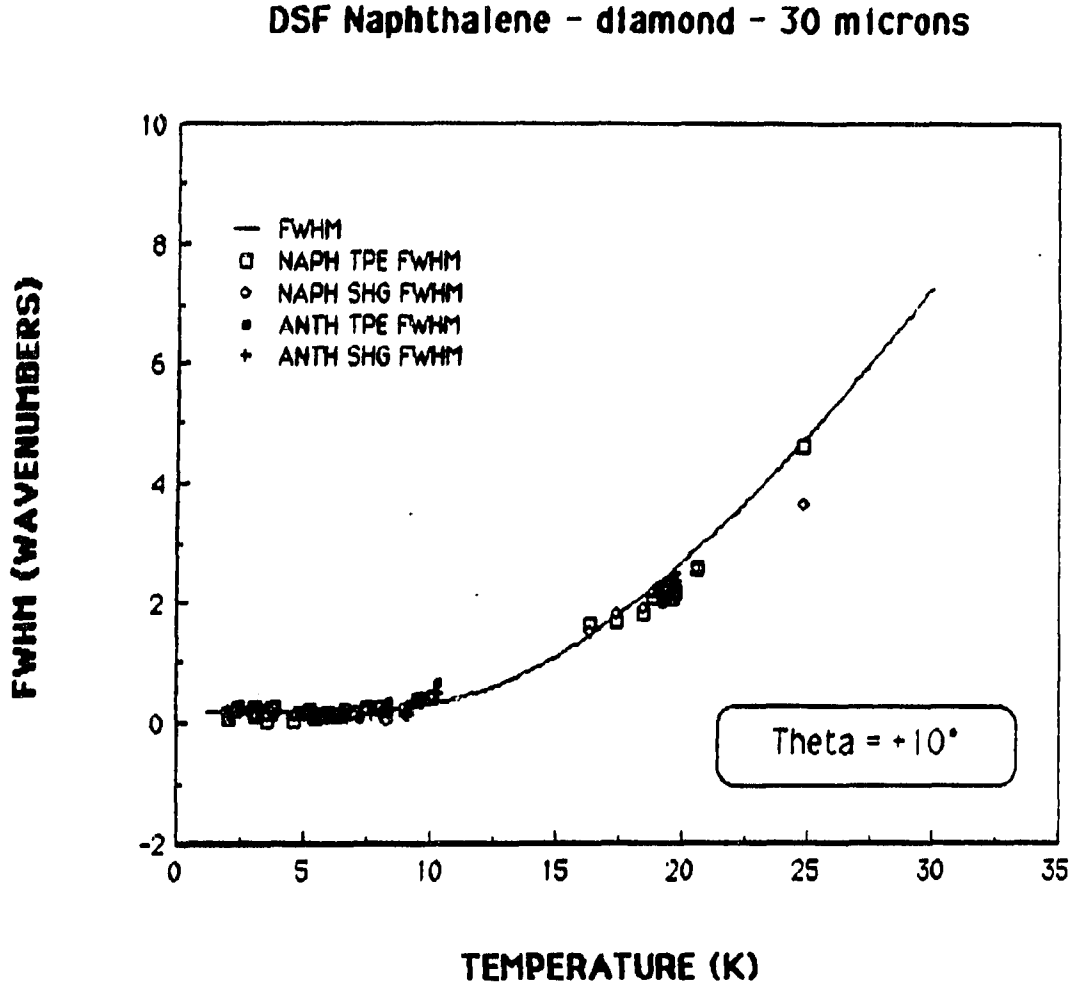

Figure 11. Temperature broadening data for the naphthalene and anthracene nonlinear signals for a 30 μ DSF naphthalene crystal (diamond shape) at Θ_{ext} = +10° angle of incidence with respect to the $\underline{c}'$ axis. Data are offset by the residual low-temperature width observed for that orientation (0.50 cm^{-1} and 0.48 cm^{-1} for naphthalene TPE and SHG, and 0.49 cm^{-1} and 0.46 cm^{-1} for anthracene TPE and SHG. The solid curve is obtained from expression [40], using an effective phonon frequency of Ω = 39 cm^{-1} and preexponential value C = 43 cm^{-1}

be calculated from:

$$\Gamma = C\langle n \rangle = C\left[\exp\left(\frac{\Omega}{k_B T} \right) - 1 \right]^{-1} \qquad [49]$$

where k_B is Boltzmann's constant, T is the temperature in degrees Kelvin, and C is the preexponential factor. For single crystals of pure, strain-free (PSF) naphthalene the effective phonon frequency Ω was determined (131c) to be 39 cm^{-1} and C was found to be 43 cm^{-1}.

Figures 5 and 6 present experimental data and calculated curves for a PSF 27 μ naphthalene crystal (Figures12 and 13 from reference (131c)). Figures 7 and 8 show data collected for two PSF naphthalene crystals in this present study. Two crystal habits were observed for the pure naphthalene; the first was the hexagonal plate, the second was the diamond plate. The former was the habit observed by Stevenson (131c), and this habit showed evidence of twinning occasionally (131), however, the crystals which showed twinning and were used by Stevenson showed no difference in behavior from the untwinned crystals. The diamond plates always showed a twinning line; this is the habit observed for all anthracene-doped naphthalene crystals used in the present investigation. The question arises as to whether the observed temperature behavior is related to the crystal habit. The broadening behavior for the two different crystals habits, observed in Figures 7 and 8, appears to be the same. The fit with theory is excellent for temperatures below ≈15 K, and begins to deviate above this temperature. Looking at Figures 5 and 6, the fits to

theoretical predictions appear to be very good, but still one does begin to observe some deviations from theory, as well as scatter in the data, as the temperature is raised. It should be pointed out that the temperatures attained by Stevenson (131c) rarely exceeded 20 K, and it is possible that the theory begins to break down at higher temperatures. It may also be that the theory breaks down at somewhat lower temperatures in the case for doped crystals, in which case the fits would show deviations at lower temperatures. This point will be alluded to again in the next subsection.

Generally, the thermal broadening behavior is consistent for both the naphthalene and the anthracene TPE signals. The behavior is also consistent between the TPE and SHG signals, as was observed by Stevenson (131c). It should be pointed out that an advantage of the present experimental arrangement is that the SHG signal is identical for both the anthracene and naphthalene TPE signal collections; that is, the TPE signals are collected using filters to pass either the naphthalene or the anthracene signals, but the SHG is not filtered as such. Therefore, the SHG signal acts as a check on experimental errors and technical problems, such as a drop in laser power.

Temperature dependence of TPE and SHG intensities

The temperature dependence of the TPE and SHG intensities for PSF naphthalene crystals is well established by Stevenson (131c). Following the theoretical development presented in reference (131c), data for PSF and DSF naphthalene crystals are presented and compared with theory in this subsection. The expressions derived by Stevenson and Small (131) for

the SHG and TPE signal intensities, expressed as functions of the damping scattering) frequency γ, crystal thickness L, and polariton group velocity v_{pol}, were given by equation [15] and are repeated here for convenience:

$$I_{SHG} = \frac{v_{pol}}{\gamma L}\left[1 - \exp\left(\frac{-\gamma L}{v_{pol}}\right)\right] \qquad [50a]$$

$$I_{TPE} = 1 - \frac{v_{pol}}{\gamma L}\left[1 - \exp\left(\frac{-\gamma L}{v_{pol}}\right)\right] = 1 - I_{SHG} \qquad [50b]$$

Temperature-dependent intensity data were collected for several crystals in the thickness range of 27-36 μ. Data were collected over the temperature range of 1.6 K to 30 K and for several polariton velocities, attained by angle-tuning the crystal with respect to the incident laser beam. The velocities for the doped crystals were assumed to be the same as for the pure crystals (131c). The data are presented in Figures 12-18 on the following pages.

The theoretical fits to Stevenson's data (131c) are observed to be fairly good for all angles (velocities) shown for the 55 μ PSF crystal (see Figure 12), although the experimental SHG data seem to fall off somewhat more rapidly than predicted by theory, most noticeably for $\Theta_{ext} = +25°$. The data for the 27 μ PSF crystal presented in Figure 13 also show reasonable fits, but there is more deviation from the fit than in the thicker crystal, particularly the smaller angles. Again the data presented in Figures 8 and 9 are for temperatures below 20 K. Figure 14 presents data obtained in the present study for a 35 μ PSF naphthalene crystal

(hexagonal habit). The deviation from theory, particularly for the TPE intensity behavior, is immediately obvious. The TPE starts out at a higher relative intensity than predicted, and for temperatures above ≈17 K the TPE intensity begins to drop off instead of reaching a plateau value. This type of behavior was not observed by Stevenson (131c). If only the data below 20 K are plotted, as illustrated in Figure 15, the TPE intensity does appear to be approaching a plateau value. This point will be discussed in greater detail later.

The temperature intensity behavior for a 34 μ PSF naphthalene crystal (diamond habit) is presented in Figure 16. The lines are visual guides only. The intensity behavior of both the TPE and SHG signals are obviously quite different from that behavior observed in the PSF hexagonal crystal. The TPE signal starts out almost at a plateau and begins to drop off in intensity at ≈7 K. The SHG signal also drops off rapidly, reaching a value of 0.5 at ≈6 K, as opposed to ≈9 K predicted by theory. It seems likely that this effect is related to the crystal habit. Similar behavior is observed for the DSF crystals (Figures 13 and 14); once again the lines are visual guides only. For all DSF crystals studied, the TPE intensity was observed to increase from a constant low temperature value and then decrease at temperatures above ≈7-10 K. Although it appears that the crystal habit may be related to this observed intensity decrease, it may also be a real effect, in as much as a tendency toward this intensity decrease also was observed for the PSF hexagonal crystal at higher temperatures. Additional studies of PSF crystals, both hexagonal and diamond habits, over wider ranges of temperatures (at least to T = 30 K) might help to elucidate this

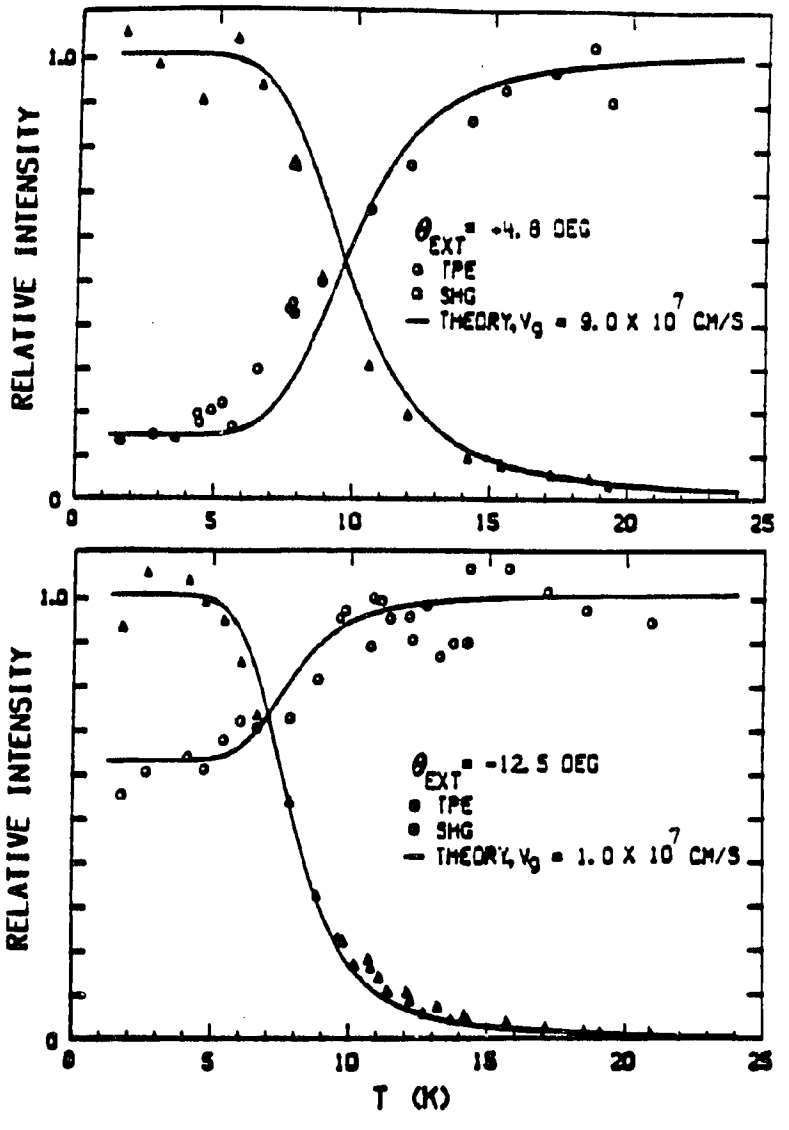

Figure 12. Integrated intensities of TPE and SHG profiles as a function of temperature at four orientations for a 55 μ PSF naphthalene crystal. The solid lines are computed from the fusion rate expressions [40] using the experimentally determined temperature-dependent damping with $\gamma_0 = 4 \times 10^9 \text{sec}^{-1}$ (from reference (131c))

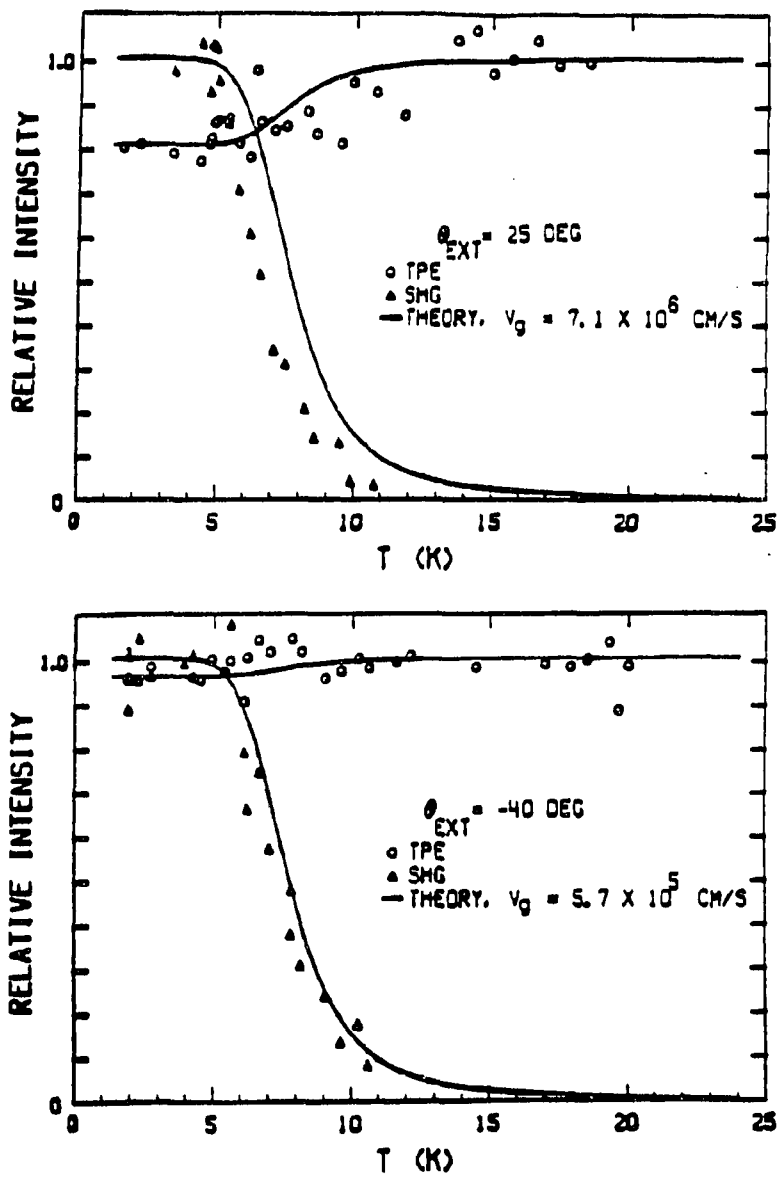

Figure 12. (continued)

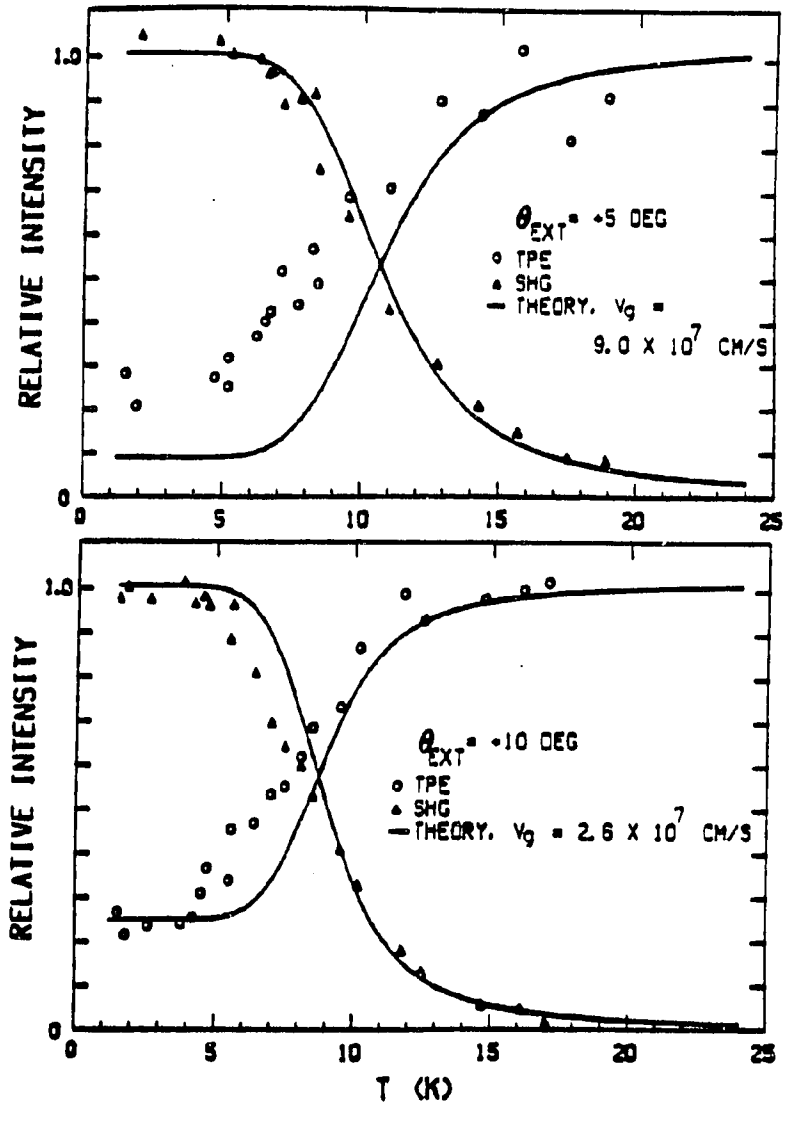

Figure 13. Integrated intensities of TPE and SHG profiles as a function of temperature at four orientations for a 27 μ PSF naphthalene crystal. The solid lines are computed from the fusion rate expressions [40] using the experimentally determined temperature-dependent damping with $\gamma_0 = 4 \times 10^9 \text{sec}^{-1}$ (from reference (131c))

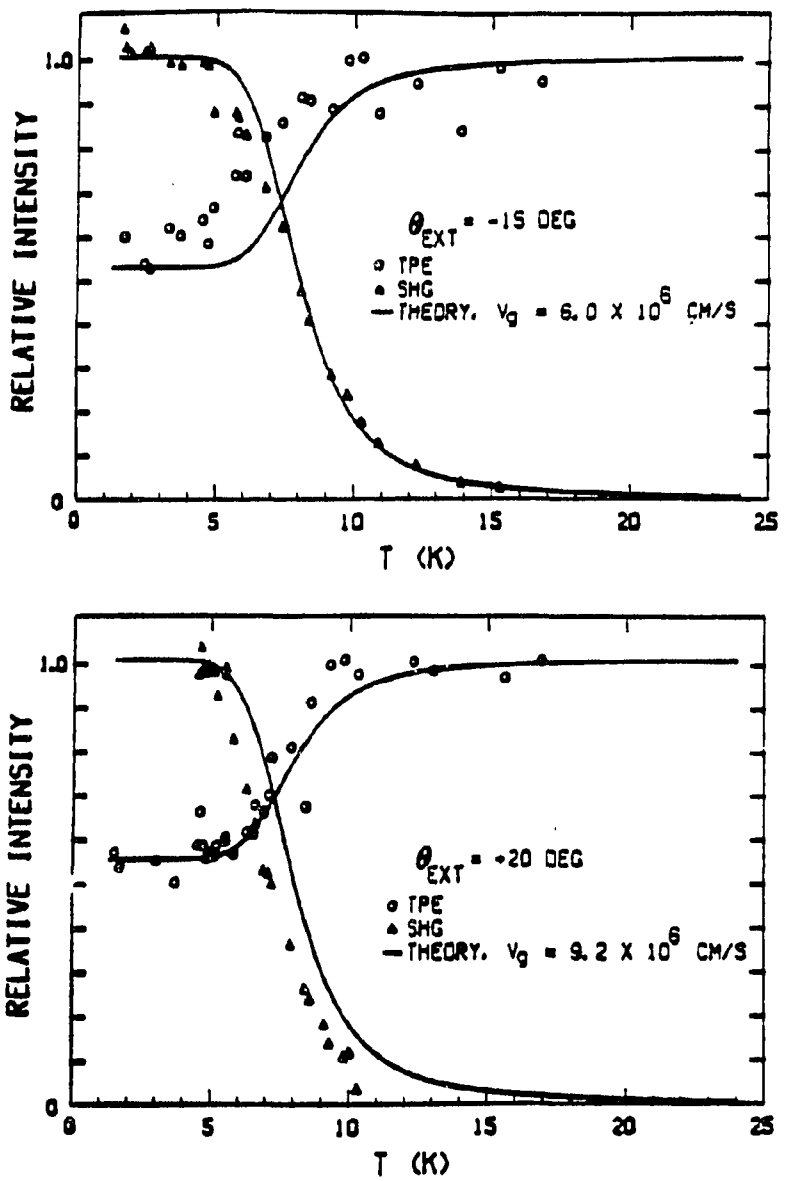

Figure 13. (continued)

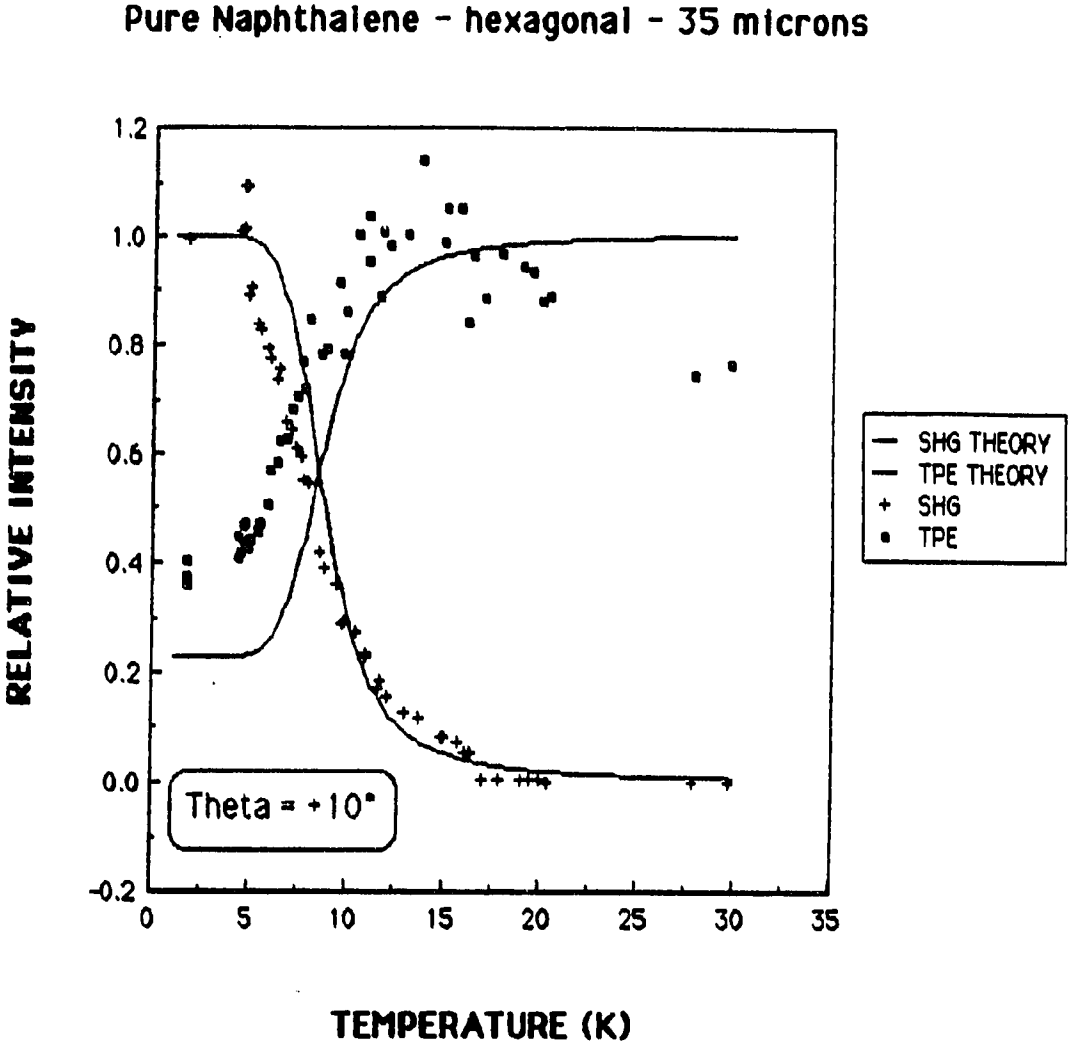

Figure 14. Integrated intensities of TPE and SHG profiles as a function of temperature at $\Theta_{ext} = +10°$ for a 35 μ PSF naphthalene crystal. The solid lines are computed from the fusion rate expressions [40] using the experimentally determined temperature-dependent damping with $\gamma_0 = 4 \times 10^9 \, sec^{-1}$

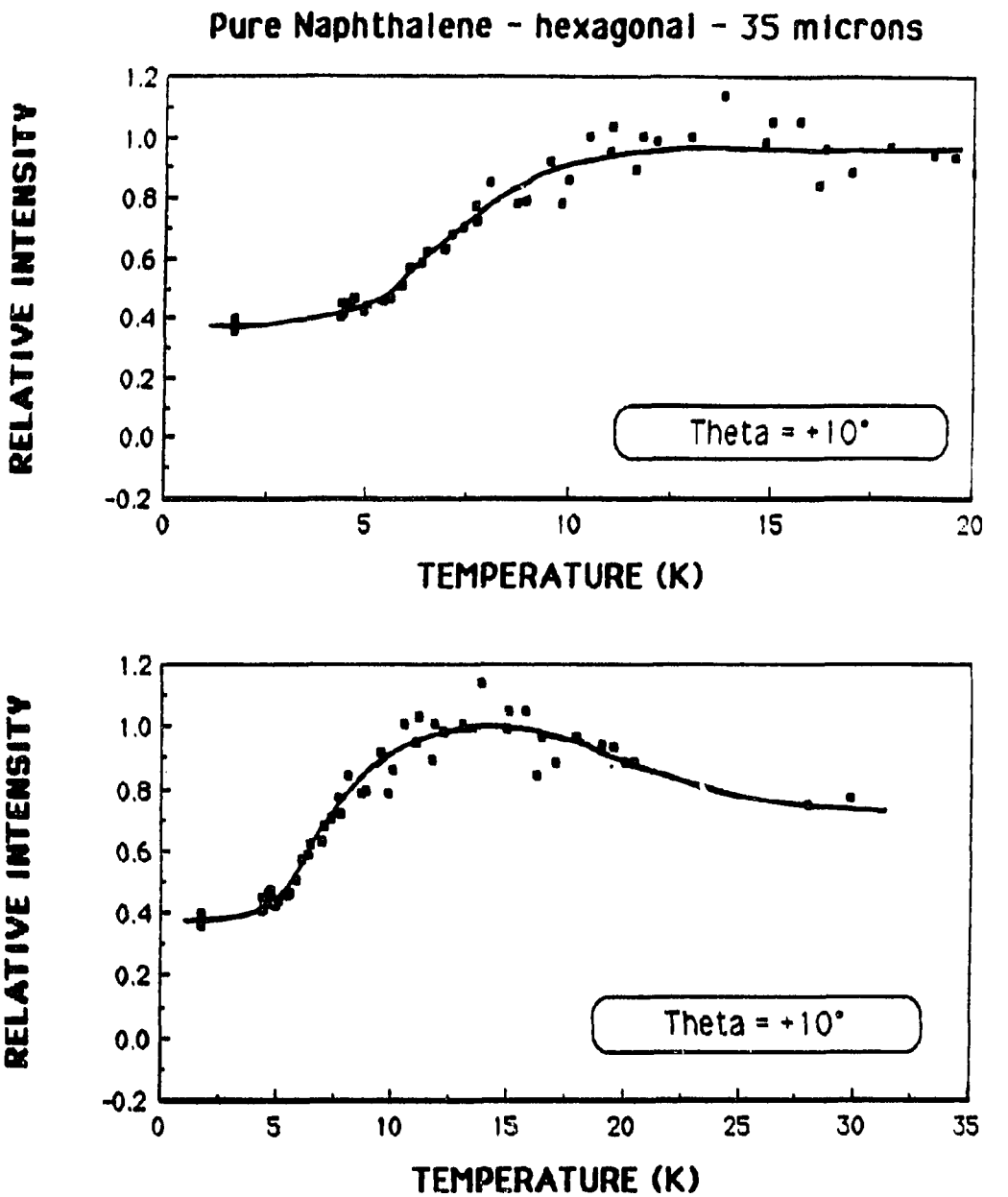

Figure 15. Integrated intensities of TPE profiles as a function of temperature at Θ_{ext} = +10° for a 35 μ PSF naphthalene crystal. The solid lines are intended as visual guides only

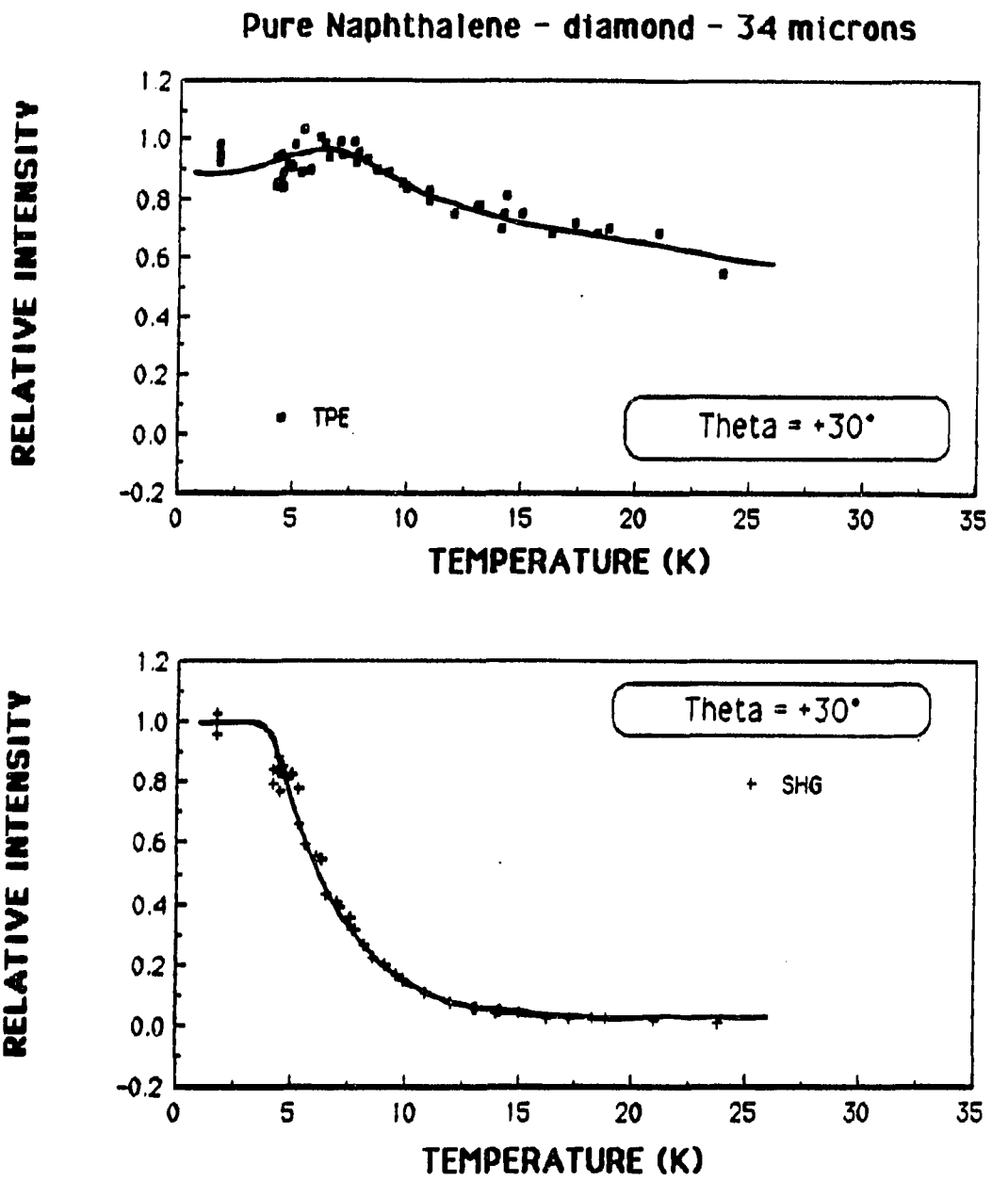

Figure 16. Integrated intensities of TPE and SHG profiles as a function of temperature at Θ_{ext} = +30° for a 34 μ PSF naphthalene crystal (diamond habit). The solid lines are intended as visual guides only

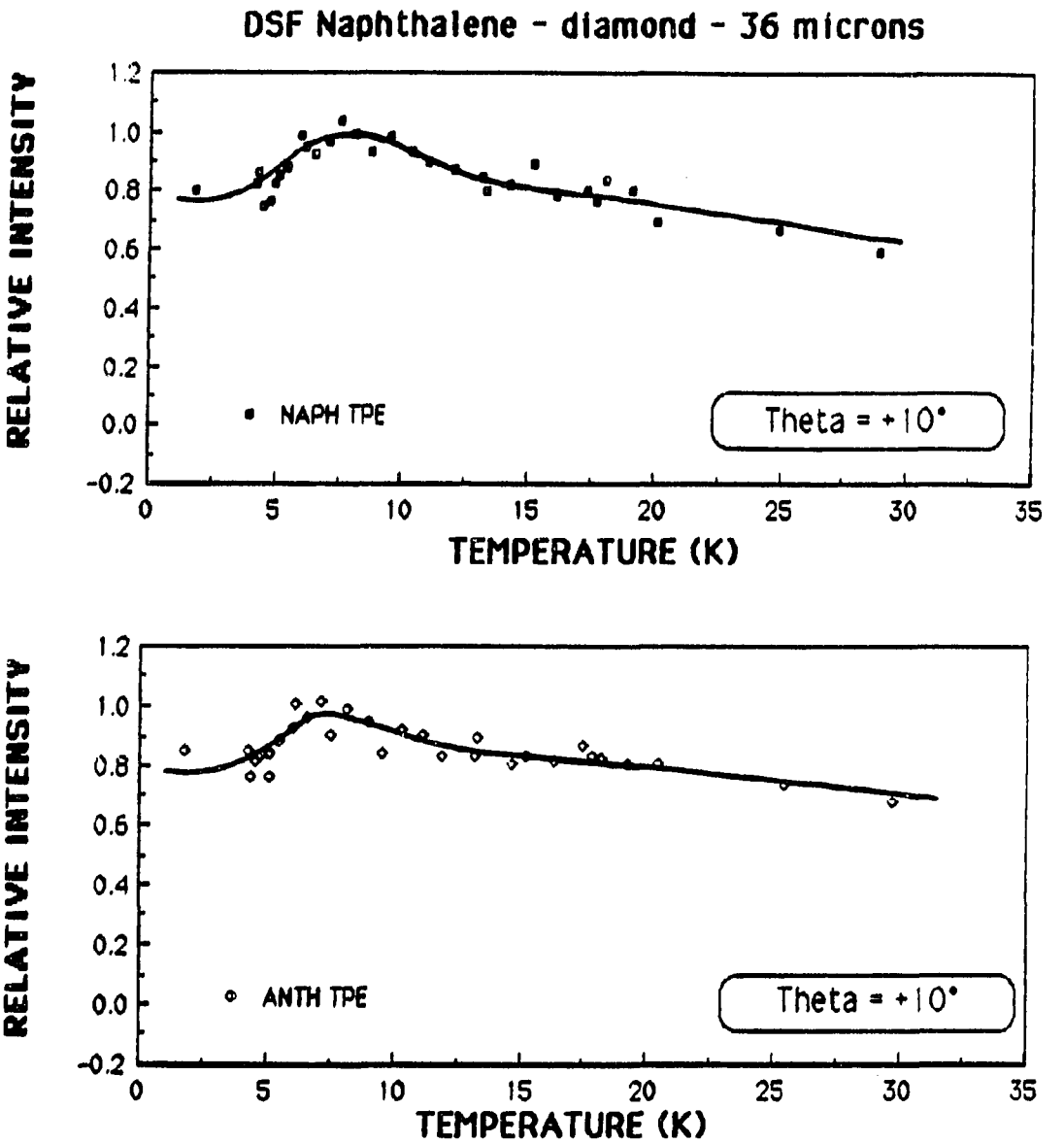

Figure 17. Integrated intensities of naphthalene and anthracene TPE and SHG profiles as a function of temperature at $\Theta_{ext} = +10°$ and $\Theta_{ext} = +30°$ for a 36 μ DSF naphthalene crystal (diamond habit). The solid lines are intended as visual guides only

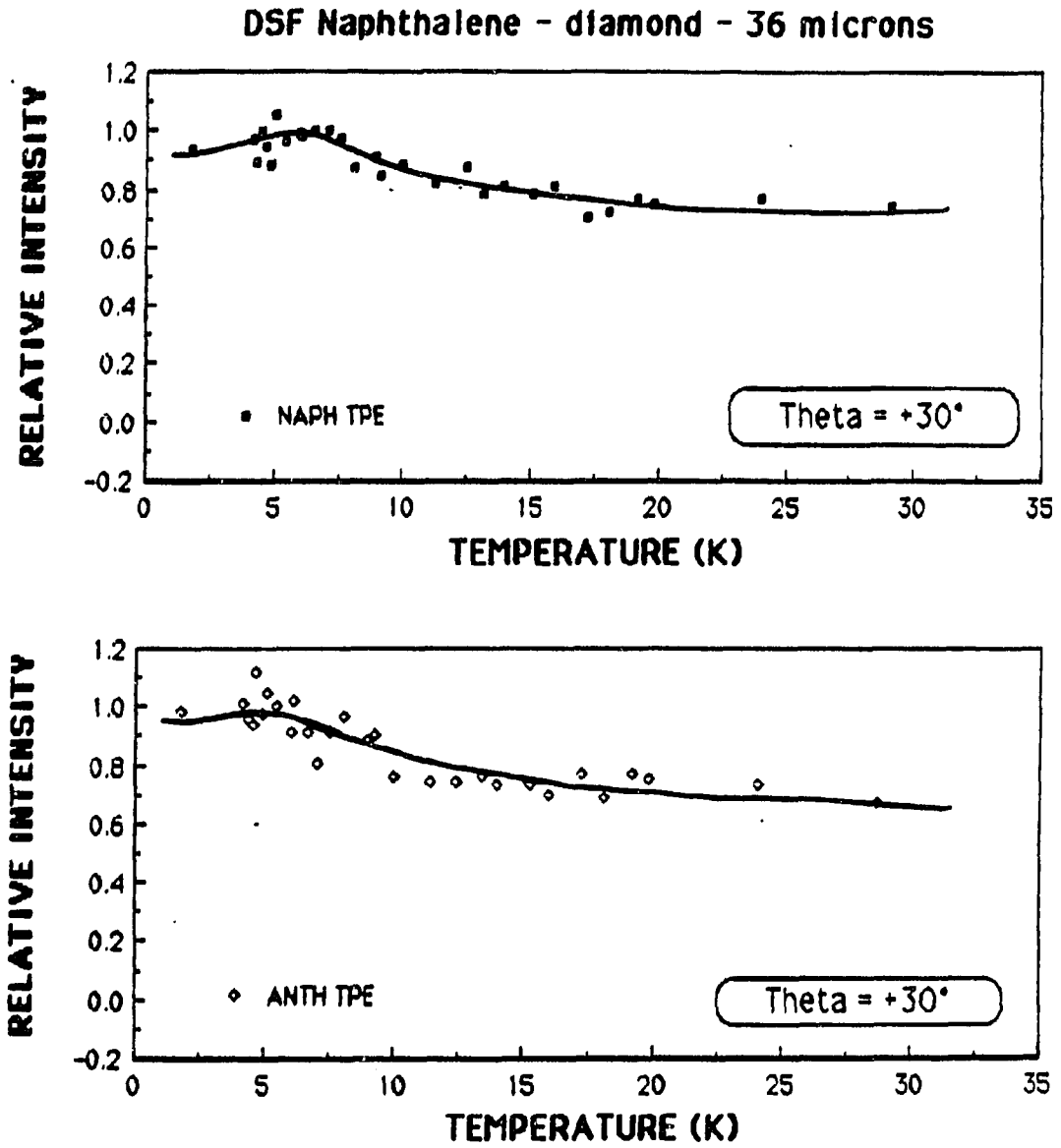

Figure 17. (continued). The solid lines are intended as visual guides only

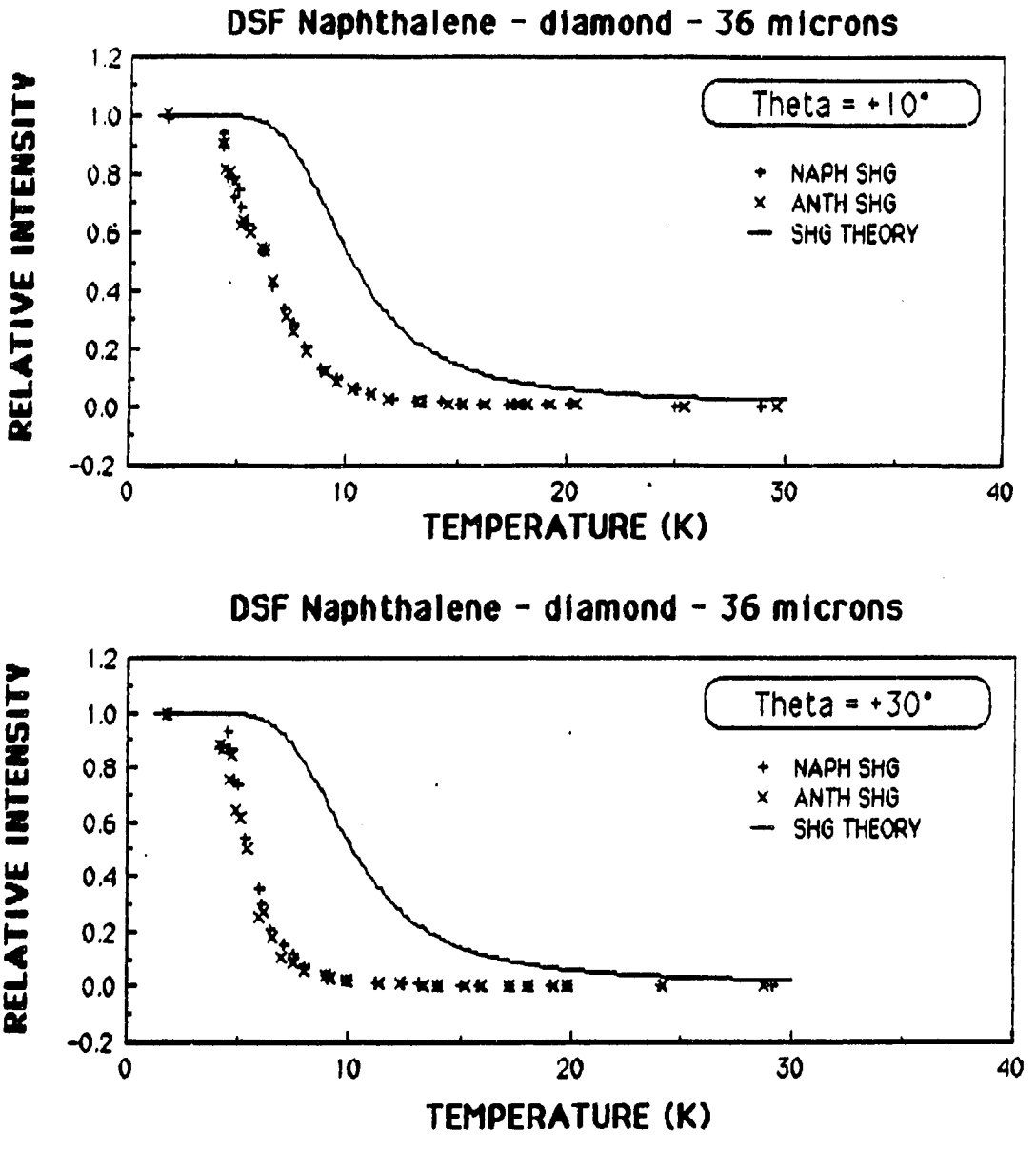

Figure 17. (continued). The solid lines are computed from the fusion rate expressions [40] using the experimentally determined temperature-dependent damping with $\gamma_0 = 3 \times 10^{10}\,\mathrm{sec}^{-1}$

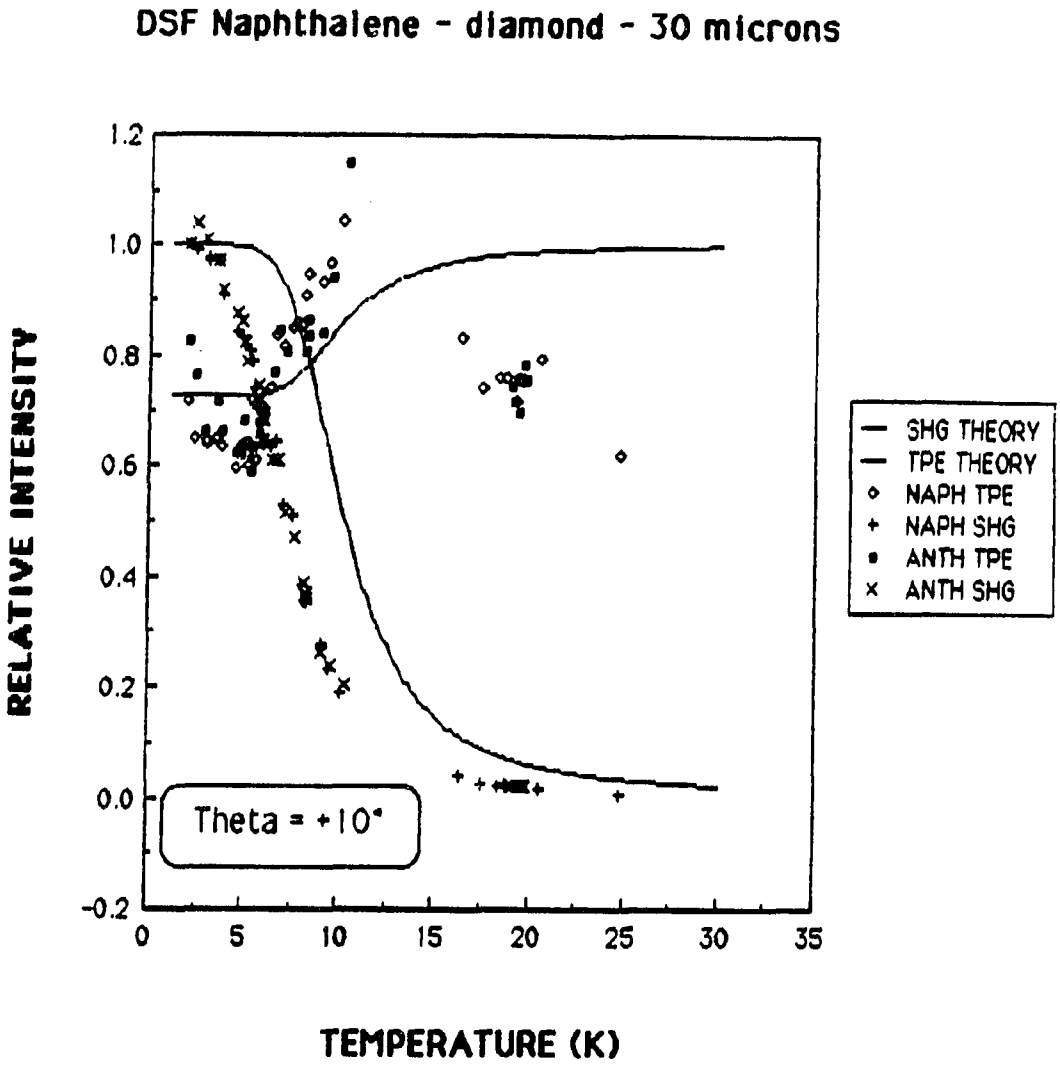

Figure 18. Integrated intensities of naphthalene and anthracene TPE and SHG profiles as a function of temperature at $\Theta_{ext} = +10°$ for a 30μ DSF naphthalene crystal (diamond habit). The solid lines are computed from the fusion rate expressions [40] using the experimentally determined temperature-dependent damping with $\gamma_0 = 3 \times 10^{10}$ sec^{-1}

anomalous behavior.

Directional Dispersion Behavior and Longitudinal Excitons

An earlier study by Stevenson (131c) provided frequency dispersion curves for several thicknesses of PSF naphthalene crystals. One thick crystal (55 μ) exhibited an interesting feature; that is, an additional peak in the TPE signal near the transverse exciton resonance. The observed behavior is shown in Figure 19. This additional peak displayed no orientational frequency dispersion, and the data were discussed in terms of the excitation of a longitudinal exciton (131c,227,228). A longitudinal exciton has its dipole moment of transition parallel to the propagation wavevector, $\underline{k}$, and does not interact with a transverse electric field (159). Therefore, the longitudinal exciton is expected to be dispersionless, as was observed by Stevenson (131c).

This same type of behavior also has been observed in the present study of PSF and DSF naphthalene crystals. At small angles of incidence, $|\Theta_{ext}| < 10°$, the additional signal intensity is comparable with the TPE signal. At angles $|\Theta_{ext}| > 10°$ the TPE signal was strong enough to preclude observation of the additional peak. No additional peak of this type was observed for SHG. The experimentally determined frequency dispersion curves for a 34 μ PSF naphthalene crystal (diamond habit) and several DSF naphthalene crystals are presented in Figures 21-24. Data in Figures 21-23 were obtained at liquid helium temperatures; data in Figure 24 were obtained at T = 5 K. Dispersion studies were also performed at

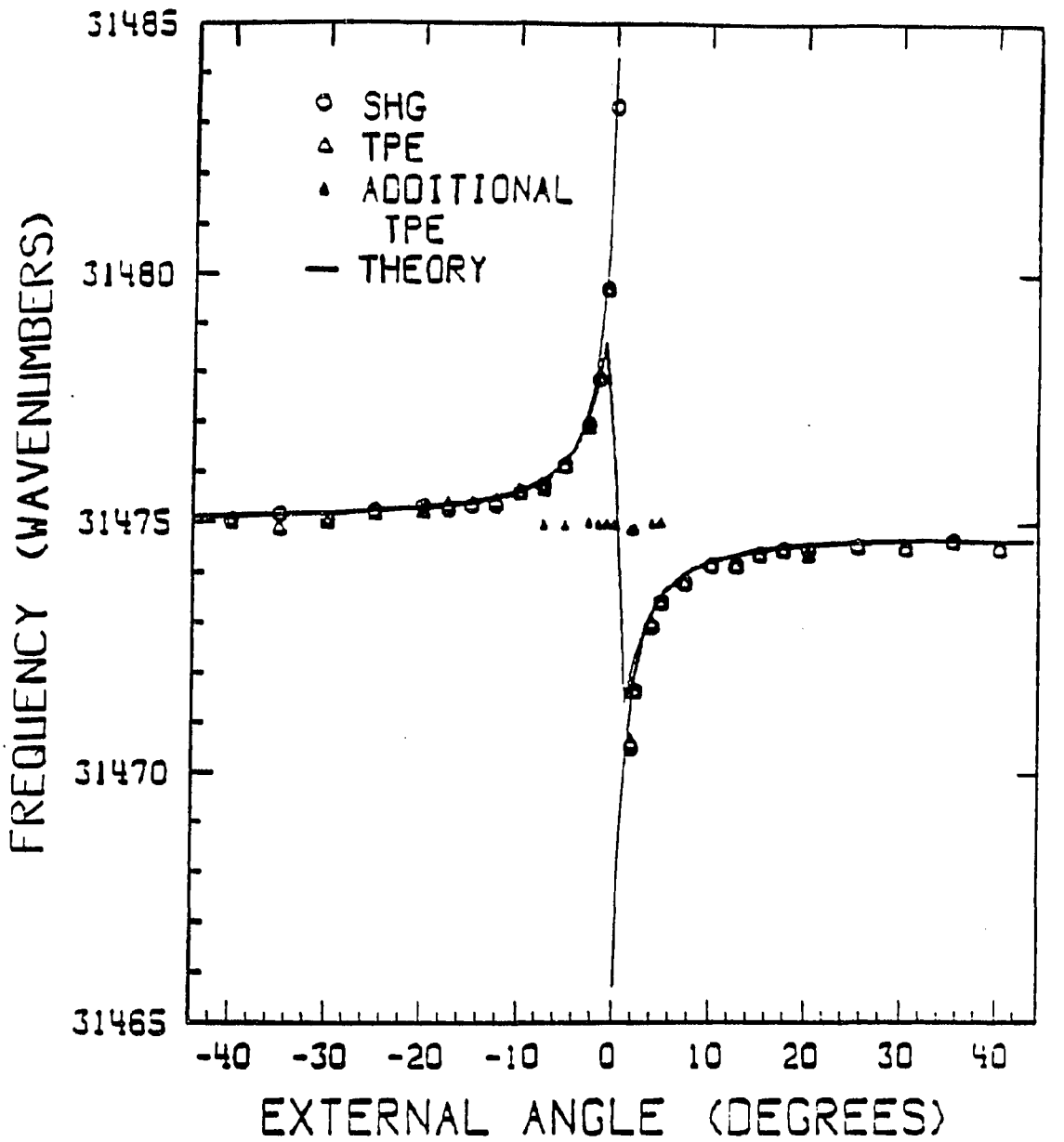

Figure 19. Experimentally determined directional dispersion of the extraordinary polariton in a 55 μ PSF naphthalene crystal (hexagonal habit). The theoretical curves are computed from equations [75] and [76] of reference (131c)

T = 20 K, however, the additional peak was not observed at this temperature, presumably due to the thermal broadening of the regular TPE and additional (longitudinal exciton) TPE signals.

The temperature broadening behavior also was studied for the crystals in this investigation. The experimental data are presented in Figure 24 along with a theoretical fit calculated from equation [49] using the previously determined (131,197) one-photon absorption phonon frequency, Ω, equal to 12 cm^{-1} and preexponential value, C, equal to 13 cm^{-1}; . The theoretical curve fits the longitudinal exciton broadening data quite well.

It is believed that this is the first observation of a longitudinal exciton in a mixed molecular organic crystal system. Details of the dynamics of the excitation are not fully understood.

It is interesting to note that Stevenson (131c) observed the longitudinal exciton only for a very thick crystal (55 μ); the 30 μ crystal studied by Stevenson (131c) showed no evidence of a longitudinal exciton. In the present investigation, however, the longitudinal exciton was observed for DSF and PSF crystals in the thickness range of 30-36 μ. The difference may have to do with the diamond crystal habit observed in the present investigation; the PSF crystals studied by Stevenson (131c) were all hexagonal habit (recall the discussion of the anomalous temperature behavior for diamond habit crystals, vide supra).

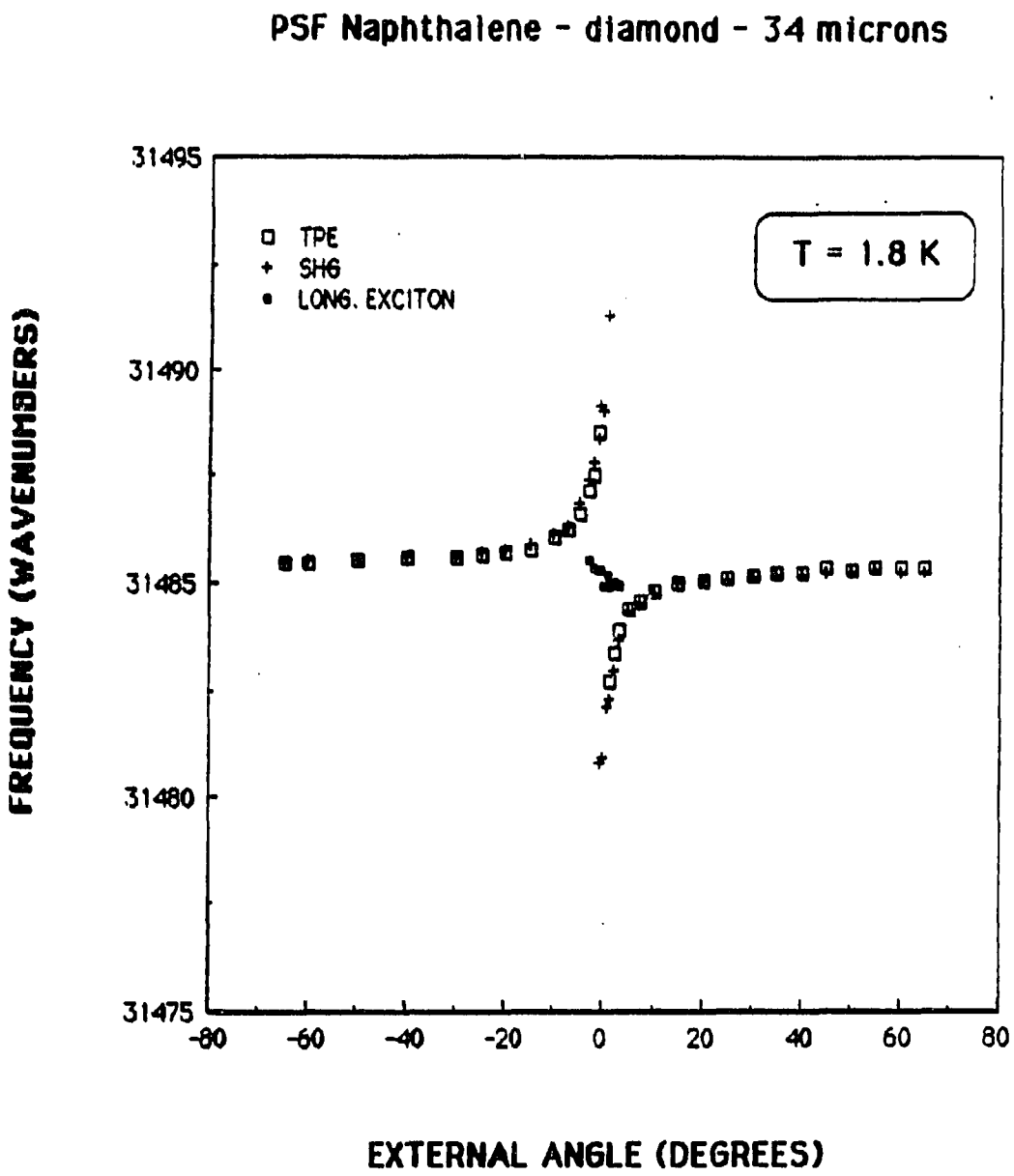

Figure 20. Experimentally determined directional dispersion of the extraordinary polariton in a 34 μ PSF naphthalene crystal (diamond habit) obtained at liquid helium temperature

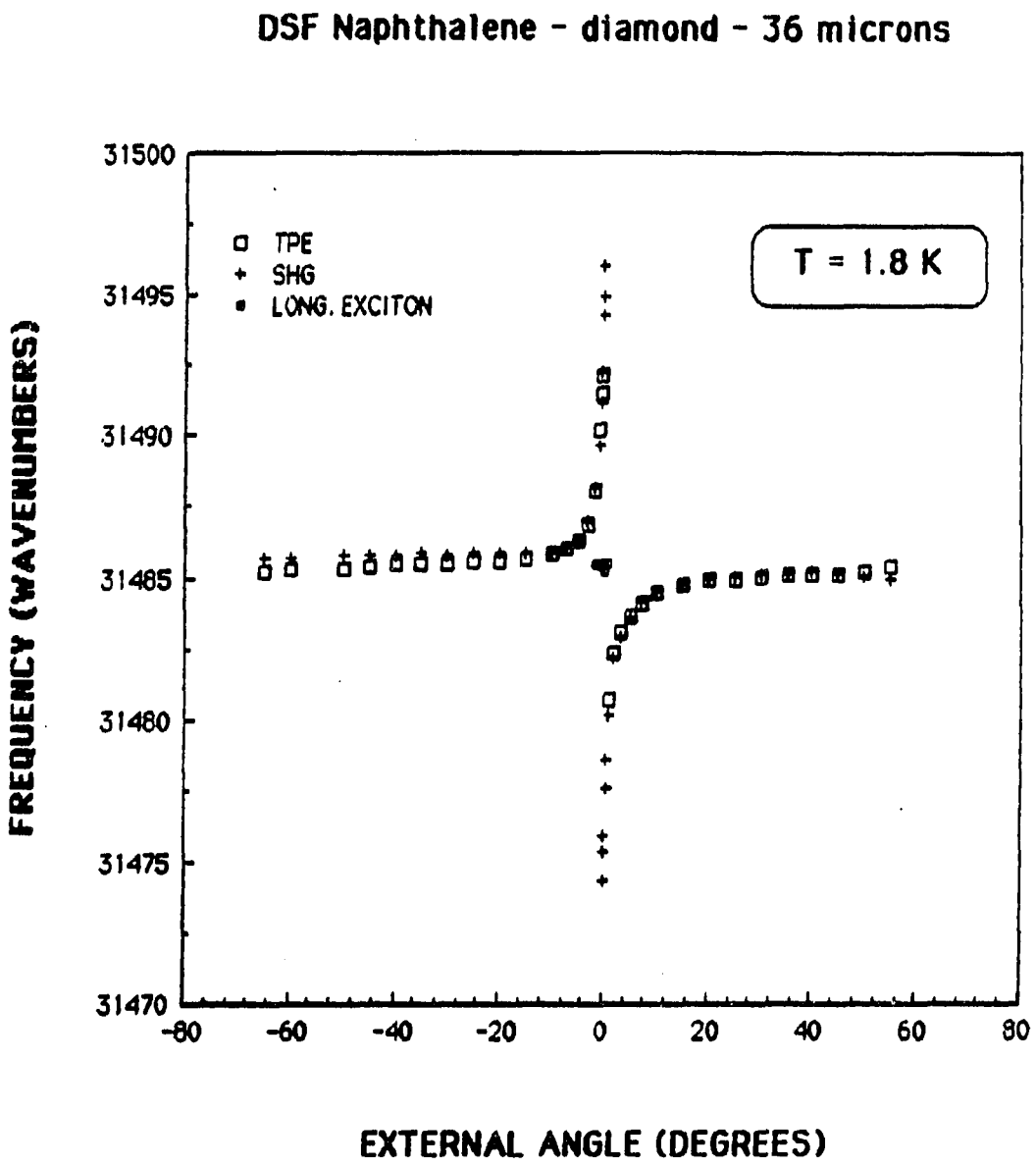

Figure 21. Experimentally determined directional dispersion of the extraordinary polariton in a 36 μ DSF naphthalene crystal (diamond habit) obtained at liquid helium temperature

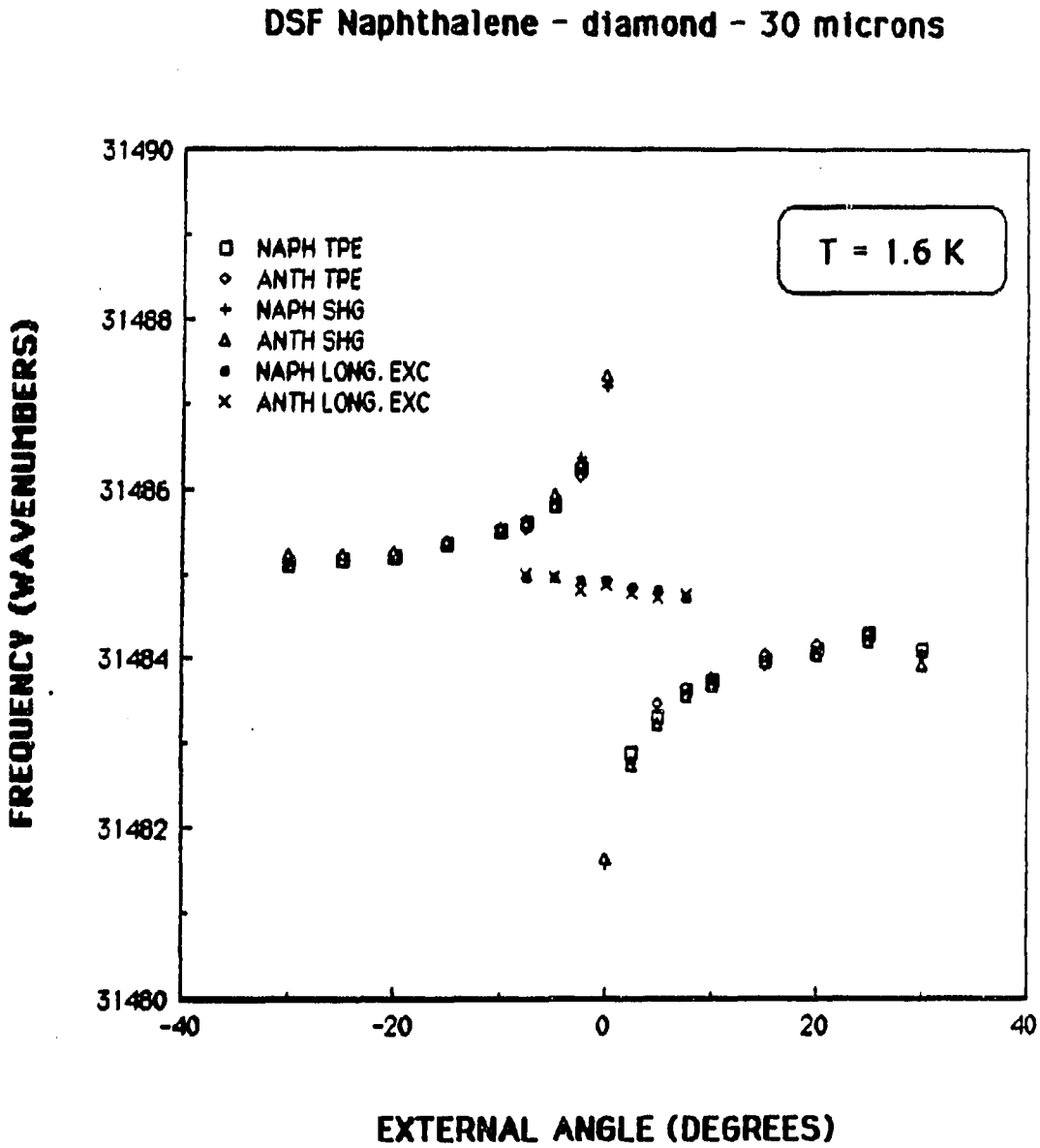

Figure 22. Experimentally determined directional dispersion of the extraordinary polariton in a 30 μ DSF naphthalene crystal (diamond habit) obtained at liquid helium temperature

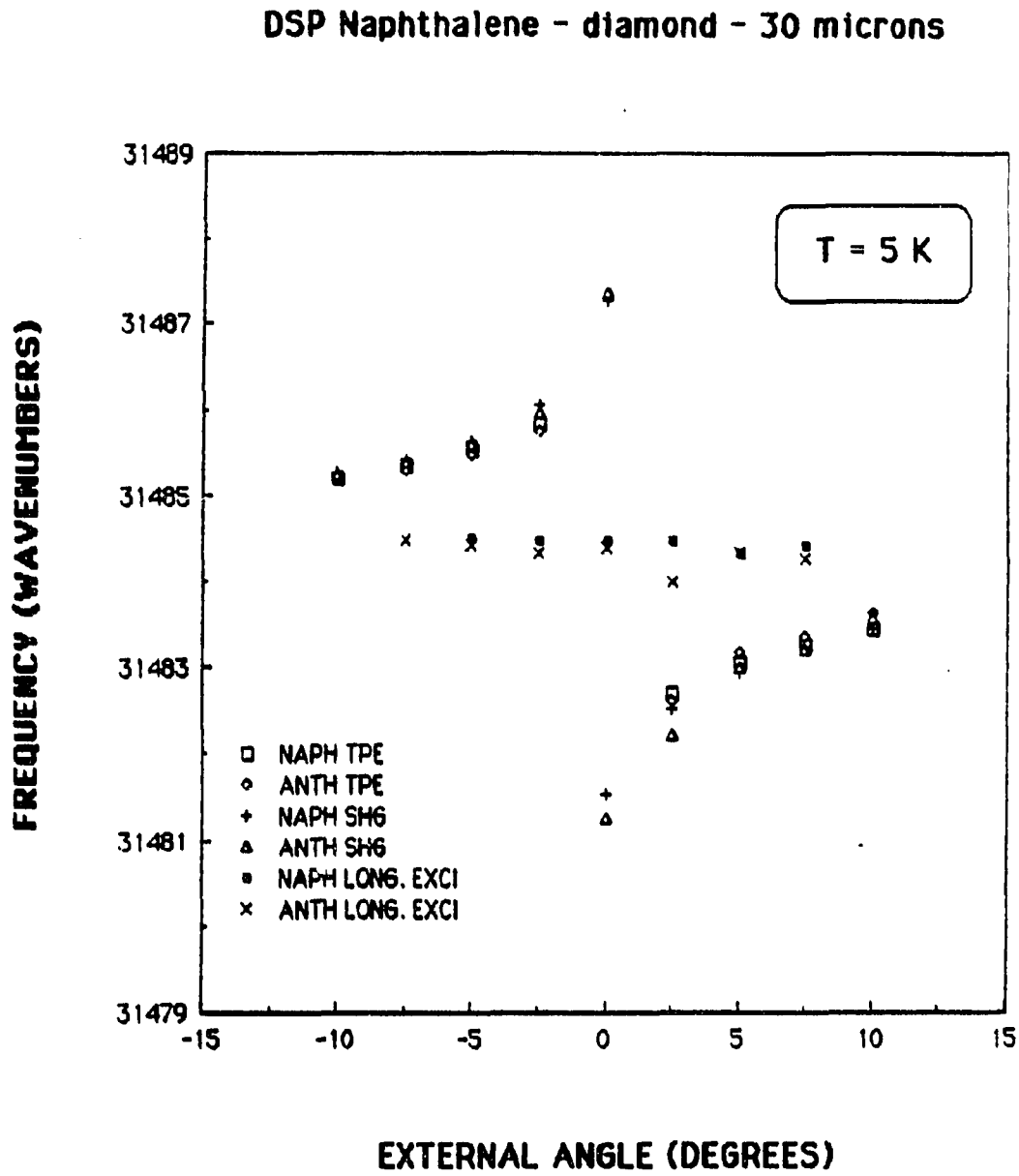

Figure 23. Experimentally determined directional dispersion of the extraordinary polariton in a 30 μ DSF naphthalene crystal (diamond habit) obtained at T - 5 K

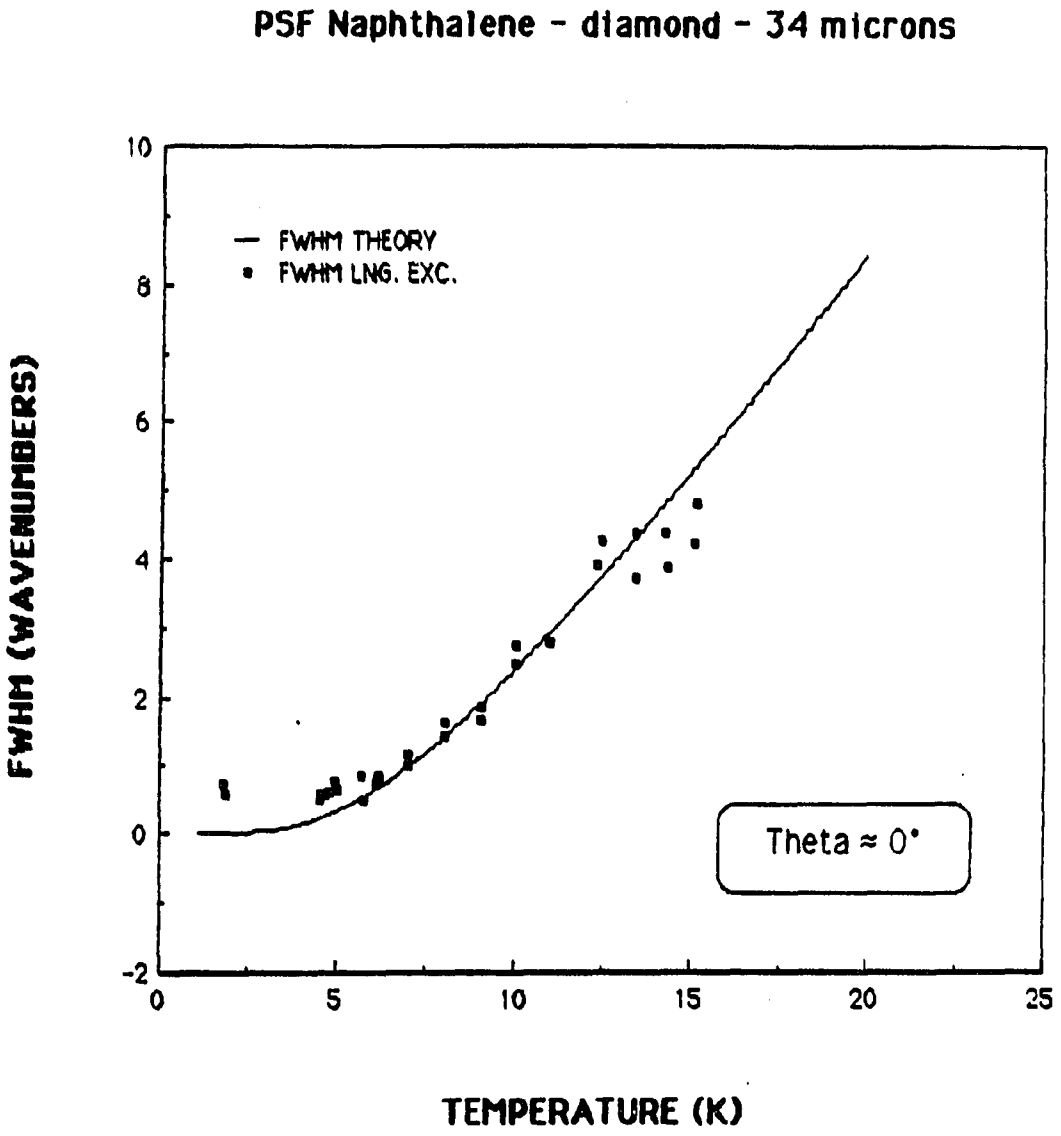

Figure 24. Temperature broadening data for the longitudinal exciton in a 34 μ PSF naphthalene crystal at near normal angle of incidence with respect to the c' axis. Data are offset by the residual low-temperature width, 0.64 cm^{-1}. The solid curve is obtained from expression [40], using phonon frequency of Ω = 12 cm^{-1} and preexponential value C = 13 cm^{-1}

CHAPTER V. SUMMARY AND CONCLUSIONS

Two-photon fluorescence excitation and second harmonic generation techniques have been used to prepare well-defined coherent polaritons in anthracene-doped, strain-free mounted naphthalene single crystals in the frequency region of the lowest singlet exciton system of naphthalene. Experiments have been performed under a variety of conditions, including low (1.6 K) and high (20-25 K) temperatures, and excitation of the (0,0) transition (coherent excitation) and excitation into the 311 cm^{-1} vibronic transition (incoherent excitation). The ratios of the intensity of the naphthalene signal to the intensity of the anthracene signal have been determined, and the results have been explained in terms of coherent electronic energy transfer at liquid helium temperatures. The ratio for coherent excitation at low temperature (I_N / I_A = 1.2) was found to be less than the ratio for coherent excitation at high temperature (I_N / I_A = 1.6). This result is consistent with the interpretation of coherent electronic energy transfer at low temperature and incoherent electronic energy transfer at high temperature. The intensity ratios were found to be equivalent for coherent excitation at high temperatures and incoherent excitation at both low and high temperatures. This result proved to be an important check on the experimental procedure.

Migration, i.e., motion, limited and capture, i.e., trapping, limited energy transfer regimes have been discussed. In the migration limited regime, the migration, or motion, of the excitation occurs on a timescale which is long compared to that of the trapping event; in the capture

limited regime, the migration occurs on a timescale which is short compared to the trapping event.

The migration limited regime is expected to be appropriate for polariton velocity-dependent scattering frequencies. However, previous studies (131) of pure strain-free (PSF) naphthalene crystals showed the scattering frequency to be velocity independent for velocities which were varied by three orders of magnitude. The velocity independence suggests, then, that the migration limited regime is inappropriate, and that the capture limited regime is in effect for the PSF naphthalene system. In the present study, it is argued that the anthracene-doped, strain-free mounted (DSF) naphthalene system is also in the capture limited regime. Since the distance between scatterers is shorter in the DSF crystals than in the PSF crystals, the time it takes to reach the scatterers is less. Additionally, in the present investigation of DSF crystals, no velocity dependence was found for the scattering frequency; this result further supports the argument for capture limited energy transfer.

A derivation of the trapping and trap scattering frequencies has been presented, and the result, $\gamma_T = 2\pi a^3 n_T p$, was found to be a function of the trapping or scattering radius, a, the number density of traps, n_T, and the trapping or scattering probability, p. The result obtained for the trapping or scattering frequency, γ_T, was compared to the result reported by Parris and Kenkre (78) for the capture limited regime and was found to be formally identical.

The trapping mechanism was discussed in terms of: 1. the polariton scattering off a trap with subsequent trapping (at trapping frequency γ_{tr})

and 2. the polariton scattering off a trap (at scattering frequency γ_{sc}), without subsequent trapping, followed by thermalization of the polariton (different $\underline{k}$-sense). A derivation of the branching ratio of these two types of trap-related events has been presented, and the branching ratio, γ_{sc}/γ_{tr}, of the trap scattering frequency, γ_{sc}, to the trapping (capture) frequency, γ_{tr}, was calculated using the experimentally determined naphthalene-to- anthracene two-photon fluorescence excitation (TPE) intensity ratios presented in Table I. The branching ratio, γ_{sc}/γ_{tr}, was found to be approximately 5 to 1. This result is significant, because, in most theoretical (and also experimental) treatments, the possibility of scattering with the trap <u>not</u> followed by trapping has been sadly neglected!

The branching ratio result, then, was used to determine the trap scattering and capture frequencies; the trap scattering frequency, γ_{sc}, was calculated to be 2.5×10^{10} sec^{-1}, and the capture frequency, γ_{tr}, was determined to be 5×10^{9} sec^{-1}. The scattering and capture probabilities, p_{sc} and p_{tr}, respectively, have been calculated for several values of the trap radius, and the results have been compared to the rate of encounters of the polariton with a trap, R_{enc}. For a trap radius smaller than about 100 Å, the encounter rate is less than the trapping event probability, and, therefore, the motion limited regime is suggested. For trap radii larger than 100 Å, the encounter rate is greater than the trapping event probability, and, therefore, the capture limited regime applies.

The temperature behavior of the TPE and SHG signals has been examined in the framework of the polariton fusion theory. Thermal broadening data generally show good agreement with theory at low

temperatures (T< 7 K), but deviations from theory are observed as the temperature is increased, with the broadening, generally, occurring at a faster rate, with respect to temperature, than in PSF crystals. The temperature behavior of the nonlinear signal intensities also has been studied. Poor agreement with theory was observed. For all DSF crystals studied, the TPE signal was observed to increase from a constant low temperature value to a maximum at temperatures in the range ≈6 K to 10 K, followed by a decrease in the intensity. This behavior has been discussed in terms of the crystal habit, i.e., hexagonal plates and diamond plates, and real temperature effects which may be exhibited at lower temperatures for doped crystals than for pure crystals. The decrease in TPE signal intensity was observed in this study for a hexagonal habit PSF naphthalene crystal; the decrease begins around 15 K and may not have been observed previously because of the shorter temperature range covered in studies performed by Stevenson (131c). The results for a diamond habit PSF naphthalene crystal, in the present investigation, show the decrease in intensity occurring at lower temperatures (6-8 K); this result for the diamond habit PSF crystal is the same as that observed for the diamond habit DSF crystals.

The directional dispersion behavior was studied for a 34 μ diamond habit PSF crystal, and for a 36 μ and a 30 μ diamond habit DSF crystal. Anomalous behavior was observed for all three crystals; at external angles, Θ_{ext}, between -10° and +10°, a second peak was observed in the TPE signal. This peak showed no orientational dispersion, like that which is observed for the regular TPE signal, and was observed to broaden much

more rapidly with increasing temperature than the regular TPE signal. A similar peak was not observed for the second harmonic generation (SHG) signal. The additional peak is attributed to a longitudinal exciton. It is interesting to note that Stevenson (131c) observed a longitudinal exciton for a thick (55 μ) PSF crystal, but did not observe the longitudinal exciton for thinner crystals, including a 30 μ crystal. The observation again is made that the PSF crystals studied by Stevenson (131c) were of the hexagonal habit, and one must consider the possibility that, in the present investigation, the observation of the longitudinal exciton for crystal thicknesses of 30-36 μ is related to the crystal habit.

The dynamics of the scattering process involved in populating the longitudinal exciton is not well understood, but the thermal broadening of the longitudinal exciton was observed to be the same as the thermal broadening of the one-photon absorption (OPA) signal (see references 131a,c).

It is clear from the results presented in this dissertation that coherent electronic energy transport does occur at low temperatures in the anthracene-doped naphthalene system studied. The advantage of the method used in this investigation over the methods used by others (5,16-20,37,62-69,224) is the preparation of polaritons with well-defined directionality, or $\underline{k}$-sense, in the present study. Future studies should include more experiments, of the type discussed in this dissertation, on both hexagonal habit and diamond habit pure, strain-free naphthalene crystals. Such studies, hopefully, will provide an understanding of the apparent crystal habit-related behavior.

REFERENCES

1. Bernard, J.E.; Berry, D.E.; Williams, F.: in Energy Transfer Processes in Condensed Matter , ed. B. DiBartolo, Plenum Press, New York (1984), p.1.

2. a. Silbey, R.: Ann. Rev. Phys. Chem. 27 , 203 (1976).
   b. Silbey, R.: in Spectroscopy and Excitation Dynamics of Condensed Molecular Systems, ed. V.M. Agranovich and R.M. Hochstrasser, North-Holland Publishing, New York (1983), p.1.

3. Harris, C.B.; Zwemer, D.A.: Ann. Rev. Phys. Chem. 29 , 473 (1978).

4. Wolf, H.C.: in Organic Molecular Aggregates , ed. P. Reineker; H. Haken; H.C. Wolf, Springer-Verlag, New York (1983), p.2.

5. Kopelman, R.: in Spectroscopy and Excitation Dynamics of Condensed Molecular Systems, ed. V.M. Agranovich and R.M. Hochstrasser, North-Holland Publishing, New York (1983), p.139.

6. Kenkre, V.M.: in Energy Transfer Processes in Condensed Matter , ed. B. DiBartolo, Plenum Press, New York (1984), p.205.

7. Haarer, D.; Philpott, M.R.: in Spectroscopy and Excitation Dynamics of Condensed Molecular Systems, ed. V.M. Agranovich and R.M. Hochstrasser, North-Holland Publishing, New York (1983), p.27.

8. Wolf, H.C.; Benz, K.W.: Pure Appl. Chem. 27 , 439 (1970).

9. Peter, G.; Ries, B.; Bässler, H.: Chem. Phys. 80 , 289 (1983).

10. Vankan, J.M.J.; Veeman, W.S.: Chem. Phys. Lett. 92 , 519 (1982).

11. Williams, J.O.; Clarke, B.P.; Thomas, J.M.; Shaw, M.J.: Chem. Phys. Lett. 38 , 41 (1976).

12. Weinzierl, G.; Friedrich, J.: Chem. Phys. Lett. 83 , 204 (1981).

13. a. Giachiano, G.G.; Kearns, D.R.: J. Chem. Phys. 52, 2964 (1970).
b. Giachiano, G.G.; Kearns, D.R.: J. Chem. Phys. 53, 3886 (1970).

14. a. Yamauchi, S.; Saigusa, H.; Azumi, T.: J. Chem. Phys. 74, 5335 (1981).
b. Yamauchi, S.; Komada, Y.; Hirota, N.: Chem. Phys. Lett. 93, 133 (1982).

15. Powell, R.C.; Soos, H.G.: J. Lumin. 11, 1 (1975).

16. a. Powell, R.C.; Kepler, R.G.: Phys. Rev. Lett. 22, 636 (1969).
b. Powell, R.C.; Kepler, R.G.: Phys. Rev. Lett. 22, 1232 (1969).
c. Powell, R.C.; Kepler, R.G.: J. Lumin. 1, 254 (1969).

17. a. Powell, R.C.: Phys. Rev. B 2, 1159 (1970).
b. Powell, R.C.: Phys. Rev. B 4, 628 (1971).
c. Powell, R.C.: J. Chem. Phys. 58, 920 (1973).

18. Rosenstock, H.B.: Phys. Rev. 187, 1166 (1969).

19. Powell, R.C.: Phys. Rev. B 2, 1207 (1970).

20. Powell, R.C.; Soos, Z.G.: Phys. Rev. B 5, 1547 (1972).

21. Soos, Z.G.; Powell, R.C.: Phys. Rev. B 6, 4035 (1972).

22. a. Blumen, A.; Zumofen, G.: J. Chem. Phys. 75, 892 (1981).
b. Zumofen, G.; Blumen, A.: J. Chem. Phys. 76, 3713 (1982).
c. Blumen, A.; Zumofen, G.: J. Chem. Phys. 77, 5127 (1982).

23. a. Zumofen, G.; Blumen, A.: Chem. Phys. Lett. 88, 63 (1982).
b. Blumen, A.; Klafter, J.; Zumofen, G.: Phys. Rev. B 27, 3429 (1983).
c. Blumen, A.; Zumofen, G.: J. Stat. Phys. 30, 487 (1983).
d. Zumofen, G.; Blumen, A.: Chem. Phys. Lett. 98, 393 (1983).

24. Klafter, J.; Silbey, R.: J. Chem. Phys. 74, 3510 (1981).

25. Dlott, D.D.; Fayer, M.D.; Wieting, R.D.: J. Chem. Phys. 67, 3808 (1977).

26. Klafter, J.; Blumen, A.: in Energy Transfer Processes in Condensed Matter, ed. B. DiBartolo, Plenum Press, New York (1984), p.621.

27. Chow, H.C.; Powell, R.C.: Phys. Rev. B 21, 3785 (1980).

28. Shelby, R.M.; Zewail, A.H.; Harris, C.B.: J. Chem. Phys. 64, 3192 (1976).

29. Guttler, W.; Von Schutz, J.U.; Wolf, H.C.: Chem. Phys. 24, 159 (1977).

30. Heidersdorf, C.P.: Mol. Cryst. Liq. Cryst. 27, 141 (1974).

31. Aartsma, T.J.; Wiersma, D.A.: Chem. Phys. Lett. 54, 415 (1978).

32. Skinner, J.L.; Anderson, H.C.; Fayer, M.D.: J. Chem. Phys. 75, 3195 (1981).

33. Fayer, M.D.: in Spectroscopy and Excitation Dynamics of Condensed Molecular Systems, ed. V.M. Agranovich and R.M. Hochstrasser, North-Holland Publishing, New York (1983), p.186.

34. Talapatra, G.B.; Misra, T.N.: J. Chem. Phys. 75, 3684 (1981).

35. Kazzaz, A.A.; Zahlan, A.B.: Phys. Rev. 124, 90 (1961).

36. a. Agranovich, V.M.; Konobeev, Y.V.: Sov. Phys.- Solid State 5, 999 (1963).
b. Agranovich, V.M.; Konobeev, Y.V.: Phys. Status Solidi 27, 435 (1968).

37. Auweter, H.; Mayer, U.; Schmid, D.: Z. Naturforsch. 33A, 651 (1978).

38. Shatz, S.; Halpern, V.: Chem. Phys. 91, 237 (1984).

39. Burland, D.M.; Konzelmann, U.; Macfarlane, R.M.: J. Chem. Phys. 67, 1926 (1977).

40. Fayer, M.D.; Harris, C.B.: Phys. Rev. B 9 , 748 (1974).

41. Diott, D.D.; Schosser, C.L.; Chronister, E.L.: Chem. Phys. Lett. 90 , 386 (1982).

42. Hess, L.A.; Prasad, P.N.: J. Chem. Phys. 78 , 626 (1983).

43. Hesp, B.H.; Wiersma, D.A.: Chem. Phys. Lett. 75 , 423 (1980).

44. a. Francis, A.H.; Harris, C.B.: J. Chem. Phys. 55 , 3595 (1971).
b. Francis, A.H.; Harris, C.B.: Chem. Phys. Lett. 9 , 181 (1971).
c. Francis, A.H.; Harris, C.B.: Chem. Phys. Lett. 9 , 188 (1971).

45. a. Zewail, A.H.; Harris, C.B.: Chem. Phys. Lett. 28 , 8 (1974).
b. Zewail, A.H.; Harris, C.B.: Phys. Rev. B 11 , 935 (1975).
c. Zewail, A.H.; Harris, C.B.: Phys. Rev. B 11 , 952 (1975).

46. a. Botter, B.J.; Dicker, A.I.M.; Schmidt, J.: Mol. Phys. Lett. 36 , 129 (1978).
b. Botter, B.J.; Nonhof, C.J.; Schmidt, J.; Van der Waals, J.H.: Chem. Phys. Lett. 43 , 210 (1976).

47. Harris, C.B.; Fayer, M.D.: Phys. Rev. B 10 , 1784 (1974).

48. Schmidt, J.: in Organic Molecular Aggregates , ed. P. Reineker; H. Haken; H.C. Wolf, Springer-Verlag, New York (1983), p.56.

49. a. Schmidberger, R.; Wolf, H.C.: Chem. Phys. Lett. 25 , 185 (1974).
b. Schmidberger, R.; Wolf, H.C.: Chem. Phys. Lett. 32 , 21 (1975).

50. Haken, H.; Strobl, T.: Z. Phys. 262 , 135 (1973).

51. Park, J.M.; Reddoch, A.H.: Chem. Phys. Lett. 91 , 117 (1982).

52. Schmid, U.; Reineker, P.: Chem. Phys. Lett. 94 , 510 (1983).

53. Lewellyn, M.T.; Zewail, A.H.; Harris, C.B.: J. Chem. Phys. 63 , 3687 (1975).

54. Vaubel, G.; Bässler, H.: Mol. Cryst. Liq. Cryst. 12, 47 (1970).

55. Cohen, M.D.; Klein, E.; Ludmer, Z.: Chem. Phys. Lett. 37, 611 (1976).

56. a. Kallmann, H.; Vaubel, G.; Bässler, H.: Phys. Status Solidi B44, 813 (1971).
b. Vaubel, G.; Bässler, H.; Mobius, D.: Chem. Phys. Lett. 10, 334 (1971).
c. Kurczewska, H.; Bässler, H.: J. Lumin. 15, 261 (1977).

57. Glushko, E.Y.: Sov. Phys. Solid State 25, 488 (1983).

58. Heisel, F.; Miehe, J.A.; Schott, M.; Sipp, B.: Mol. Cryst. Liq. Cryst. 4, 251 (1978).

59. Yuan, W.; Rabinovich, B.S.: J. Chem. Phys. 80, 1687 (1984).

60. Greene, B.I.; Millard, R.R.: Phys. Rev. Lett. 55, 1331 (1985).

61. a. Brown, R.; Lemaistre, J.P.; Megel, J.; Pee, P.; Dupuy, F.; Kottis, P.: J. Chem. Phys. 76, 5719 (1982).
b. Brown, R.; Pee, P.; Dupuy, F.; Kottis, P.: J. Phys. C76, 5549 (1984).

62. a. Argyrakis, P.; Kopelman, R.: J. Chem. Phys. 66, 3301 (1977).
b. Argyrakis, P.; Kopelman, R.: Chem. Phys. Lett. 61, 187 (1979).
c. Kopelman, R.; Argyrakis, P.: J. Chem. Phys. 72, 3053 (1980).
d. Argyrakis, P.; Kopelman, R.: Chem. Phys. 51, 9 (1980).
e. Argyrakis, P.; Kopelman, R.: Chem. Phys. 78, 251 (1983).

63. a. Monberg, E.M.; Kopelman, R.: Chem. Phys. Lett. 58, 492 (1978).
b. Monberg, E.M.; Kopelman, R.: Chem. Phys. Lett. 58, 497 (1978).

64. a. Argyrakis, P.; Anacker, L.W.; Kopelman, R.: J. Stat. Phys. 36, 579 (1984).
b. Argyrakis, P.; Blumen, A.; Kopelman, R.; Zumofen, G.: J. Phys. Chem. 88, 1973 (1984).
c. Keramiotis, A.; Argyrakis, P.; Kopelman, R.: Phys. Rev. B 31, 4617

(1985).
d. Argyrakis, P.; Kopelman, R.: Phys. Rev. B 29, 511 (1984).
e. Argyrakis, P.; Kopelman, R.: J. Chem. Phys. 81, 1015 (1984).
f. Argyrakis, P.; Kopelman, R.: Phys. Rev. B 31, 6008 (1985).
g. Argyrakis, P.; Kopelman, R.: J. Chem. Phys. 83, 3099 (1985).
h. Argyrakis, P.; Kopelman, R.: J. Chem. Phys. 84, 1047 (1986).

65. Kopelman, R.: J. Stat. Phys. 42, 185 (1986).

66. a. Kopelman, R.; Klymko, P.W.; Newhouse, J.S.; Anacker, L.W.: Phys. Rev. B 29, 3747 (1984).
b. Newhouse, J.S.; Argyrakis, P.; Kopelman, R.: Chem. Phys. Lett. 107, 48 (1984).
c. Anacker, L.W.; Kopelman, R.; Newhouse, J.S.: J. Stat. Phys. 36, 591 (1984).
d. Anacker, L.W.; Kopelman, R.: J. Chem. Phys. 81, 6402 (1984).
e. Newhouse, J.S.; Kopelman, R.: Phys. Rev. B 31, 1677 (1985).
f. Anacker, L.W.; Kopelman, R.: J. Phys. Chem. 89, 4758 (1985).
g. Kopelman, R.: J. Physique 46, 9 (1985).
h. Kopelman, R.: in Fractals in Physics, ed. L. Pietronero, E. Tosatti, Elsevier Science, New York (1986), p.369.
i. Kopelman, R; Parus, S.; Prasad, J.: Phys. Rev. Lett. 56, 1742 (1986).

67. a. Gentry, S.T.; Kopelman, R.: J. Phys. Chem. 88, 3170 (1984).
b. Gentry, S.T.; Kopelman, R.: J. Chem. Phys. 81, 3014 (1984).
c. Gentry, S.T.; Kopelman, R.: J. Chem. Phys. 81, 3022 (1984).

68. a. Gentry, S.T.; Kopelman, R.: Chem. Phys. Lett. 93, 264 (1982).
b. Gentry, S.T.; Kopelman, R.: J. Chem. Phys. 78, 373 (1983).

69. a. Parson, R.P.; Kopelman, R.: Chem. Phys. Lett. 87, 528 (1982).
b. Parson, R.P.; Kopelman, R.: Chem. Phys. Lett. 104, 320 (1984).
c. Parson, R.P.; Kopelman, R.: Chem. Phys. 89, 265 (1984).
d. Parson, R.P.; Kopelman, R.: J. Phys. Chem. 88, 2931 (1984).
e. Parson, R.P.; Kopelman, R.: J. Chem. Phys. 82, 3692 (1985).

70. Colson, S.D.; George, S.M.; Keyes, T.; Vaida, V.: J. Chem. Phys. 67, 4941

(1977).

71. Anderson, P.W.: Phys. Rev. 109, 1492 (1958).

72. Rips, I.; Jortner, J.: Chem. Phys. 99, 207 (1985).

73. a. Kenkre, V.M.; Knox, R.S.: Phys. Rev. B 9, 5279 (1974).
b. Kenkre, V.M.; Knox, R.S.: Phys. Rev. Lett. 33, 803 (1974)

74. Kenkre, V.M.: Phys. Rev. B 18, 4064 (1978).

75. a. Wong, Y.M.; Kenkre, V.M.: Phys. Rev. B 20, 2438 (1979).
b. Kenkre, V.M.: Chem. Phys. 36, 377 (1979).

76. Kenkre, V.M.; Wong, Y.M.: Phys. Rev. B 23, 3748 (1981).

77. a. Kenkre, V.M.: Chem. Phys. Lett. 93, 260 (1982).
b. Kenkre, V.M.; Parris, P.E.: Phys. Rev. B 27, 3221 (1983).

78. Parris, P.E.; Kenkre, V.M.: Chem. Phys. Lett. 125, 189 (1986).

79. Kenkre, V.M.; Schmid, D.: Chem. Phys. Lett. 94, 603 (1983).

80. Kenkre, V.M.; Parris, P.E.; Schmid, D.: Phys. Rev. B 32, 4946 (1985).

81. Kenkre, V.M.; Schmid, D.: Preprint, Chem. Phys. (1984)

82. Honig, A.; Moroz, M.: Solid State Commun. 44, 1481 (1982).

83. Travnikov, V.V.; Krivolapchuk, V.V.: JETP Lett. 37, 496 (1983).

84. Masumoto, Y.; Shionoya, S.: Phys. Rev. B 30, 1076 (1984).

85. a. Aoyagi, Y.; Segawa, Y.; Namba, S.: Phys. Rev. B 25, 1453 (1982).
b. Segawa, Y.; Aoyagi, Y.; Komuro, S.; Namba, S.: Phys. Rev. Lett. 50, 436 (1983).

86. Klingshirn, C.: in Energy Transfer Processes in Condensed Matter, ed.

B. DiBartolo, Plenum Press, New York (1984), p.285.

87. Blasse, G.: in Energy Transfer Processes in Condensed Matter, ed. B. DiBartolo, Plenum Press, New York (1984), p.251.

88. Boulon, G.: in Energy Transfer Processes in Condensed Matter, ed. B. DiBartolo, Plenum Press, New York (1984), p.603.

89. Powell, R.C.: in Energy Transfer Processes in Condensed Matter, ed. B. DiBartolo, Plenum Press, New York (1984), p.655.

90. Schwentner, N.; Koch, E.E.; Jortner, J.: in Energy Transfer Processes in Condensed Matter, ed. B. DiBartolo, Plenum Press, New York (1984), p.417.

91. Soos, Z.: Ann. Rev. Phys. Chem. 25, 121 (1974).

92. McClure, D.S.: Solid State Phys. 8, 1 (1960).

93. Wolf, H.C.: Solid State Phys. 9, 1 (1961).

94. Hochstrasser, R.M.: Rev. Mod. Phys. 34, 531 (1962).

95. Armstrong, J.A.; Bloembergen, N.; Ducuing, J.; Pershan, P.S.: Phys. Rev. 127, 1918 (1962).

96. a. Shen, Y.R.: Rev. Mod. Phys. 48, 1 (1976).
b. Shen, Y.R.: in Proc. Intl. Sch. Phys. "Enrico Fermi" Course LXIV, ed. N. Bloembergen, North-Holland, New York (1977), p.170.

97. a. Bloembergen, N.: Rev. Mod. Phys. 54, 685 (1982).
b. Bloembergen, N.: Science 216, 1057 (1982).

98. Hochstrasser, R.M.; Trommsdorff, H.P.: Acc. Chem. Res. 16, 376 (1983).

99. Butcher, P.N.: Nonlinear Optical Phenomena, Bulletin 200, Engineering Experimental Station, Ohio State University, Columbus,

Ohio (1965).

100. Bloembergen, N.: Nonlinear Optics , W.A. Benjamin, Reading, Mass. (1965).

101. Franken, P.A.; Hill, A.E.; Peters, C.W.; Weinrich, G.: Phys. Rev. Lett. 7 , 118 (1961).

102. Kaiser, W.; Garrett, C.G.B.: Phys. Rev. Lett. 7 , 229 (1961).

103. Göppert-Mayer, M.: Ann. Physik 9 , 273 (1931).

104. Pao, Y.H.; Rentzepis, P.M.: J. Chem. Phys. , 1281 (1965).

105. Honig, B.; Jortner, J.; Szöke, A.: J. Chem. Phys. 46 , 2714 (1967).

106. Mahan, G.D.: Phys. Rev. 170 , 825 (1968).

107. Bader, T.R.; Gold, A.: Phys. Rev. 171 , 997 (1968).

108. Denisov, M.M.; Makarov, V.P.: J. Phys. C 5 , 2651 (1972).

109. Swofford, R.L.; McClain, W.M.: Chem. Phys. Lett. 34 , 455 (1975).

110. a. Hopfield, J.J.; Worlock, J.M.: Phys. Rev. Lett. 11 , 414 (1963).
b. Hopfield, J.J.; Worlock, J.M.: Phys. Rev. 137 , A1455 (1965).

111. Peticolas, W.L.; Rieckhoff, K.E.: J. Chem. Phys. 39 , 1347 (1963).

112. a. Hochstrasser, R.M.; Wessel, J.E.: Chem. Phys. Lett. 24 , 1 (1974).
b. Hochstrasser, R.M.; Klimcak, C.M.; Meredith, G.R.: J. Chem. Phys. 70, 870 (1979).
c. Ho, F.; Tsay, W.S.; Trout, J.; Velsko, S.; Hochstrasser, R.M.: Chem. Phys. Lett. 97 , 141 (1983).

113. Mikami, N.; Ito, M.: J. Chem. Phys. 64 , 3077 (1976).

114. a. Hochstrasser, R.M.; Sung, H.N.; Wessel, J.E.: J. Chem. Phys. 58 , 4694

(1973).
b. Hochstrasser, R.M.; Sung, H.N.; Wessel, J.E.: Chem. Phys. Lett. 24, 168 (1974).
c. Hochstrasser, R.M.; Sung, H.N.: J. Chem. Phys. 66, 3276 (1977).

115. Fang, H.L.; Gustafson, T.L.; Swofford, R.L.: J. Chem. Phys. 78, 1663 (1983).

116. Dick, B.; Hohlneicher, G.: Chem. Phys. Lett. 84, 471 (1981).

117. Stevenson, S.H.; Johnson, C.K.; Small, G.J.: J. Phys. Chem. 85, 2709 (1981).

118. Iannuzzi, M.; Polacco, E.: Phys. Rev. Lett. 13, 371 (1964).

119. Bergman, A.; Jortner, J.: Chem. Phys. Lett. 15, 309 (1972).

120. a. Sethuraman, V.; Edelson, M.C.; Johnson, C.K.; Sethuraman, C.; Small, G.J.: Mol. Cryst. Liq. Cryst. 57, 89 (1980).
b. Johnson, C.K.: Ph.D. dissertation, Iowa State University (1981).

121. Bree, A.; Edelson, M.; Taliani, C.: Chem. Phys. 30, 343 (1978).

122. Giordmaine, J.A.: Phys. Rev. Lett. 8, 19 (1962).

123. Ovander, L.N.; Petrenko, A.D.: J. Appl. Spectrosc. 21, 1309 (1974).

124. Meredith, G.R.: J. Chem. Phys. 75, 4317 (1981).

125. a. Bloembergen, N.; Lee, C.H.: Phys. Rev. Lett. 19, 835 (1967).
b. Bloembergen, N.; Chang, R.K.; Jha, S.S.; Lee, C.H.: Phys. Rev. 174, 813 (1968).
c. Bloembergen, N.; Simon, H.J.; Lee, C.H.: Phys. Rev. 181, 1261 (1969).

126. Shigorin, V.D.; Shipulo, G.P.: Sov. Phys. Crystallogr. 19, 622 (1975).

127. Katriel, J.; Moiseyev, N.: J. Chem. Phys. 78, 876 (1983).

128. Weiner, A.M.: IEEE J. Quan. Electronics QE-19, 1276 (1983).

129. a. Wynne, J.J.: Phys. Rev. Lett. 52, 751 (1984).
b. Wynne, J.J.: Phys. Rev. Lett. 52, 1255 (1984).

130. Hochstrasser, R.M.; Meredith, G.R.: J. Chem. Phys. 67, 1273 (1977).

131. a. Stevenson, S.H.; Small, G.J.: Chem. Phys. Lett. 95, 18 (1983).
b. Stevenson, S.H.; Small, G.J.: Chem. Phys. Lett. 100, 334 (1983).
c. Stevenson, S.H.: Ph.D. dissertation, Iowa State University (1985).

132. a. Johnson, C.K.; Small, G.J.: J. Chem. Phys. 76, 3837 (1982).
b. Johnson, C.K.; Small, G.J.: Chem. Phys. 64, 83 (1982).

133. Kielich, S.; Zawodny, R.: in Optical Properties of Highly Transparent Solids, ed. S.S. Mitra, B. Bendow, Plenum Press, New York (1975), p.393.

134. a. Meredith, G.R.; Krongauz, V.; Williams, D.J.: Chem. Phys. Lett. 87, 289 (1982).
b. Meredith, G.R.; Williams, D.J.; Fishman, S.N.; Goldburt, E.S.; Krongauz, V.A.: J. Phys. Chem. 87, 1697 (1983).

135. Lam, Y.T.; Thirunamachandran, T.: J. Chem. Phys. 77, 3810 (1982).

136. Tweig, R.; Azema, A.; Jain, K.; Cheng, Y.Y.: Chem. Phys. Lett. 92, 208 (1982).

137. Zel'dovich, B.Y.; Kuz'michev, S.D.: JETP Lett. 37, 103 (1983).

138. Meredith, G.R.; VanDusen, J.G.; Williams, D.J.: Macromolecules 15, 1385 (1982).

139. Driscoll, T.A.; Guidotti, D.: Phys. Rev. B 28, 1171 (1983).

140. a. Andrews, D.L.: J. Chem. Phys. 77, 2831 (1982).
b. Andrews, D.L.: J. Chem. Phys. 78, 1731 (1983).

141. a. Meredith, G.R.: Phys. Rev. B 24 , 5522 (1981).
b. Meredith, G.R.: J. Chem. Phys. 77 , 5863 (1982).
c. Meredith, G.R.: J. Chem. Phys. 78 , 1533 (1983).
d. Meredith, G.R.: J. Chem. Phys. 78 , 1543 (1983).

142. Burland, D.M.; Haarer, D.: IBM J. Res. Develop. 23 , 534 (1979).

143. Edelson, M.C.; Hayes, J.M.; Small, G.J.: Chem. Phys. Lett. 60 , 307 (1979).

144. Akhmanov, S.A.; Aslanyan, L.S.; Bunkin, A.F.; Gadzhiev, F.N.; Koroteev, N.I.; Shumai, I.L.: in Light Scattering in Solids , ed. J.L. Birman, H.Z. Cummins, K.K. Rabane, Plenum Press, New York (1979), p.409.

145. Bloembergen, N.: in Light Scattering in Solids , ed. J.L. Birman, H.Z. Cummins, K.K. Rabane, Plenum Press, New York (1979), p.423.

146. a. Hochstrasser, R.M.; Abram, I.I.: in Light Scattering in Solids , ed. J.L. Birman, H.Z. Cummins, K.K. Rabane, Plenum Press, New York (1979), p.447.
b. Hochstrasser, R.M.; Meredith, G.R.; Trommsdorff, H.P.: J. Chem. Phys. 73 , 1009 (1980).
c. Dick, B.; Hochstrasser, R.M.: J. Chem. Phys. 78 , 3398 (1983).

147. Oudar, J.L.; Smith, R.W.; Shen, Y.R.: Appl. Phys. Lett. 34 , 758 (1979).

148. Antcliff, R.R.; Jarrett, O.: Appl. Opt. 22 , 1954 (1983).

149. Kosic, T.J.; Cline, R.E.; Dlott, D.D.: Chem. Phys. Lett. 103 , 109 (1983).

150. a. Chen, C.K.; DeCastro, A.R.B.; Shen, Y.R.: Phys. Rev. Lett. 43 , 946 (1979).
b. Heinz, T.F.; Chen, C.K.; Ricard, D.; Shen, Y.R.: Chem. Phys. Lett. 83 , 180 (1981).
c. Chen, C.K.; Heinz, T.F.; Ricard, D.; Shen, Y.R.: Phys. Rev. Lett. 46 , 1010 (1981).
d. Chen, C.K.; Heinz, T.F.; Ricard, D.; Shen, Y.R.: Phys. Rev. B 27 , 1965 (1983).

e. Heinz, T.F.; Tom, H.W.K.; Shen, Y.R.: Phys. Rev. A 28 , 1883 (1983).

151. Agarwal, G.S.; Jha, S.S.: Phys. Rev. B 26 , 482 (1982).

152. a. Stegeman, G.I.; Liao, C.; Karaguleff, C.: Opt. Commun. 46 , 253 (1983).
b. Moshrefzadeh, R.; Fortenberry, R.; Karaguleff, C.; Stegeman, G.I.; VanWijck, N.E.; Hetherington, W.H.: Opt. Commun. 46 , 257 (1983).

153. Reider, G.A.; Schmidt, A.J.: Opt. Commun. 47 , 223 (1983).

154. Tien, P.K.; Ulrich, R.; Martin, R.J.: Appl. Phys. Lett. 17 , 447 (1970).

155. Burns, W.K.; Lee, A.B.: Appl. Phys. Lett. 24 , 222 (1974).

156. Stolen, R.H.; Lin, C.: in Optical Properties of Highly Transparent Solids, ed. S.S. Mitra, B. Bendow, Plenum Press, New York (1975), p.307.

157. a. Frenkel, J.: Phys. Rev. 37 , 17 (1931).
b. Frenkel, J.: Phys. Rev. 37 , 1276 (1931).

158. a. Davydov, A.S.; Lubchenko, A.F.: Sov. Phys. JETP 35 , 1048 (1959).
b. Davydov, A.S.: Sov. Phys. JETP 16 , 1293 (1963).
c. Davydov, A.S.: Sov. Phys. JETP 16 , 496 (1964).
d. Davydov, A.S.: Phys. Status Solidi 20 , 143 (1967).
e. Davydov, A.S.; Myasnikov, E.N.: Phys. Status Solidi 20 , 153 (1967).
f. Davydov, A.S.; Myasnikov, E.N.: Phys. Status Solidi B63 , 325 (1974).

159. Davydov, A.S.: Theory of Molecular Excitons , Plenum Press, New York (1971).

160. Knox,R.S.: Theory of Excitons , Academic Press, New York (1963).

161. Ueta, M.; Kanzaki, H.; Kobayashi, K.; Toyozawa, Y.; Hanamura, E.: Excitonic Processes in Solids , Springer-Verlag, New York (1986).

162. Pekar, S.I.: Sov. Phys. JETP 11, 1286 (1960).

163. a. Agranovich, V.M.: Sov. Phys. Solid State 3, 592 (1961).
b. Agranovich, V.M.; Ginzburg, V.L.: Sov. Phys. Usp. 5, 323 (1962).
c. Agranovich, V.M.; Ginzburg, V.L.: Sov. Phys. Usp. 5, 675 (1963).
d. Agranovich, V.M.; Toshich, B.S.: Sov. Phys. JETP 26, 104 (1968).

164. Philpott, M.R.: Adv. Chem. Phys. 23, 227 (1973).

165. a. Craig, D.P.; Walmsley, S.H.: Mol. Phys. 4, 113 (1961).
b. Craig, D.P.; Walmsley, S.H.: Mol. Phys. 4, 97 (1961).

166. a. Greer, W.L.; Rice, S.A.; Jortner, J.; Silbey, R.: J. Chem. Phys. 48, 5667 (1968).
b. Silbey, R.; Jortner, J.; Vala, M.T.; Rice, S.A.: J. Chem. Phys. 42, 2948 (1965).

167. a. McClure, D.S.: J. Chem. Phys. 22, 1668 (1954).
b. McClure, D.S.: J. Chem. Phys. 24, 1 (1956).

168. a. Krivenko, T.A.; Sheka, E.F.; Rashba, E.I.: Mol. Cryst. Liq. Cryst. 47, 119 (1978).
b. Meletov, K.P.; Sheka, E.F.; Rashba, E.I.: Mol. Cryst. Liq. Cryst. 57, 65 (1980).

169. Davydov, A.S.; Sheka, E.F.: Phys. Status Solidi 11, 877 (1965).

170. Matsui, A.; Ishii, Y.: J. Phys. Soc. Japan 23, 581 (1967).

171. Philpott, M.R.: J. Chem. Phys. 54, 111 (1971).

172. a. Morris, G.C.; Rice, S.A.; Sceats, M.G.; Martin, A.E.: J. Chem. Phys. 55, 5610 (1971).
b. Morris, G.C.; Sceats, M.G.: Chem. Phys. 3, 332 (1974).
c. Morris, G.C.; Sceats, M.G.: Chem. Phys. 3, 342 (1974).

173. Craig, D.P.; Dissado, L.A.: Proc. R. Soc. Lond. A. 363, 153 (1978).

174. Craig, D.P.; Gordon, R.D.: Proc. R. Soc. Lond. A. 288 , 69 (1965).

175. Agranovich, V.M.; Konobeev, Y.V.: Sov. Phys. Solid State 6 , 644 (1964).

176. Cho, K.; Toyozawa, Y.: J. Phys. Soc. Japan 30 , 1555 (1971).

177. Colson, S.D.; Netzel, T.L.; van Pruyssen, J.M.: J. Chem. Phys. 62 , 606 (1975).

178. Kopelman, R.; Ochs, F.W.; Prasad, P.N.: J. Chem. Phys. 57 , 5409 (1972).

179. Sumi, H.: J. Chem. Phys. 67 , 2943 (1977).

180. Craig, D.P.: Chem. Phys. Lett. 88 , 362 (1982).

181. Klafter, J.; Jortner, J.: J. Chem. Phys. 77 , 2812 (1982).

182. Munn, R.W.: Chem. Phys. 84 , 413 (1984).

183. Huang, K.: Proc. R. Soc. London A208 , 352 (1951).

184. Fano, U.: Phys. Rev. 103 , 1202 (1956).

185. Hopfield, J.J.: Phys. Rev. 112 , 1555 (1958).

186. Agranovich, V.M.: Sov. Phys. JETP 37 , 307 (1960).

187. Benson, H.J.; Mills, D.L.: Phys. Rev. B 1 , 4835 (1970).

188. Lang, M.: Phys. Rev. B 2 , 4022 (1970).

189. Sumi, H.: J. Phys. Soc. Japan 41 , 526 (1976).

190. Philpott, M.R.: Phys. Rev. B 14 , 3471 (1976).

191. Hopfield, J.J.: J. Phys. Soc. Japan 21 , 77 (1966).

192. Johnson, C.K.; Small, G.J.: in Excited States , vol.6, ed. E.C. Lim, Academic Press, New York (1982), p.97.

193. a. Boggett, D.; Loudon, R.: Phys. Rev. Lett. 28 , 1051 (1972).
b. Boggett, D.; Loudon, R.: J. Phys. C 6 , 1763 (1973).

194. a. Hopfield, J.J.; Thomas, D.G.: Phys. Rev. Lett. 15 , 22 (1965).
b. Henry, C.H.; Hopfield, J.J.: Phys. Rev. Lett. 15 , 964 (1965).

195. Ferguson, J.: Chem. Phys. Lett. 36 , 316 (1975).

196. Permogorov, S.; Travnikov, V.: Phys. Status Solidi B78 , 389 (1976).

197. a. Robinette, S.L.; Small, G.J.: J. Chem. Phys. 65 , 837 (1976).
b. Robinette, S.L.; Small, G.J.; Stevenson, S.H.: J. Chem. Phys. 68 , 4790 (1978).
c. Robinette, S.L.; Stevenson, S.H.; Small, G.J.: J. Chem. Phys. 69 , 5231 (1978).
d. Robinette, S.L.; Stevenson, S.H.; Small, G.J.: J. Lumin. 18/19 , 457 (1979).

198. Galanin, M.D.; Khan-Magometova, S.D.; Myasnikov, E.N.: Mol. Cryst. Liq. Cryst. 57 , 119 (1980).

199. a. Vidmont, N.A.; Maksimov, A.A.; Tartakovskii, I.I.: Sov. Phys. Solid State 24, 784 (1982).
b. Vidmont, N.A.; Maksimov, A.A.; Tartakovskii, I.I.: JETP Lett. 37 , 689 (1983).

200. Coffinet, J.P.; DeMartini, F.: Phys. Rev. Lett. 22 , 60 (1969).

201. a. Frohlich, D.; Mohler, E.; Wiesner, P.: Phys. Rev. Lett. 26 , 554 (1971).
b. Frohlich, D.; Mohler, E.; Uihlein, C.: Phys. Status Solidi B55 , 175 (1973).

202. Haueisen, D.C.; Mahr, H.: Phys. Rev. B 8 , 2969 (1973).

203. Duong, P.H.; Itoh, T.; Lavallard, P.: Solid State Commun. 43 , 879 (1982).

204. Lyssenko, V.G.; Kempf, K.; Bohnert, K.; Schmieder, G.; Klingshirn, C.; Schmitt-Rink, S.: Solid State Commun. 42 , 401 (1982).

205. Frohlich, D.; Holscher, H.; Nothe, A.: Solid State Commun. 48 , 217 (1983).

206. Broude, V.L.; Rashba, E.I.; Sheka, E.F.: Spectroscopy of Molecular Excitons , Springer-Verlag, New York (1985).

207. Loudon, R.: in Proc. Intl. Sch. Phys. "Enrico Fermi" Course LXIV , ed. N. Bloembergen, North-Holland, New York (1977), p.296.

208. DeMartini, F.: in Proc. Intl. Sch. Phys. "Enrico Fermi" Course LXIV , ed. N. Bloembergen, North-Holland, New York (1977), p.319.

209. a. Munn, R.W.; Silbey, R.: J. Chem. Phys. 68 , 2439 (1978).
b. Munn, R.W.; Silbey, R.: Mol. Cryst. Liq. Cryst. 57 , 131 (1980).

210. a. Haken, H.; Strobl, G.: in The Triplet State , ed. A. Zahlan, Cambridge University Press, London (1967), p.311.
b. Haken, H.; Reineker, F.: Z. Phys. 249 , 253 (1972).

211. Reineker, P.: in Exciton Dynamics in Molecular Crystals and Aggregates , ed. G. Hohler, Springer-Verlag, New York (1982), p.111.

212. Grover, M.; Silbey, R.: J. Chem. Phys. 54 , 4843 (1971).

213. Kenkre, V.M.: in Exciton Dynamics in Molecular Crystals and Aggregates , ed. G. Hohler, Springer-Verlag, New York (1982), p.1.

214. a. Hoshen, J.; Kopelman, R.; Monberg, E.M.: J. Stat. Phys. 19 , 219 (1978).
b. Hoshen, J.; Klymko, P.; Kopelman, R.: J. Stat. Phys. 21 , 583

(1979).

215. Abram, I.I.; Silbey, R.: J. Chem. Phys. 63, 2317 (1975).

216. Allan, J.W.; Silbey, R.: Chem. Phys. 43, 341 (1979).

217. Munn, R.W.: J. Chem. Phys. 58, 3230 (1972).

218. Reineker, P.; Kühne, R.: Phys. Rev. B 21, 2448 (1980).

219. a. Ovander, L.N.: Sov. Phys. Solid State 5, 641 (1963).
b. Ovander, L.N.: Sov. Phys. Usp. 86, 337 (1965).

220. Fearey, B.L.: Ph.D. dissertation, Iowa State University (1986).

221. Chang, T.C.: Ph.D. dissertation, Iowa State University (1985).

222. Hayes, J.M.: Ames Laboratory U.S.D.O.E., Ames, Iowa, unpublished work.

223. Small, G.J.: Department of Chemistry, Iowa State University and Ames Laboratory U.S.D.O.E., Ames, Iowa, unpublished results.

224. Schmid, D.: in Organic Molecular Aggregates, ed. P. Reineker, H. Haken, H.C. Wolf, Springer-Verlag, New York (1983), p.184.

225. Chandrasekhar, S.: Rev. Mod. Phys. 15, 1 (1943).

226. Stevenson, S.H.: Experimental Station, Dupont Corporation, Wilmington, Delaware, personal communication.

227. Hopfield, J.J.; Thomas, D.G.: J. Phys. Chem. Solids 12, 276 (1960).

228. Johnson, C.K.: Ph.D. dissertation, Iowa State University (1981).

ACKNOWLEDGMENTS

The completion of one's graduate career is certainly a time for celebration, however such a celebration is only justified if it is shared with all of the many persons who have given support during the years of study. I have had the great fortune to meet with and be influenced by many wonderful people during my graduate school years, and I wish to express my gratitude to them now.

I am grateful to my research advisor, Professor Gerald J. Small, for his help and patience during my tenure at Iowa State University. His support and his willingness to discuss the good, the bad and the ugly at any time were a great advantage to me. His confidence in my results, even at times when I thought I was hexed, was greatly appreciated. I am also grateful for his patience, understanding and restraint (from committing bodily harm on my person) when once paired as foosball partners, what can I say except that eye-hand coordination never has been my forte!

I am grateful also to Dr. Sylvia H. Stevenson for her help in the laboratory during the early days at ISU and for many helpful long-distance discussions of perplexing data after her departure. In addition to the fine lab-related rapport, I would like to thank both Sylvia and Doug Adelman for their out-of-lab friendship. Please note that the next time we get together for a quick game of bridge I will come prepared with a can of carpet cleaner (birthday parties too!)! Until then, go easy on the pistachios!

Dr. John M. Hayes also deserves many thanks. John wrote several programs used in my data collection and analysis and was very helpful in

the initial stages of the move from the beloved NRG to the Quantel. Thanks also to both John and Rita and their entire family for their friendship past, present and future!

I would like to thank my office mates Mike Kenney and Bryan Isaac for lots of good company and conversation. I would especially like to thank Mike for cheerfully accepting and efficiently performing the role of legman during this past year. And by the way, Mike, which version of FIGURE are you up to now? My thanks to Kevin Gillie for helping us keep the tomatoes picked and, more importantly, for taking all of the beets! Steve Johnson and Scott (Scumby) Cooper, thanks for being great friends. We've enjoyed the beer, margaritas, mild tacos, pool, and Trivial Pursuit! We await your visit - R.S.'s Hot Rocks awaits!

Many thanks to Dr. Ryszard Jankowiak for many enjoyable conversations at the lab and outside. My best wishes for your continued success in your new home. We look forward to seeing you, Marzenna, and the kids again.

To Jon Andy Warren, Monie says thanks for the memories, especially those of Thunder Bay! Should you ever plan a return trip, count me in (this offer applies to summer months only!).

To all members of the Small group, past and present, thanks for having such a great sense of humor. The subtle (and not-so-subtle) practical jokes gave me great enjoyment (although I ***never*** had anything to do with them, ***honest***!).

I would also like to thank Evan and Darlene Fearey for their encouragement during my studies.

I would like to express my sincere appreciation to my parents, Mr. and Mrs. Walter E. Connolly, without whose support and understanding it would have been nearly impossible for me to return to school for "a few years" (yes, I realize it turned into a decade, but making estimates has never been a strongpoint of mine!). I will always be grateful for everything you have done for me.

Finally, I would like to thank my husband, Dr. Bryan L. Fearey, for his continuous support, understanding and encouragement throughout my entire time at ISU. You more than anyone else have helped me tremendously in my efforts. You have been there for me during the bad times as well as the good times, and for this I always will be grateful. I thank you also for your occasional help in the laboratory, for the fast food deliveries during my marathon laboratory sessions, and for your help in compiling and editing this thesis.